NATIONAL ADVISORY COMMITTEE FOR AERONAUTICS

WARTIME REPORT

ORIGINALLY ISSUED
September 1944 as
Memorandum Report

AIRFOIL SECTION DATA FROM TESTS OF 10 PRACTICAL-CONSTRUCTION SECTIONS OF HELICOPTER ROTOR BLADES SUBMITTED BY THE SIKORSKY AIRCRAFT DIVISION, UNITED AIRCRAFT CORPORATION

By Neal Tetervin

Langley Memorial Aeronautical Laboratory
Langley Field, Va.

WASHINGTON

NATIONAL ADVISORY COMMITTEE FOR AERONAUTICS

MEMORANDUM REPORT

for the

Army Air Forces, Materiel Command

AIRFOIL SECTION DATA FROM TESTS OF 10 PRACTICAL-CONSTRUCTION SECTIONS OF HELICOPTER ROTOR BLADES SUBMITTED BY THE SIKORSKY AIRCRAFT DIVISION, UNITED AIRCRAFT CORPORATION

By Neal Tetervin

SUMMARY

At the request of the Army Air Forces, Materiel Command, 10 practical-construction models of sections of helicopter rotor blades built by the Sikorsky Aircraft Division, United Aircraft Corporation, were tested in the NACA two-dimensional low-turbulence pressure tunnel at atmospheric pressure.

Lift, drag, and pitching-moment characteristics of blades representing the present method of construction of the YR-4A helicopter were determined. Similar data were obtained for other models representing the YR-4A, XR-6, and XR-5 helicopters to determine the effect of an abrasion strip at the leading edge, of improving the surface fairness and smoothness near the leading edge, of halving the rib spacing, of making the blades entirely of plywood, of using a combination plywood and fabric construction, and of using a thinner airfoil section. The effects of various model internal pressures on the characteristics of the fabric-covered models were determined. Internal pressures corresponding to various tip-vent positions were measured on one of the two tip sections. The spanwise variation of section drag was also obtained for the tip sections. The tests were made over a range of Reynolds numbers from 0.74×10^6 to 3.46×10^6 and a corresponding range of Mach numbers from 0.130 to 0.376.

The aerodynamic characteristics of the fabric-covered models used in the present tests were markedly affected by variations of the internal pressure. Usually the most desirable pressure in the hollow rear portion of the model was one equal to the free-stream static pressure. An internal pressure greater than that of the free stream usually produced an increase in section drag coefficient, a decrease in section maximum lift coefficient, and a forward movement of the aerodynamic center. An internal pressure less than that of the free-stream static pressure usually produced a slight increase in a section drag coefficient, a slight increase in section maximum lift coefficient, and a slight rearward movement of the aerodynamic center.

Halving the rib spacing of a fabric-covered model made the aerodynamic characteristics less sensitive to the model internal pressure.

Blades having plywood surfaces had maximum lift coefficients no higher than those of fabric-covered models and drag coefficients about 0.0013 less than those of the best fabric-covered models.

INTRODUCTION

The characteristics of smooth and fair airfoil sections specified for use on helicopters have been known for some time as a result of tests in essentially two-dimensional nonyawed flow. It has been realized, however, that the characteristics of actual rotor-blade sections are different from those of smooth and fair airfoils because of manufacturing irregularities, distortions of the blade-section shape that occur in flight, and the yawed conditions in which the blade sections operate.

At the request of the Army Air Forces, Materiel Command, 10 practical-construction models of sections of helicopter rotor blades built by the Sikorsky Aircraft Division, United Aircraft Corporation, were tested in the NACA two-dimensional low-turbulence pressure tunnel at atmospheric pressure. Although these tests did not simulate the effects of yaw, data were obtained to determine the relative merit of various practical types of construction.

Lift, drag, and pitching-moment characteristics of blades representing the present method of construction of the YR-4A helicopter were determined. Similar data were obtained for other models representing the YR-4A, XR-6, and XR-5 helicopters to determine the effect of an abrasion strip at the leading edge, of improving the surface fairness and smoothness near the leading edge, of halving the rib spacing, of making the blades entirely of plywood, of using a combination plywood and fabric construction, and of using a thinner airfoil. The effects of various internal pressures on the characteristics of the fabric-covered models were determined. Internal pressures corresponding to various tip-vent positions were measured. The spanwise variation of section drag was also obtained for the tip sections. The tests were made over a range of Reynolds numbers from 0.74×10^6 to 3.46×10^6 and a corresponding range of Mach numbers from 0.130 to 0.376.

MODELS

Models representing sections of rotor blades from three helicopters, the YR-4A, XR-6, and XR-5 were tested. The YR-4A models consisted of a group of five camouflage-painted fabric-covered models, the no. 1, no. 3, no. 4, no. 6, and no. 10, representing sections in the region from the blade tip to approximately 9 feet from the tip. The YR-4A no. 10 model was built with half the rib spacing of the others and the YR-4A no. 4 was built without a leading-edge abrasion strip. In addition to tests in its original condition, the YR-4A no. 10 was also tested with the forward third of the model surfaces faired to the contour of the NACA 0012 airfoil section with pyroxylin glazing putty and sanded smooth. Although the texture of the finish over the forward third of the model surfaces was made smooth to the touch, there were local bumps just to the rear of the quarter-chord line that could not be removed by sanding. The YR-4A no. 10 model with the forward third made smooth and fair is called the YR-4A no. 10 (Smooth Forward Portion). The models were to represent the NACA 0012 airfoil section but, as constructed, were about $12\frac{1}{2}$ percent thick. Additional information for these models is given in table I and figures 1 to 6. The crack at the juncture of the leading-edge abrasion strip and the remainder of the

model that can be noticed in figure 6(a) occurred after the model tests had been completed.

Three XR-6 blade sections, the XR-6 no. 1, no. 5, and no. 7 models representing the portion of the blade between the tip and approximately 9 feet from the tip were tested. The models were of plywood construction and were painted with camouflage paint by the manufacturer. Measurements of the models showed them to be just about 12 percent thick. Additional information for these models is given in table I and figures 7 to 9.

Two XR-5 blade sections which represented the portion of the blade close to the tip were tested. The models were of combination plywood and fabric construction having plywood laid over ribs and camouflage-painted fabric over the plywood. The two XR-5 models differed from one another in the extent of plywood on one of the surfaces. The ordinates of the two XR-5 sections, obtained from measurements of one of the models, are approximately those of the NACA 0010-64 airfoil section (reference 1). Additional information for these models is given in table I and figures 10 and 11.

All the models were tested as received except for filling a few gouges obviously caused by handling and lightly sanding the upper surface of the XR-6 no. 2 tip section before testing. After the drag measurements for the YR-4A no. 1 tip section were completed, six vent holes were installed. The model internal pressures were then measured with all the vent holes sealed, except the one for which data were being obtained. The vent holes were all of $\frac{3}{16}$-inch diameter. Five were on the lower surface $\frac{1}{2}$-inch inboard of the solid wood which formed the outer $6\frac{3}{8}$ inches of the tip section and were located at 38, 50, 60, 70, and 80 percent of the chord from the leading edge in a plane perpendicular to the quarter-chord line. The vent holes were made by doping a strip of aircraft fabric over the model fabric in the region in which the holes were to be located, cutting the holes through the two thicknesses of aircraft fabric, and smoothing their edges. The sixth vent hole was drilled from the extreme tip through the solid tip portion and into the hollow part of the model. The location of the tip-vent hole is given in figure 12.

TEST PROCEDURE

The tests in the NACA two-dimensional pressure tunnel were made at atmospheric pressure in order to keep the same relation between the Reynolds number, Mach number, and dynamic pressure as in flight.

The wind tunnel is briefly described in reference 2. All the models except the two tip sections extended almost from wall to wall of the tunnel. Gaps just large enough to allow the model to pitch freely during measurements of the pitching moments were left at the model ends. Because of the small size of the end gaps, about 1/32 of an inch, it is believed that the effect of any air flow through these gaps on the measured lifts, drags, and pitching moments was negligible. The two tip sections were mounted cantilever from one wall of the tunnel leaving an 11-inch gap between the model tip and the other wall of the tunnel.

The aerodynamic data were obtained at the smallest Reynolds number first and the highest last. The chords used in calculating the Reynolds number are given in table II. The lifts were measured by evaluating the reaction of the model on the floor and ceiling of the tunnel from measurements of the pressures on the floor and ceiling (reference 2). Although the models did not have uniform chord along the span, no change was made in the usual method of obtaining the lift. Any error caused by the taper of the models is believed to be small.

The drag coefficients for the complete span models, obtained by the wake-survey method, were the average coefficients over the center portion of the models. In table II, which lists the tests of each model, are given the spanwise distances over which the drags were measured. The drag coefficient of the two tip sections has been based on a 10-inch chord. The variation of chord along the span of the two tip sections is given in figure 13.

The pitching-moment coefficients were obtained from measurements on a balance (reference 2).

Because some of the test Mach numbers were higher than those at which tests are usually made in the

NACA two-dimensional pressure tunnel, the customary methods of computing the data were modified to include the compressibility correction to the measured dynamic pressure. The wake-survey method of obtaining drag was corrected for compressibility by using the charts in reference 3.

The usual corrections to the lift, drag, and pitching-moment coefficients for tunnel-wall effect have been applied to the data for all the models except the two tip sections. The corrections used were:

$$c_l = 0.995c_l'$$

$$c_d = 0.998c_d'$$

$$c_m = 0.998c_m'$$

$$\alpha_o = 1.004\alpha_o'$$

for the YR-4A no. 3, no. 4, no. 10, no. 10 (Smooth Forward Portion), and XR-6 no. 5 models. For the YR-4A no. 6, XR-5(a), XR-5(b), and XR-6 no. 7 models, the corrections were:

$$c_l = 0.991c_l'$$

$$c_d = 0.997c_d'$$

$$c_m = 0.997c_m'$$

$$\alpha_o = 1.006\alpha_o'$$

The primed symbols denote values obtained in the tunnel.

Tunnel-wall corrections have not been applied to the data for the tip sections because of the small magnitude of the corrections for a full-span model of the size of the tip sections and because the corrections usually applied were derived for constant chord models which completely span the tunnel. Because of the questionable accuracy of profile-drag measurements made by the wake-survey method in the region of strong trailing vortices, such as were present in the tip region of the models, the compressibility corrections have not been applied to the measured drags for the two tip sections. The corrections would reduce the drag coefficients by approximately $2\frac{1}{2}$ percent at a Mach number of 0.280 and

5 percent at a Mach number of 0.375. During tests of the tip sections, the wake-survey rate was about $2\frac{1}{2}$ feet behind the trailing edge of the models.

The full-span fabric-covered models and the fabric-covered tip section were tested with the internal pressure in the hollow rear portions of the models equal to the free-stream static pressure and to pressures greater and less than the free-stream static pressure by 20 inches of water. The free-stream static pressure is the pressure that would exist in the tunnel test section for the conditions at which the tests were made but with the tunnel test section empty. The desired model internal pressures were obtained by connecting the interior of the models to a pump through a hollow pin that helped hold the models in place. The model internal pressures were measured by connecting the hollow rear portion of the models to a suitable manometer.

The internal pressures of the fabric-covered tip section were measured with all the holes sealed except the one for which data were being obtained. The measured pressures have not been corrected for tunnel-wall effect.

During the tests the fabric on some of the models cracked or split, thus causing leaks. The cracks were repaired by applying dope; the tears were repaired by covering the region of the tear with aircraft tape and applying a few coats of dope. A list and the type of repairs are given in table III. The aerodynamic characteristics of the models were not noticeably affected by changes in surface conditions caused by the repairs. To eliminate the possibility of model failure at the highest test dynamic pressures the angle-of-attack range was restricted to values below the stall.

RESULTS

The results are presented in groups of blade sections which have similar construction features. The pitching-moment coefficients have been presented about both the aerodynamic centers and quarter-chord points for all cases except those where the slope of the curve of pitching-moment coefficient about the quarter-chord point

was practically zero. All the aerodynamic centers are located on the chord line.

The first group consists of the YR-4A no. 3 and the YR-4A no. 6 blade sections. The results for the YR-4A no. 3 blade section are given in figures 14 to 16. Upon inspecting the model at the completion of the test at a Reynolds number of 1.84×10^6, it was found that the fabric covering over the hollow rear portion of the airfoil had become flabby. The tests at a Reynolds number of 2.58×10^6 were conducted with the fabric in this condition. The fabric flabbiness magnified the effects of the different internal pressures and allowed the external suctions to have a relatively large effect at the higher dynamic pressures for the condition of zero-internal-pressure difference. The results for the YR-4A no. 6 blade section are contained in figures 17 to 20. The fabric tension decreased slightly during the tests.

The second group consisted of the YR-4A no. 4, YR-4A no. 10, and YR-4A no. 10 (Smooth Forward Portion) sections. The YR-4A no. 4 blade section was used to determine the effect of a leading-edge abrasion strip on the characteristics of the models in the first group. The results are given in figure 21. The YR-4A no. 10 blade section was tested to determine the effect on the aerodynamic characteristics of models in group one of halving the rib spacing. The results are given in figures 22 to 24. The YR-4A no. 10 (Smooth Forward Portion) was used to determine the effect of smoothing and fairing the forward third of the airfoil section on the aerodynamic characteristics of models similar to the YR-4A no. 10 blade section. The results are contained in figures 25 and 26.

The third group consisted of the XR-6 no. 5 and XR-6 no. 7 blade sections and indicate the results to be expected from plywood-covered blades. The data for the XR-6 no. 5 are presented in figure 27 and the data for the XR-6 no. 7, in figure 28.

The fourth group consisted of the XR-5(a) and XR-5(b) sections and indicates the effect on the aerodynamic characteristics of changing the airfoil section from the NACA 0012 to the NACA 0010-64 and indicates the results to be expected from blade sections having the combination plywood and fabric construction used for the XR-5 models. The results for the XR-5(a) blade specimen

are given in figures 29 and 30. The results for the XR-5(b) blade specimen are contained in figures 31 to 33.

The fifth group consisted of the two blade tip sections. Neither lift nor pitching moments were measured during tests of the two tip sections. Section drag coefficients over the outer portion of the span are presented in table IV for the YR-4A no. 1 tip section and in table V for the XR-6 no. 2 tip section. Data of table IV at one test condition and four angles of attack were plotted in figure 34 to show the variation of section drag coefficient along the span of the YR-4A no. 1 tip section. Similar data for the XR-6 no. 2 tip section from table V are presented in figure 35. In figure 36 data are presented in the form of curves of $\Delta p/q$ versus α for the various vent-hole positions, where

Δp model internal static pressure minus free-stream static pressure

q free-stream dynamic pressure

DISCUSSION

Aerodynamic Characteristics of Fabric-Covered Models as Affected by Internal Pressure

The blade sections were tested at internal pressures greater and less than that of the free-stream static pressure because the internal static pressures of rotor blades in flight differ from atmospheric pressure. The column of air contained in the rotating blade is acted upon by centrifugal forces and for the XR-5, XR-6, and YR-4A helicopters it is possible for the static pressure in the tip portion of the blade to be about 280 pounds per square foot greater than atmospheric pressure at sea level. This is based on the assumption of an internal pressure at the blade root equal to the atmospheric static pressure and an airtight blade. By sealing the blade at the root and leaving the tip portion open to the atmosphere it would be possible to get an internal static pressure in the blade at the root less than atmospheric pressure by about 280 pounds per square foot.

Such large pressure differences from atmospheric pressure are probably not encountered in practice because the blades are vented to the atmosphere and may have leaks or partitions along the span. A pressure difference of 20 inches of water, corresponding to a pressure of 104 pounds per square foot, was chosen as being sufficiently large to show clearly the effects of internal pressure on the aerodynamic characteristics and yet not be large enough to cause structural failure of the blades during the tests.

The YR-4A no. 3 test section was chosen to illustrate the effects of internal pressure on the aerodynamic characteristics of a typical fabric-covered model.

Section maximum lift coefficient.- The effect of variations of internal pressure on the section maximum lift coefficients of fabric-covered models with normal rib spacing is illustrated by the data for the YR-4A no. 3 section, at a Reynolds number of 1.84×10^6, given in the following table and in figure 15(b):

Internal pressure (in. H_2O)	Section maximum lift coefficient
20	1.15
0	1.25
-20	1.32

Increasing the internal pressure caused the section maximum lift coefficients to decrease. Decreasing the internal pressure caused the opposite effect. The effect of internal pressure increased as the test dynamic pressure increased (figs. 14(b) and 15(b)).

The effects of internal pressure on other models, which had approximately the same rib spacing (YR-4A no. 4, YR-4A no. 6), were about the same.

Section lift-curve slope.- The effect of variations of the internal pressure on the slope of the lift curve is illustrated in the following table and in figures 14(b), 15(b), and 16(b) for the YR-4A no. 3 test section.

Internal pressure ($in. H_2O$)	Section lift-curve slope		
	$R = 0.91 \times 10^6$ $q = 26.0$ lb/sqft	$R = 1.84 \times 10^6$ $q = 102$ lb/sq ft	$R = 2.58 \times 10^6$ $q = 210$ lb/sqft
20	0.104	0.095	0.102
0	.104	.112	.112
-20	.106	.112	.119

Increasing the internal pressure reduced the slope of the lift curve from that obtained at zero internal-pressure difference and decreasing the internal pressure caused the slope of the lift curve to increase.

The values in the table also indicate that the effect of internal pressure became larger with increasing airspeed. Increasing the airspeed caused the dynamic pressure to increase and therefore caused the pressure differences acting across the fabric surfaces to increase. The increased pressure differences caused increasing changes in model contour.

Section drag coefficient.- The effect on the section drag coefficient of varying the internal pressure is illustrated by the data for the YR-4A no. 3 test section. The data for a moderate lift coefficient, 0.4, and a Reynolds number of 1.84×10^6 are given in the following table and in figure 15(a):

Internal pressure ($in. H_2O$)	Section drag coefficient
20	0.0115
0	.0098
-20	.0107

The table is representative of the general conclusions drawn from the data in the figures. These are that zero internal-pressure difference produced the lowest section drag coefficients and that the suction condition produced slightly higher section drag. Positive internal pressures produced the largest drag coefficients.

Section aerodynamic center.- The effect of variations of the internal pressure on the position of the aerodynamic center is illustrated by the data given in the

following table and in figure 15(d) for the YR-4A no. 3 model at a Reynolds number of 1.84×10^6.

Internal pressure (in. H_2O)	Position of the aerodynamic center
20	0.212
0	.241
-20	.258

Changing the model internal pressure thus had a large effect on the position of the aerodynamic center. Positive internal pressures caused the aerodynamic centers to move forward fairly large distances from the positions for no internal-pressure difference. In most cases, suction caused a slight rearward movement of the aerodynamic center. The reason for the movement of the aerodynamic center with internal pressure is believed to be the change in the airfoil shape in the trailing-edge region as the internal pressure was varied. A thick blunt trailing-edge region results in a forward position of the aerodynamic center; a fine cusp-like trailing-edge position results in a rear position of the aerodynamic center (unpublished data from LMAL).

Effect on the Aerodynamic Characteristics of Increasing the Airspeed

Section maximum lift coefficient.- The effect on the section maximum lift coefficient of increasing the airspeed is illustrated by the data for the YR-4A no. 3 section contained in the following table and in figures 14(b) and 15(b):

R	Section maximum lift coefficient		
	Internal pressure (in. H_2O)		
	20	0	-20
0.91×10^6	1.20	1.17	1.23
1.84	1.15	1.25	1.32

As the airspeed increased the section maximum lift coefficient obtained at the condition of positive internal pressure decreased. At both zero internal-pressure

difference and suction the section maximum lift coefficient increased with increasing airspeed. The changes were fairly small.

The change in maximum section lift coefficient with airspeed depended on the relative effects of the change in Reynolds number, Mach number, and airfoil contour. Increasing the Reynolds number in the range covered by the present tests would be expected to increase the maximum section lift coefficient but increasing the Mach number would decrease the maximum section lift coefficient. An example of the effect of Mach number on the maximum section lift coefficient is given by the data in figures 25(b) and 26(b). The section maximum lift coefficient decreased from 1.25 to 1.04 as the Mach number increased from 0.262 to 0.375.

In reference 4 are given data indicating that the effect of Mach number on the maximum lift coefficient of the NACA 0012 airfoil becomes important at Mach numbers greater than 0.17. The effect of increasing the dynamic pressure would be to increase the maximum section lift coefficient if the effect of increasing camber at the rear of the airfoil, caused by the fabric deflections, were greater than the effect of thickening the airfoil at the rear. For the condition of suction the effect of increasing camber was probably greater than that of airfoil thickening. At the condition of positive internal pressure the airfoil probably bulged out so much that the effect of increasing camber was overshadowed by the change in airfoil thickness distribution.

Section lift-curve slope.- As an illustration of the variation of section lift-curve slope with airspeed the values for the YR-4A no. 3 model for the suction condition are given below:

R	M	Slope of section lift curve
0.91×10^6	0.131	0.106
1.84	.262	.112
2.58	.375	.119

The section lift-curve slopes increased with airspeed. Because the slope of the lift curve for rigid

airfoils, in the test range of Reynolds numbers (reference 5), is practically independent of Reynolds number, the change in slope of the lift curve was caused either by Mach number, dynamic pressure, or a combination of both.

The section lift-curve slope may be expected to increase with Mach number in the manner given by Glauert's factor $1/\sqrt{1 - M^2}$ (reference 6). For all models tested with internal pressure, except the two XR-5 models, the increase of the slope of the lift curve with Mach number, at internal pressures equal to and less than the free-stream static pressure by 20 inches of water, was greater than would be expected from Glauert's factor. For positive internal pressures the increase was greater than that given by the factor $1/\sqrt{1 - M^2}$ for the YR-4A no. 6 model but less than expected for the YR-4 no. 3 and YR-4A no. 10 models. The increase of lift-curve slope with Mach number for the XR-6 no. 5 plywood-covered model was about equal to the increase expected from Glauert's factor. The XR-6 no. 7 model showed an unexplained increase in lift-curve slope with Mach number that was about 10 percent greater than expected from Glauert's factor.

A contributing factor to the excessive lift-curve slopes for the fabric-covered models may have been a camber increasing fabric deflection at the rear of the airfoils that increased with increase in dynamic pressure and angle of attack. The effect of the camber increasing fabric deflections on the lift was probably greatest at the condition of suction and least at the positive internal-pressure condition because of the bulging of the airfoil thickness distribution in the trailing-edge region as the internal pressure increased.

Section drag coefficient.- The variation of section drag coefficient with airspeed is given in the following table and in figures 14(a), 15(a), and 16(a) for the YR-4A no. 3 test section:

Internal pressure (in. H_2O)	Section drag coefficient at $c_l = 0$	Section drag coefficient at $c_l = 0.8$
$R = 0.92 \times 10^6$		
20	0.0091	0.0162
0	.0086	.0134
-20	.0102	.0144
$R = 1.84 \times 10^6$		
20	0.0104	0.0172
0	.0092	.0120
-20	.0098	.0132
$R = 2.58 \times 10^6$		
20	0.0114	0.0156
0	.0095	.0132
-20	.0098	.0125

There were no important differences between the variation of section drag coefficient obtained for this model and the other fabric-covered models. In general, the fabric-covered models at small values of c_l did not show the usual decrease of section drag coefficient with Reynolds number as the airspeed increased. The cause is believed to be the distortion of the airfoil shape with increase in airspeed and the fact that the model surfaces were not aerodynamically smooth. At the higher section lift coefficients the section drag decreased slightly between the lowest and highest airspeeds.

The section drag coefficients for the XR-6 no. 5 and XR-6 no. 7 plywood-covered models (figs. 27(a) and 28(a)) at zero lift rose by about 0.0008 as the airspeed increased. At the larger lift coefficients the section drag coefficients decreased by about 0.0020 as the airspeed increased.

Section aerodynamic center.- The movement of the aerodynamic center of the YR-4A no. 3 section as the airspeed was varied is given in figures 14(d), 15(d), and 16(d) and in the following table:

R	Aerodynamic center position, x/c		
	Internal pressure (in. H_2O)		
	20	0	-20
0.91×10^6	0.242	0.245	0.253
1.84	.212	.241	.258
2.58	.206	.227	.262

The variation in position of the aerodynamic center for the different internal pressures increased with increasing airspeed. The same effect was present on the other fabric-covered models. The cause was the increasing change caused in the model contour by the internal pressure as the dynamic pressure increased.

The movement of the aerodynamic center of the XR-6 no. 5 plywood-covered model with change in airspeed is presented in figure 27(d) and in the following table:

R	Aerodynamic center position, x/c
0.92×10^6	0.247
1.78	.242
2.68	.237

The small forward movement of the aerodynamic center with increasing airspeed was also obtained on the XR-6 no. 7 test section (fig. 28(d)). Because of the rigid plywood surfaces the dynamic pressure probably did not cause a sufficiently large change in model contour to affect the aerodynamic characteristics. Reference 7 indicates that a forward movement of the aerodynamic center with increasing Mach number is to be expected. The measured movement for the two plywood models (figs. 27(d) and 28(d)) is close to the value, 0.9 percent, which would be expected from reference 7 for the test range of Mach numbers.

Effect of Leading-Edge Abrasion Strip on the Aerodynamic Characteristics

The effect of a leading-edge abrasion strip on the aerodynamic characteristics of a typical fabric-covered

model can be obtained from a comparison of the data for the YR-4A no. 3 and YR-4A no. 4 test sections at a Reynolds number of 1.87×10^6. These sections were practically identical except for the painted leading-edge abrasion strip on the YR-4A no. 3 test section and a possible difference in fabric tension.

Section maximum lift coefficient.- The leading-edge abrasion strip had no important effect on the section maximum lift coefficient (figs. 15(b) and 21(b)).

Section lift-curve slope.- From comparison of figures 15(b) and 21(b) it is apparent that the leading-edge abrasion strip causes no important change in slope over the straight portion of the lift curve.

Section drag coefficient.- The addition of a leading-edge abrasion strip reduced the section drag coefficient by about 0.0008 in the range of moderate section lift coefficients at zero internal-pressure difference. At positive internal pressures the effect of the leading-edge abrasion strip was masked by the effects of fabric deflection so that the model with the leading-edge abrasion strip, the YR-4A no. 3, had higher section drag than the model without the leading-edge strip. The effect of the leading-edge abrasion strip on section drag coefficient depends on the relative smoothness of the leading-edge abrasion strip. For the region of the span over which drags were taken the leading-edge abrasion strip was fairly smooth; at other points blobs of paint were present.

Section aerodynamic center.- The difference between the section aerodynamic centers for the two test sections (figs. 15(d) and 21(d)) is not believed to have been caused by the difference in surface conditions at the leading edge. The difference may have been caused by a difference in fabric tension.

Effect on the Aerodynamic Characteristics of Fabric-Covered Models of Halving the Rib Spacing

The effect on the aerodynamic characteristics of a fabric-covered model of halving the rib spacing is

illustrated by the data for the YR-4A no. 10 and YR-4A no. 3 test specimens. The major difference between the two models was the difference in rib spacing (table I).

Section maximum lift coefficient.- A table of the section maximum lift coefficients is given below:

Internal pressure (in. H_2O)	YR-4A no. 3	YR-4A no. 10
$R = 0.91 \times 10^6$		
20	1.20	1.17
0	1.17	1.19
-20	1.23	1.18
$R = 1.84 \times 10^6$		
20	1.15	1.25
0	1.25	1.25
-20	1.32	1.25

These results indicate that at the smallest test Reynolds number the section maximum lift coefficients for both test specimens were about the same (figs. 14(b) and 22(b)). At the intermediate Reynolds number 1.84×10^6 the section maximum lift coefficient of the YR-4A no. 10 section was independent of internal pressure and equal to 1.25 (fig. 23(b)). The section maximum lift coefficient of the YR-4A no. 3 blade section varied from 1.15 with the blade at a positive internal pressure to 1.32 with the blade interior under suction (fig. 15(b)). Although the greatest maximum section lift coefficient for the YR-4A no. 10 section was less than the greatest for the YR-4A no. 3 section, the halving of the rib spacing eliminated the variation of maximum section lift coefficient with internal pressure.

Section lift-curve slope.- For the conditions of positive and zero internal-pressure difference the slope of the lift curve of the YR-4A no. 10 section divided by the slope of the lift curve of the YR-4A no. 3 section varied from 1.02 at the lowest to 1.08 at the highest Mach number. At negative internal pressures the difference between the slope of the lift curves was less than about 2 percent for all the test conditions.

Section drag coefficient.- The following table of section drag coefficients at $c_l = 0.4$ illustrates the difference in section drag coefficients obtained for the YR-4A no. 3 and YR-4A no. 10 models:

Internal pressure (in. H_2O)	YR-4A no. 3	YR-4A no. 10
$R = 0.91 \times 10^6$		
20	0.0125	0.0094
0	.0101	.0098
-20	.0115	.0101
$R = 1.84 \times 10^6$		
20	0.0115	0.0101
0	.0098	.0100
-20	.0105	.0103
$R = 2.58 \times 10^6$		
20	0.0122	0.0102
0	.0104	.0099
-20	.0106	.0102

These results indicate that halving the rib spacing reduced the variation of section drag coefficient with internal pressure to an almost negligible amount. Although not apparent from the values in the table which are for $c_l = 0.4$, the YR-4A no. 10 specimen at all internal pressures at the lower lift coefficients had about the same section drags as the YR-4A no. 3 had at the condition of zero internal-pressure difference (figs. 15(a) and 23(a)). When the internal pressure of the YR-4A no. 3 test section was greater or less than the free-stream static pressure by 20 inches of water the section drag coefficients were larger than those obtained at the condition of zero internal-pressure difference. The YR-4A no. 10 model at all internal pressures, therefore, had smaller section drag coefficients than those obtained for the YR-4A no. 3 model at internal pressures greater or less than the free-stream static pressure by 20 inches of water.

Section pitching-moment coefficient.- Halving the rib spacing reduced but did not eliminate the movement of

the aerodynamic center with change in dynamic pressure. The movement of the aerodynamic center during the tests was reduced from a movement between 26.2 and 20.6 percent of the chord for the YR-4A no. 3 (fig. 16(d)) to a movement between 25.0 and 22.6 percent of the chord for the YR-4A no. 10 (fig. 24(d)).

Comparison between the Aerodynamic Characteristics of a Fabric-Covered Model Having Half the Normal Rib Spacing and a Model Having Rigid Surfaces

To investigate the effect on the aerodynamic characteristics of changing the method of construction from the fabric-covered type with half the normal rib spacing to the plywood-covered type of construction the data for the YR-4A no. 10 fabric-covered section are compared with those for the XR-6 no. 5 plywood-covered model.

Section maximum lift coefficient.- A table giving the section maximum lift coefficients for the two test sections is given below:

R	YR-4A no. 10	XR-6 no. 5
0.92×10^6	1.13	1.14
1.78	1.25	1.19

At both the smallest and intermediate Reynolds numbers the fabric-covered YR-4A no. 10 section had slightly higher section maximum lift coefficients than the plywood covered XR-6 no. 5 section (figs. 22(b), 23(b), and 27(b)). The difference in section maximum lift coefficients, although small, was consistent and may have been caused by a slight difference in leading-edge radius between the two test sections.

Section lift-curve slope.- The section lift-curve slope was slightly greater for the YR-4A no. 10 model than for the XR-6 no. 5 model at both the suction and zero internal-pressure difference conditions. The difference increased from about 2 to about 7 percent of the lift-curve slope of the XR-6 no. 5 section as the test Mach number increased from the lowest to the highest. For a positive internal pressure of 20 inches of water

the YR-4A no. 10 model had a slope of the lift curve less than that of the XR-6 no. 5 section by about 7 percent at a Mach number of 0.262; at a Mach number of 0.376 the slopes were about the same.

Section drag coefficient.- In the range of moderate lift coefficients at the lowest Reynolds number the plywood-covered blade had about the same section drag coefficients as the lowest for YR-4A no. 10 (figs. 22(a) and 27(a)). At the intermediate Reynolds number the section drag coefficients for the XR-6 no. 5 section were lower than those for the YR-4A no. 10 section by approximately 0.0014 through the range of moderate lift coefficients (figs. 23(a) and 27(a)). At the highest Reynolds number the difference was about the same, approximately 0.0013 (figs. 24(a) and 27(a)). The XR-6 no. 5 plywood-covered blade thus had lower drags than the fabric-covered YR-4A no. 10 blade specimen. The difference in section drag coefficient was believed to be caused by a difference in the surface conditions between the two models.

Section aerodynamic center.- The XR-6 no. 5 plywood-covered section had a rigid surface and so its aerodynamic characteristics were obtained without any adjustment to its internal pressure. The maximum variation in the position of the aerodynamic center from the lowest to the highest Reynolds numbers was 1 percent from 24.7 percent of the chord to 23.7 percent of the chord (fig. 27(d)). The extreme movement of the aerodynamic center during the tests of the YR-4A no. 10 model was 2.4 percent of the chord from 25.0 to 22.6 percent of the chord (fig. 24(d)).

Effect on the Aerodynamic Characteristics of Smoothing the Forward Portion of the Airfoil

Section maximum lift coefficient.- Comparison of the data for the YR-4A no. 10 and YR-4A no. 10 (Smooth Forward Portion) indicates no important effect on maximum section lift coefficient.

Section lift-curve slope.- Smoothing and fairing the forward portion of the airfoil made no change in the slope of the lift curve.

Section drag coefficient.- At lift coefficients less than about 0.7 the airfoil with the smooth forward portion had less drag than the airfoil having the usual finish. The difference in section drag was about 0.0013 over part of the range of moderate lift coefficients at all Reynolds numbers for which comparable data are available.

Section aerodynamic center position.- The differences in the section aerodynamic center positions were small and were probably caused by slight changes in fabric tension rather than by changes in the surface of the forward portion of the model.

Aerodynamic Results Obtained for the Two XR-5 Test Specimens

The data in figure 29(b) for the XR-5(a) test section indicates a shift in the lift curve between the conditions of suction and zero internal-pressure difference and the condition of positive internal pressure. In addition, although the airfoil section was symmetrical, the lift at zero angle of attack was negative. The shift in the lift curve may be explained by a change in model contour during the tests. During the test at a Reynolds number of 2.40×10^6, it was noticed that the fabric on the upper surface had pulled away from the plywood which it covered and ballooned out, thereby changing the model contour. The fabric probably began to pull away from the wood during the test at a Reynolds number of 1.19×10^6 and a pressure difference of 20 inches of water. This probably explains the upward shift of the lift curve at $\alpha_0 = 0^\circ$ for the positive internal-pressure condition at $R = 1.19 \times 10^6$ because bulging fabric over the upper surface would be equivalent to an increase in airfoil camber. Because of the change in model contour caused by the bulging fabric, tests on the model were discontinued. The explanation for the apparent existence of negative lift at zero angle of attack is that the model was twisted in such a manner that zero angle of attack at the end used to set the angle corresponded to a negative angle of attack over most of the span.

The XR-5(b) model was not tested at internal pressure greater than the free-stream static pressure because it was found before beginning the tests that application of a small positive internal pressure caused the fabric to begin to tear away from the plywood which it covered and balloon out. The section drag coefficients in figure 33(a), for internal pressures less than and equal to that of the free-stream static pressure, have been plotted against the lift coefficients obtained at an internal pressure equal to that of the free stream. The data at the highest Reynolds number are incomplete because the fabric had loosened from the plywood enough to balloon out over the forward portion of the upper surface as mounted in the tunnel. Because of the change in model contour the tests were discontinued. External suctions over the forward portion of the upper surface at moderate and high lift coefficients during the tests at the lower Reynolds numbers had probably caused the fabric to tear away from the plywood. A partial explanation for the relatively low maximum lift coefficients obtained with the XR-5 sections is that the sections were about 10 percent thick whereas the others were about 12 percent thick.

This portion of the discussion is based on the data for the XR-5(b) model because the data obtained for the XR-5(a) twisted model may not be representative.

Maximum section lift coefficient.- The maximum section lift coefficient was lower than obtained in tests of the models using the NACA 0012 contour. The value of the maximum section lift coefficient varied from 0.87 at a Reynolds number of 1.20×10^6, to at least 1.05 at a Reynolds number of 3.16×10^6. Although part of the increase in maximum section lift may have been caused by the fabric leaving the upper surface of the forward portion of the airfoil, it appears probable that this effect was small. An increase in the effective camber would normally show itself in an upward shift of the lift curve if the camber increase were independent of angle of attack or in an abnormally large slope of the lift curve if the camber increased with angle of attack. The upward shift of the section lift curve was only 0.04 and the section lift curve did not have an abnormally large slope. Thus, the effect of a change in the airfoil contour was probably small and most of the effect appears to have been caused by Reynolds number.

Section lift-curve slope.- The slope of the lift curve was slightly less than that of the other models and showed no abnormal increase with Mach number.

Section drag coefficient.- The section drag coefficient was low at zero lift at the lowest Reynolds number but increased at higher lift coefficients and Reynolds numbers until it was no lower than the section drag coefficients obtained for the YR-4A no. 10 model. The low values of the maximum lift coefficient caused the section drag to increase to large values at lower values of the section lift coefficient than for the other models.

Section aerodynamic center position.- The aerodynamic center was at the quarter-chord point for all the tests at internal pressures less than and equal to that of the free-stream static pressure. Because the XR-5(b) model was not tested with internal pressures greater than that of the free stream, no data on the effect of positive internal pressures on the position of the aerodynamic center are available.

Comparison of Aerodynamic Data for the Test Specimens with that Obtained for a Smooth and Fair NACA 0012 Airfoil Section

For purposes of comparison, data for a smooth and fair NACA 0012 airfoil have been included in figure 37. Pitching moments were not obtained during the test of the smooth and fair airfoil.

Maximum section lift coefficient.- The Mach numbers for most of the present tests at Reynolds numbers close to 1.8 million are approximately 0.260. In spite of the unfavorable effect of Mach number on maximum lift coefficient at Mach numbers larger than about 0.170 (reference 4) the test specimens had maximum lift coefficients which were fairly close to that obtained for the smooth and fair section at a Reynolds number of 1.79 million and a Mach number of 0.130.

Section lift-curve slope.- The slope of the lift curves for all the models at zero internal-pressure

difference and a Mach number of 0.130 were just about the same as that for the smooth and fair airfoil.

Section drag coefficient.- The section drag coefficients of the fair and smooth NACA 0012 airfoil were smaller than those obtained for any of the NACA 0012 test specimens, including those covered with plywood. The difference in section drag between the plywood covered and the smooth and fair section varied between approximately 0.0005 and 0.0025; the largest differences occurred in the range of moderate lift coefficients. In figure 37 the drag curve for the XR-6 no. 5 model at $R = 1.78 \times 10^6$ has been included for comparison.

YR-4A no. 1 and XR-6 no. 2 Blade Tip Sections

The angle of attack given in the data for the two tip sections is the geometric angle of attack at the root of the model. Because of the finite span, trailing vortices were present at all angles at which any portion of the models had lift. These vortices produced vertical velocities at the models that caused the aerodynamic angle of attack to vary along the span.

For some high drag conditions at the higher tunnel dynamic pressures the deflections in the manometer used to measure drag exceeded the range of the instrument. Therefore, the drag coefficients at these points could not be obtained. These points are indicated in the tables by an asterisk. When the variation of drag coefficient along the span, at a particular angle of attack, does not change much from the lower to the higher test Reynolds numbers, the profile-drag coefficients at the missing points may be estimated from the values at the lowest Reynolds number.

The large spanwise variation of section drag coefficient of the YR-4A no. 1 tip section (fig. 34) was probably caused in part by the type of model surface, ribs and fabric, and partly by the variation of lift coefficient along the span. The lift coefficient varied over the span of the model because of the geometric twist of about 2° (table I) and because of the usual variation of angle of attack along the span of a finite span model. As the angle of attack increased the spanwise variation

of section drag coefficient also increased. With increasing angle of attack the boundary layer over the upper surface became thick and therefore was more easily deflected in a spanwise direction by any pressure gradients which were present. Such spanwise pressure gradients could be caused by the variation of lift along the span and by local changes in airfoil contour such as protruding ribs and bumps.

The spanwise variation of section drag coefficient for the XR-6 no. 2 plywood-covered tip section (fig. 35) was less than for the YR-4A no. 1 tip section. The major reason was probably the comparatively good surface finish of the XR-6 no. 2 tip section.

The peak in profile-drag coefficient near the tip of the models is probably caused by the tip vortex deflecting the boundary layer from a portion of the model into a small spanwise region. Regions in which the boundary layer has been deflected spanwise usually are characterized by alternating regions of high and low drag. The regions of high drag represent regions into which the boundary layer has flowed from the regions which appear as low drag regions.

The pressure transmitted into the model interior by the various vent holes are shown in figure 36. The change in $\Delta p/q$ with angle of attack decreased as the vent hole was moved toward the trailing edge because the change in pressure with angle of attack at a point on an airfoil decreases as the point moves toward the trailing edge. The curves of $\Delta p/q$ versus α are almost straight lines up to an angle of attack of 16° at $R = 0.74 \times 10^6$ and 18° at $R = 1.46 \times 10^6$. The angles of attack at which the curves suddenly change character are probably the angles at which the tip region of the model stalled. The data obtained for the tip vent indicate a very large variation of $\Delta p/q$ with angle of attack. The curves for the tip vent undergo a sudden change in character at the same angles as the chord vents, 16° at $R = 0.74 \times 10^6$ and 18° at $R = 1.46 \times 10^6$. The curve of $\Delta p/q$ reaches a maximum at approximately 3° instead of, as would be expected, at 0°. The model twist of about 2° from root to the tip region accounts for most of the difference.

CONCLUSIONS

The data obtained for the models tested indicated the following conclusions:

1. The aerodynamic characteristics of the fabric-covered models were markedly affected by variations of pressure. Usually, the most desirable pressure in the hollow rear portion of the model was one equal to the free-stream static pressure. An internal pressure greater than that of the free stream usually produced an increase in section drag coefficient, a decrease in maximum section lift coefficient, and a forward movement of the aerodynamic center. An internal pressure less than that of the free-stream static pressure usually produced a slight increase in section drag coefficient, a slight increase in maximum section lift coefficient, and a slight rearward movement of the aerodynamic center.

2. The effect of model internal pressure on the aerodynamic characteristics increased as the test dynamic pressure increased.

3. Halving the rib spacing of a fabric-covered model made the aerodynamic characteristics less sensitive to the model internal pressure.

4. Blades having plywood surfaces had maximum section lift coefficients no higher than those of fabric-covered models and drag coefficients about 0.0013 less than those of the best fabric-covered models.

5. The effect of smoothing and fairing the forward third of a typical fabric-covered test section was to reduce the section drag coefficient by about 0.0013 in the range of moderate lift coefficients.

6. Comparison of the data obtained for the practical-construction models, at internal pressures equal to and less than that of the free-stream static pressure, with those for a smooth and fair NACA 0012 airfoil section indicated no important differences in the maximum section lift coefficient. The drag coefficients for the smooth and fair NACA 0012 airfoil section were lower than the lowest obtained for the practical-construction NACA 0012 models by an amount which increased from 0.0005 to 0.0025 as the magnitude of the lift coefficient increased from zero to moderate values.

7. The effect of adding a leading-edge abrasion strip was to reduce the section drag coefficient by about 0.0008 in the range of moderate lift coefficients for zero internal-pressure difference.

8. Models which had approximately the NACA 0010-64 airfoil section had section maximum lift coefficients about 0.3 less than those obtained on airfoils built to represent the NACA 0012 airfoil section.

9. Measurements of internal pressures for vent holes located on the lower surface of the fabric-covered tip section, inboard of the tip, indicated pressures less than the free-stream static pressure at all angles of attack except the highest and a variation of pressure with angle of attack that decreased as the vent was moved toward the trailing edge. The internal static pressures for a vent placed in the extreme tip of the blade were less than that of the free stream throughout the range of angles of attack and the variation with angle of attack was very large. The values of the measured static pressure ranged from 35 percent to 230 percent of the free-stream dynamic pressure beneath that of the free-stream static pressure.

10. Measurements of the spanwise variation of section drag coefficient along the span of the two tip sections indicated a peak in the section drag coefficient about 3 inches from the blade tip that increased with increase in angle of attack.

Langley Memorial Aeronautical Laboratory
National Advisory Committee for Aeronautics
Langley Field, Va., September 6, 1944

REFERENCES

1. Stack, John, and von Doenhoff, Albert E.: Tests of 16 Related Airfoils at High Speeds. NACA Rep. No. 492, 1934.

2. Jacobs, Eastman N., Abbott, Ira H., and Davidson, Milton: Preliminary Low-Drag-Airfoil and Flap Data from Tests at Large Reynolds Numbers and Low Turbulence, and Supplement. NACA ACR, March 1942.

3. Davis, Wallace F.: Comparison of Various Methods for Computing Drag from Wake Surveys. NACA ARR, Jan. 1943.

4. Muse, Thomas C.: Some Effects of Reynolds and Mach Numbers on the Lift of an NACA 0012 Rectangular Wing in the NACA 19-Foot Pressure Tunnel. NACA CB No. 3E29, 1943.

5. Jacobs, Eastman N., and Sherman, Albert: Airfoil Section Characteristics as Affected by Variations of the Reynolds Number. NACA Rep. No. 586, 1937.

6. Glauert, H.: The Effect of Compressibility on the Lift of an Airfoil. R. & M. No. 1135, British A.R.C., 1927. (Also Proc. Roy. Soc. (London), ser. A, vol. 118, no. 779, March 1, 1928, pp. 113-119.)

7. Kaplan, Carl: Compressible Flow about Symmetrical Joukowski Profiles. NACA Rep. No. 621, 1938.

TABLE I

Model	Variation of Chord Along Span (Inches)	Construction	Rib Spacing, Inches: Large Chord End	Center Portion of Span	Small Chord End	Type of Leading Edge	Finish Over Forward Third of Model	Finish Over Rear Two-Thirds of Model	Remarks
YR-4A No. 1 Tip Section	See Figure 12	Forward third solid wood, ribs to rear. Entire assembly fabric-covered	Rib spacing varied from $3\frac{3}{8}$ to $3\frac{1}{2}$			Unpainted metal abrasion strip	Fabric grain apparent. Local nicks and bumps	Fabric grain apparent. Bumpy over ribs	Model received with twist along span. Tip region at geometric angle of attack about 2° less than root, as mounted in tunnel
YR-4A No. 3	Linear from $10\frac{5}{16}$ to $13\frac{1}{4}$	"	$4\frac{3}{8}$	4	$3\frac{3}{4}$	Painted metal abrasion strip	Local ridges at joint of abrasion strip and airfoil proper. Fabric grain apparent	Smooth between ribs, bumpy over ribs	
YR-4A No. 4	Linear from $10\frac{5}{16}$ to $13\frac{1}{8}$	"	$4\frac{3}{8}$	4	$3\frac{1}{2}$	No abrasion strip	Rough to touch. Fabric grain apparent	"	
YR-4A No. 6	Linear from $13\frac{15}{16}$ to $16\frac{15}{16}$	"	5	5	5	Half span unpainted metal abrasion strip	Fabric grain apparent	Fabric grain apparent to touch; bumpy over ribs	Vertical slots in leading-edge abrasion strip filled
YR-4A No. 10	Linear from $10\frac{5}{16}$ to $13\frac{5}{16}$	"	$2\frac{1}{4}$	2	$1\frac{3}{4}$	Unpainted metal abrasion strip	"	Bumpy and rough	
YR-4A No. 10 (Smooth Forward Portion)	"	"	"	"	"	---	---	"	Forward third faired to NACA 0012 contour with pyroxylin glazing putty and sanded. Smooth to touch except for local bumps
XR-6 No. 2 Tip Section	See Figure 12	Rigid wood surface. Outer layer of fabric for about forward 20 percent of chord	--	--	--	Small fabric-covered metal strip	Fabric grain apparent over leading edge	Smooth except for local nicks and bumps	Upper surface, as mounted in tunnel, lightly sanded before beginning tests
XR-6 No. 5	Linear from $10\frac{5}{16}$ to $13\frac{3}{16}$	"	--	--	--	"	"	"	
XR-6 No. 7	Linear from 14 to $16\frac{13}{16}$	"	--	--	--	"	Fabric grain apparent in leading-edge region	"	
XR-5 (a)	Linear from $13\frac{5}{8}$ to $17\frac{3}{16}$	One surface 50 percent wood, other 100 percent. Ribs for rear 72 percent of chord. Entire assembly fabric-covered	$3\frac{1}{2}$	$3\frac{1}{4}$	3	No abrasion strip	Fabric grain apparent, local bumps	Fabric grain apparent, local bumps. Bumpy over ribs	50-percent wood surface upper surface in tunnel. Model received with most of span twisted to negative angle of attack as mounted in tunnel
XR-5 (b)	Linear from $13\frac{5}{8}$ to $17\frac{5}{16}$	Both surfaces 50 percent wood. Ribs for rear 72 percent of chord. Entire assembly fabric-covered	$3\frac{3}{4}$	$3\frac{1}{4}$	3	"	"	"	

TABLE II

LIST OF TESTS

L - Lift, D - Drag, M - Pitching Moment

Model	Chord Used to Calculate Reynolds Number (Inches)	Portion of Span Over Which Drag Was Taken		Model Internal Pressure Inches of Water. Referred to free-stream static pressure	R × 10^{-6}	M	Dynamic pressure, q. lbs/sq ft.	Characteristics Measured
		Left of Center Line, Inches	Right of Center Line, Inches					
YR-4A No. 1 Tip Section	10.0	Outer portion of tip		0, ±20 0, ±20 0, ±20	0.74 1.46 2.09	0.130 0.260 0.375	26.0 102 209	D D D
YR-4A No. 3	11.7	4	4	0, ±20 0, ±20 0, ±20	0.91 1.84 2.58	0.131 0.262 0.375	26.0 102 210	L, D, M L, D, M L, D, M
YR-4A No. 4	11.7	4	4	0, ±20	1.87	0.261	102	L, D, M
YR-4A No. 6	15.4	5	5	0, ±20 0, ±20 0, ±20 0, ±20	1.72 2.42 2.93 3.20	0.181 0.262 0.322 0.366	56.3 102 156 201	L, D, M L, D, M L, D, M L, D, M
YR-4A No. 10	11.7	4	4	0, ±20 0, ±20 0, ±20	0.91 1.84 2.59	0.131 0.262 0.376	26.0 102 209	L, D, M L, D, M L, D, M
YR-4A No. 10 (Smooth Forward Portion)	11.7	4	4	0, -20 0, -20	1.84 2.59	0.262 0.375	102 210	L, D, M L, D, M
XR-6 No. 2 Tip Section	10.0	Outer portion of tip		Rigid surface. Internal pressure not adjusted.	0.74 1.46 2.09	0.130 0.260 0.375	26.0 102 209	D D D
XR-6 No. 5	11.7	4	4	Rigid surface. Internal pressure not adjusted.	0.92 1.78 2.68	0.131 0.262 0.375	26.0 102 210	L, D, M L, D, M L, D, M
XR-6 No. 7	15.4	4	4	Rigid surface. Internal pressure not adjusted.	1.21 2.23 3.46	0.131 0.262 0.376	26.0 102 210	L, D, M L, D, M L, D, M
XR-5 (a)	15.4	5	5	0, ±20 +20 0	1.19 2.40 2.40	0.131 0.261 0.261	26.0 102 102	L, D, M L, D, M L, D
XR-5 (b)	15.4	5	5	0, -20 0, -20 0 -20	1.20 2.30 3.16 3.16	0.136 0.262 0.373 0.373	26.0 102 201 201	L, D, M L, D, M L, D, M D

TABLE III

LIST OF REPAIRS

Model	Repairs
YR-4A No. 1 Tip Section	No repairs.
YR-4A No. 3	No repairs.
YR-4A No. 4	No repairs.
YR-4A No. 6	Cracks in fabric along ribs near trailing edge. Fabric split at trailing edge. Dope applied to cracks. Strip of aircraft tape applied to trailing edge and doped in place between runs at $R = 2.93 \times 10^6$ and $R = 3.20 \times 10^6$. (See photograph.) Fabric tension decreased during tests.
YR-4A No. 10	Local cracks in fabric. Repaired by applying dope.
YR-4A No. 10 (Smooth Forward Portion)	Local cracks in fabric repaired with dope. Fabric split on one surface on center line of model. Piece of aircraft fabric doped over split.
XR-6 No. 2 Tip Section	No repairs.
XR-6 No. 5	No repairs.
XR-6 No. 7	End rib began to work loose from main portion of span; reinforced. (See photograph.)
XR-5 (a)	No repairs.
XR-5 (b)	No repairs.

TABLE IV (a)

SPANWISE VARIATION OF DRAG COEFFICIENT FOR THE YR-4A NO. 1 HELICOPTER BLADE TIP SECTION

NATIONAL ADVISORY COMMITTEE FOR AERONAUTICS

L, Distance inboard from blade tip, inches
α, Angle of attack, degrees

Test Conditions: R = 0.74×10^6, M = 0.130, internal pressure, +20 inches of water

L \ α	-4°	-2°	0°	2°	4°	6°	8°	10°	12°	14°	16°	18°	20°
2	0.0089		0.0101		0.0032		0.0114		0.0128		0.0670		0.0714
3	.0073		.0046		.0047		.0100		.0419		.2420		.1596
4	.0109		.0134		.0060		.0126		.0079		.0139		.0658
5	.0090		.0065		.0085		.0120		.0187		.0182		.0402
6	.0074		.0115		.0129		.0144		.0218		.0128		.0554
7	.0111		.0082		.0088		.0139		.0102		.0118		.0722
8	.0161		.0077		.0079		.0109		.0156		.0153		.0918
9	.0136		.0082		.0079		.0097		.0127		.0138		.1180
10	.0096		.0101		.0100		.0082		.0170		.0184		.1461
11	.0150		.0109		.0099		.0076		.0179		.0190		.1620

Test Conditions: R = 0.74×10^6, M = 0.130, internal pressure, 0 inches of water

1									0.0119	0.0210	0.0269	0.0191	0.0430
2	0.0132	0.0097	0.0180	0.0048	0.0090	0.0097	0.0123	0.0210	.0210	.0298	.0393	.0337	.0149
3	.0180	.0130	.0050	.0068	.0050	.0066	.0096	.0380	.1021	.1385	.1625	.1204	.0240
4	.0102	.0131	.0107	.0070	.0072	.0043	.0065	.0052	.0220	.0302	.0473	.0367	.0518
5	.0077	.0067	.0077	.0069	.0079	.0107	.0084	.0107	.0154	.0112	.0705	.0289	.0418
6	.0084	.0097	.0112	.0117	.0110	.0148	.0087	.0153	.0098	.0089	.0151	.0401	.0556
7	.0101	.0078	.0090	.0140	.0139	.0150	.0157	.0071	.0046	.0115	.0120	.0499	.0750
8	.0110	.0099	.0092	.0078	.0079	.0090	.0090	.0105	.0100	.0116	.0118	.0641	.0983
9	.0086	.0092	.0086	.0086	.0092	.0092	.0100	.0105	.0184	.0120	.0145	.0808	.1231
10	.0096	.0100	.0104	.0104	.0104	.0104	.0104	.0125	.0130	.0171	.0214	.0954	.1434
11	.0109	.0104	.0089	.0087	.0104	.0128	.0154	.0158	.0183	.0193	.0264	.1124	.1550

Test Conditions: R = 0.74×10^6, M = 0.130, internal pressure, -20 inches of water

0							0.0015		0.0040				0.0051
1	0.0056		0.0030				.0077		.0179		0.0259		.0328
2	.0077		.0111		.0096		.0100		.0151		.0324		.0467
3	.0128		.0043		.0065		.0095		.0140		.2745		.2068
4	.0093		.0123		.0053		.0078		.0101		.0292		.0593
5	.0093		.0069		.0090		.0093		.0110		.0216		.0511
6	.0076		.0124		.0112		.0143		.0229		.0152		.0532
7	.0113		.0086		.0149		.0136		.0094		.0083		.0652
8	.0100		.0094		.0092		.0078		.0081		.0095		.0938
9	.0100		.0099		.0109		.0094		.0087		.0125		.1182
10	.0105		.0104		.0109		.0117		.0219		.0327		.1499
11	.0144		.0111		.0096		.0141		.0186		.0282		.1484

TABLE IV (b)

NATIONAL ADVISORY COMMITTEE FOR AERONAUTICS

Test Conditions: $R = 1.46 \times 10^6$, $M = 0.280$, internal pressure, +20 inches of water

L \ α	-4°	-2°	0°	4°	8°	12°	14°	16°	20°
- 4								0.0021	0.0008
- 3								.0028	.0009
- 2						0.0010		.0029	.0017
- 1					0.0012	.0020		.0043	.0031
0				0.0004	.0019	.0032		.0053	.0099
1	0.0042		0.0013	.0014	.0031	.0099		.0279	.0242
2	.0239		.0162	.0094	.0153	.0232		.0600	.1431
3	.0201		.0061	.0064	.0072	.0281		*	.0691
4	.0064		.0129	.0065	.0083	.0090		.0093	.0348
5	.0102		.0078	.0082	.0113	.0102		.0171	.0357
6	.0086		.0119	.0129	.0115	.0106		.0160	.0609
7	.0077		.0087	.0127	.0077	.0114		.0095	.0603
8	.0087		.0097	.0083	.0080	.0126		.0136	.0799
9	.0154		.0115	.0112	.0146	.0166		.0180	.1010
10	.0133		.0099	.0111	.0128	.0148		.0233	.1313
11	.0108		.0135	.0096	.0091	.0110		.0188	.1526

Test Conditions: $R = 1.46 \times 10^6$, $M = 0.280$, internal pressure, 0 inches of water

0					0.0014		0.0049	0.0080	0.0116
1	0.0035		0.0016	0.0003	.0028	0.0123	.0228	.0204	.0346
2	.0112		.0125	.0117	.0136	.0255	.0309	.0701	.1133
3	.0291		.0059	.0064	.0093	*	*	*	*
4	.0067		.0128	.0060	.0095	.0128	.0271	.0186	.0417
5	.0091		.0074	.0092	.0089	.0119	.0194	.0144	.0388
6	.0083		.0119	.0114	.0072	.0169	.0064	.0069	.0468
7	.0096		.0092	.0148	.0175	.0070	.0085	.0093	.0575
8	.0096		.0101	.0082	.0085	.0111	.0143	.0129	.0746
9	.0106		.0095	.0092	.0091	.0099	.0174	.0174	.0984
10	.0115		.0097	.0085	.0110	.0170	.0153	.0196	.1201
11	.0126		.0081	.0110	.0152	.0161	.0156	.0192	.1477

Test Conditions: $R = 1.46 \times 10^6$, $M = 0.280$, internal pressure, -20 inches of water

- 4								0.0021	0.0017
- 3								.0030	.0023
- 2						0.0184		.0034	.0023
- 1						.0040		.0053	.0024
0	0.0001		0.0001		0.0021	.0052		.0080	.0098
1	.0032	0.0021	.0025	.0007	.0023	.0143		.0140	.0363
2	.0195	.0125	.0138	.0126	.0122	.0268		.0580	.0883
3	.0241	.0119	.0056	.0061	.0124	.0723		*	.1839
4	.0064	.0142	.0135	.0065	.0101	.0130		.0498	.0516
5	.0091	.0084	.0076	.0092	.0075	.0114		.0365	.0414
6	.0080	.0090	.0127	.0098	.0175	.0265		.0154	.0471
7	.0130	.0088	.0093	.0185	.0156	.0085		.0090	.0566
8	.0104	.0115	.0108	.0088	.0079	.0085		.0094	.0941
9	.0105	.0096	.0100	.0105	.0095	.0085		.0116	.1244
10	.0110	.0105	.0106	.0106	.0132	.0233		.0339	.1329
11	.0103	.0104	.0088	.0113	.0145	.0171		.0237	.1759

* Drag-off scale of drag indicator

NATIONAL ADVISORY COMMITTEE FOR AERONAUTICS

TABLE IV (c)

Test Conditions: $R = 2.09 \times 10^6$, $M = 0.375$, internal pressure, +20 inches of water

L \ α	-4°	0°	4°	8°
-1				0.0015
0			0.0004	.0018
1	0.0030		.0011	.0031
2	.0134	0.0175	.0103	.0156
3	.0205	.0062	.0069	.0080
4	.0067	.0134	.0081	.0092
5	.0110	.0100	.0086	.0105
6	.0108	.0135	.0141	.0122
7	.0083	.0091	.0145	.0097
8	.0099	.0103	.0097	.0089
9	.0165	.0109	.0125	.0097
10	.0160	.0129	.0125	.0166
11	.0126	.0122	.0097	.0082

Test Conditions: $R = 2.09 \times 10^6$, $M = 0.375$, internal pressure, 0 inches of water

L \ α				
-1				0.0012
0		0.0023		.0018
1	0.0021	.0183		.0025
2	.0133	.0060	.0112	.0150
3	*	*	.0068	.0110
4	.0068	.0131	.0082	.0097
5	.0100	.0090	.0094	.0101
6	.0091	.0070	.0118	.0093
7	.0096	.0088	.0164	.0172
8	.0103	.0110	.0091	.0085
9	.0127	.0115	.0100	.0092
10	.0130	.0122	.0107	.0140
11	.0129	.0112	.0213	.0171

Test Conditions: $R = 2.09 \times 10^6$, $M = 0.375$, internal pressure, -20 inches of water

L \ α				
-1				0.0014
0	0.0002			.0021
1	.0043	0.0015	0.0010	.0026
2	.0171	.0161	.0137	.0119
3	.0223	.0058	.0064	.0175
4	.0072	.0136	.0070	.0096
5	.0103	.0076	.0093	.0086
6	.0084	.0131	.0103	.0187
7	.0116	.0100	.0149	.0176
8	.0121	.0114	.0085	.0082
9	.0115	.0113	.0106	.0090
10	.0131	.0119	.0087	.0133
11	.0152	.0104	.0132	.0188

* Drag-off scale of drag indicator

TABLE V

SPANWISE VARIATION OF DRAG COEFFICIENT FOR THE XR-6 NO. 2 HELICOPTER BLADE TIP SECTION

L, Distance inboard from blade tip, inches
α, Angle of attack, degrees

NATIONAL ADVISORY COMMITTEE FOR AERONAUTICS

Test Conditions: $R = 0.74 \times 10^6$, $M = 0.130$

L \ α	-4°	-2°	0°	2°	4°	6°	8°	10°	12°	14°	16°	18°	20°
-3									0.0031	0.0086	0.0016	0.0029	
-2									.0031	.0052	.0060	.0035	0.0029
-1								0.0034	.0040	.0060	.0075	.0080	.0058
0	0	0	0	0	0	0	0	.0054	.0074	.0125	.0296	.0390	.0265
1	.0063	.0045	0	.0040	.0098	.0112	.0188	.0228	.0236	.0175	.0220	.0652	.1331
2	.0197	.0040	.0069	.0050	.0171	.0195	.0217	.0413	.0513	.0789	.1142	.2470	.2409
3	.0048	.0067	.0074	.0064	.0071	.0150	.0248	.0316	.0800	.1902	.2480	.2092	.3587
4	.0075	.0069	.0079	.0067	.0073	.0079	.0055	.0085	.0102	.0102	.0135	.0710	.3387
5	.0079	.0087	.0076	.0068	.0063	.0071	.0091	.0104	.0100	.0095	.0085	.0437	.1645
6	.0079	.0079	.0079	.0074	.0080	.0095	.0096	.0111	.0126	.0115	.0132	.0296	.1774
7	.0084	.0084	.0083	.0078	.0080	.0098	.0110	.0122	.0126	.0134	.0149	.0527	.1107
8	.0088	.0086	.0089	.0096	.0087	.0100	.0116	.0125	.0126	.0158	.0167	.0604	.1440
9	.0101	.0089	.0093	.0095	.0104	.0105	.0130	.0135	.0144	.0162	.0182	.0730	.1636
10	.0101	.0084	.0084	.0094	.0109	.0129	.0129	.0149	.0164	.0179	.0202	.1050	.1353
11	.0105	.0086	.0084	.0086	.0111	.0139	.0133	.0153	.0169	.0189	.0222	.0921	.1829
12	.0106	.0091	.0078	.0089	.0116	.0100	.0138						

Test Conditions: $R = 1.46 \times 10^6$, $M = 0.280$

L \ α	-4°	-2°	0°	2°	4°	6°	8°	10°	12°	14°	16°	18°	20°
-4									0.0016		0.0031		0.0024
-3							0.0012		.0027		.0041		.0029
-2					0.0005		.0009		.0026		.0031		.0049
-1	0.0003				.0008		.0016		.0039		.0124		.0020
0	.0012		0		.0008		.0031		.0073		.0378		.0240
1	.0036		.0021		.0041		.0153		.0255		.0471		.0452
2	.0181		.0050		.0145		.0227		.0687		*		*
3	.0035		.0061		.0064		.0216		*		*		*
4	.0069		.0085		.0056		.0092		.0073		.0134		.0385
5	.0076		.0085		.0085		.0073		.0096		.0134		.0567
6	.0088		.0081		.0085		.0118		.0108		.0120		.0543
7	.0095		.0099		.0087		.0078		.0101		.0132		.0761
8	.0102		.0104		.0098		.0083		.0118		.0156		.1011
9	.0108		.0090		.0107		.0127		.0127		.0173		.1199
10	.0111		.0086		.0094		.0120		.0139		.0200		.1497
11	.0106		.0083		.0101		.0120		.0156		.0220		.1946

Test Conditions: $R = 2.09 \times 10^6$, $M = 0.375$

L \ α	-4°	-2°	0°	2°	4°	6°	8°	10°	12°	14°	16°	18°	20°
-1	0.0001						0.0020						
0	.0005		0.0003		0.0011		.0032						
1	.0039		.0011		.0034		.0161						
2	.0141		.0059		.0127		.0209						
3	.0047		.0083		.0088		.0122						
4	.0082		.0103		.0054		.0107						
5	.0090		.0101		.0092		.0102						
6	.0095		.0093		.0105		.0087						
7	.0102		.0103		.0090		.0094						
8	.0110		.0112		.0107		.0128						
9	.0112		.0103		.0110		.0105						
10	.0108		.0090		.0105		.0117						
11	.0108		.0098		.0118		.0120						

* Drag-off scale of drag indicator

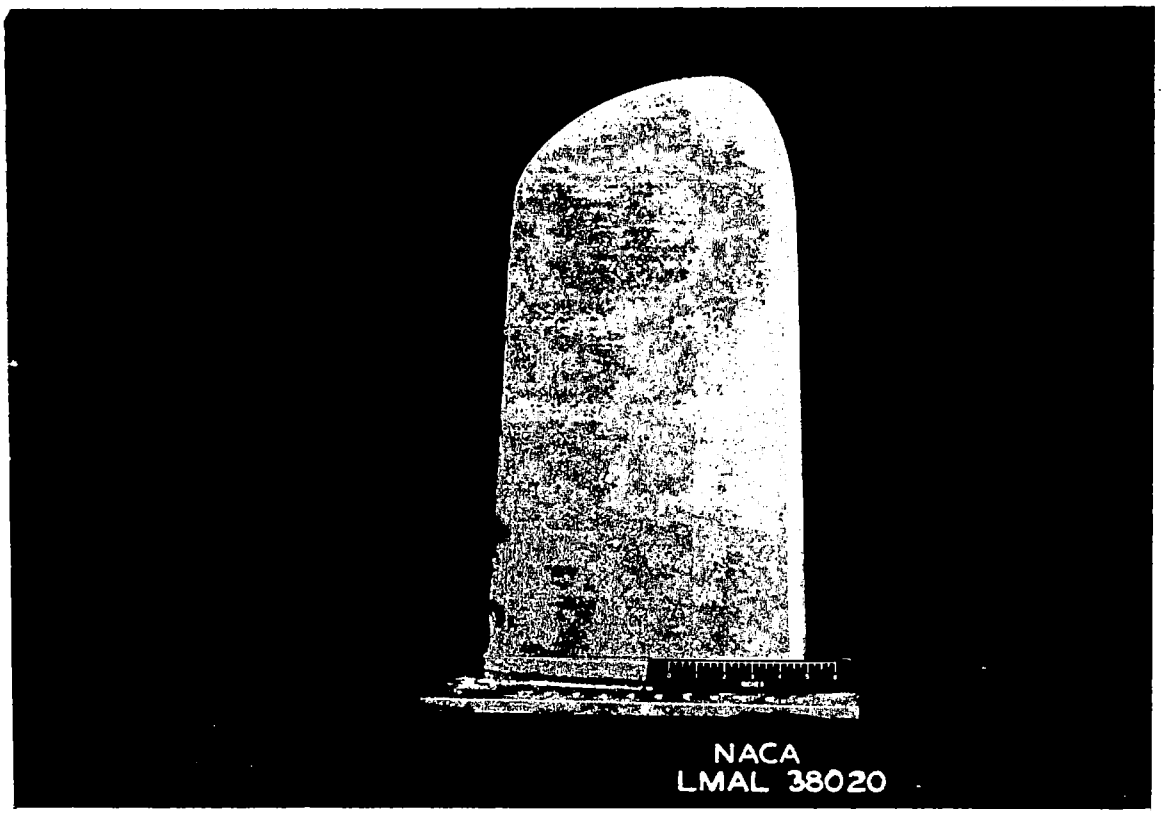

(a) Upper surface upon completion of tests.

Figure 1.- Photograph of YR-4A No. 1 tip section.

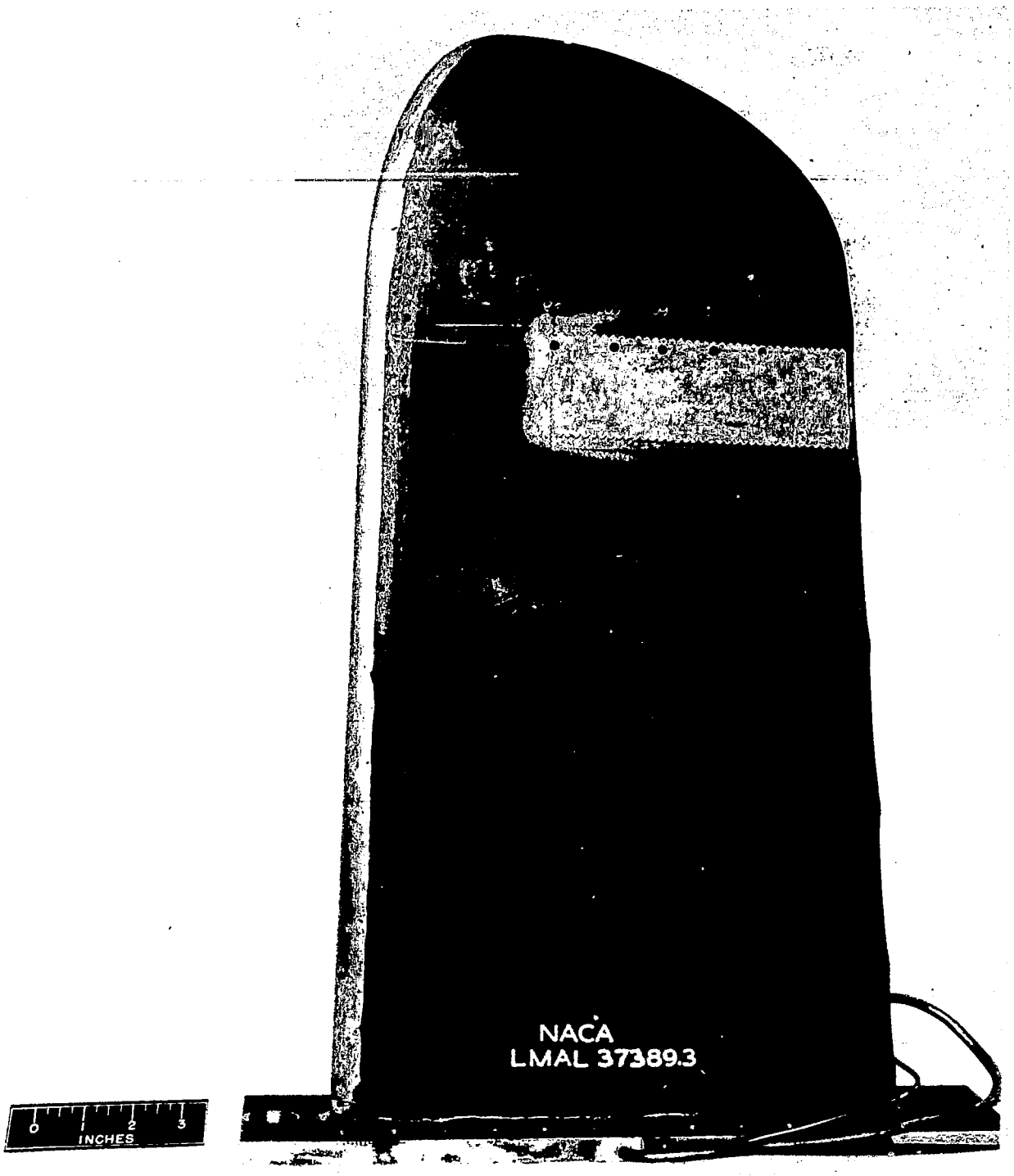

(b) Lower surface upon completion of tests.

Figure 1.- Concluded.

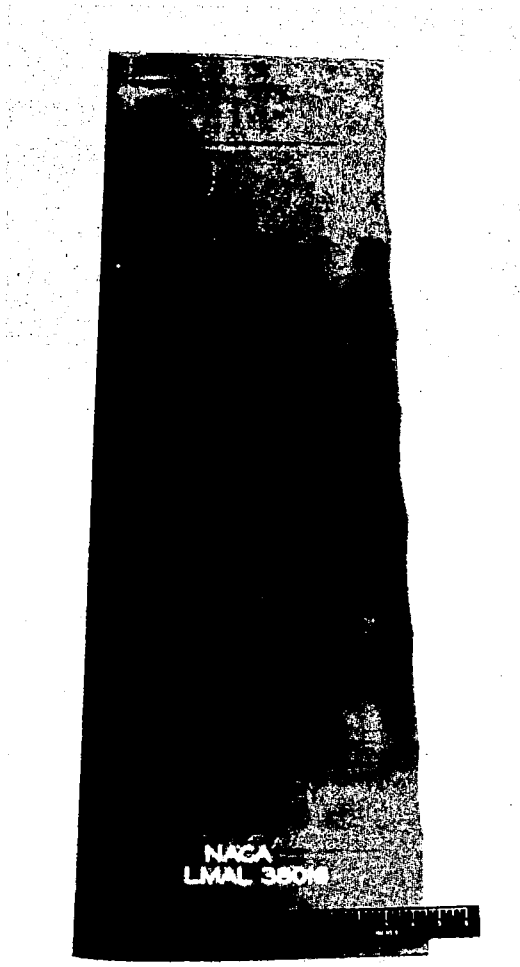

Lower surface upon completion of tests.

Figure 2.- Photograph of YR-4A No. 3 helicopter test specimen.

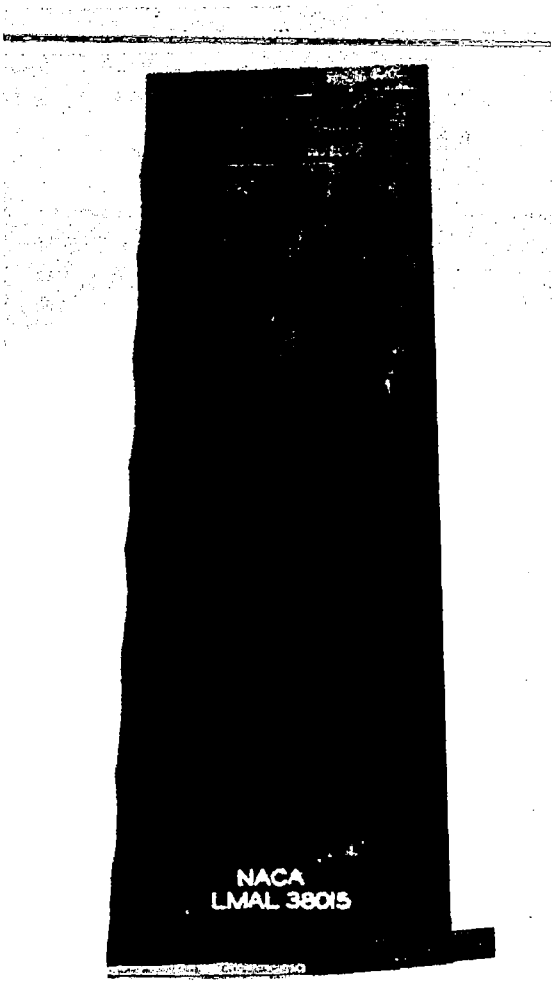

Upper surface upon completion of tests.

Figure 3.- Photograph of YR-4A No. 4 helicopter test specimen.

L-643

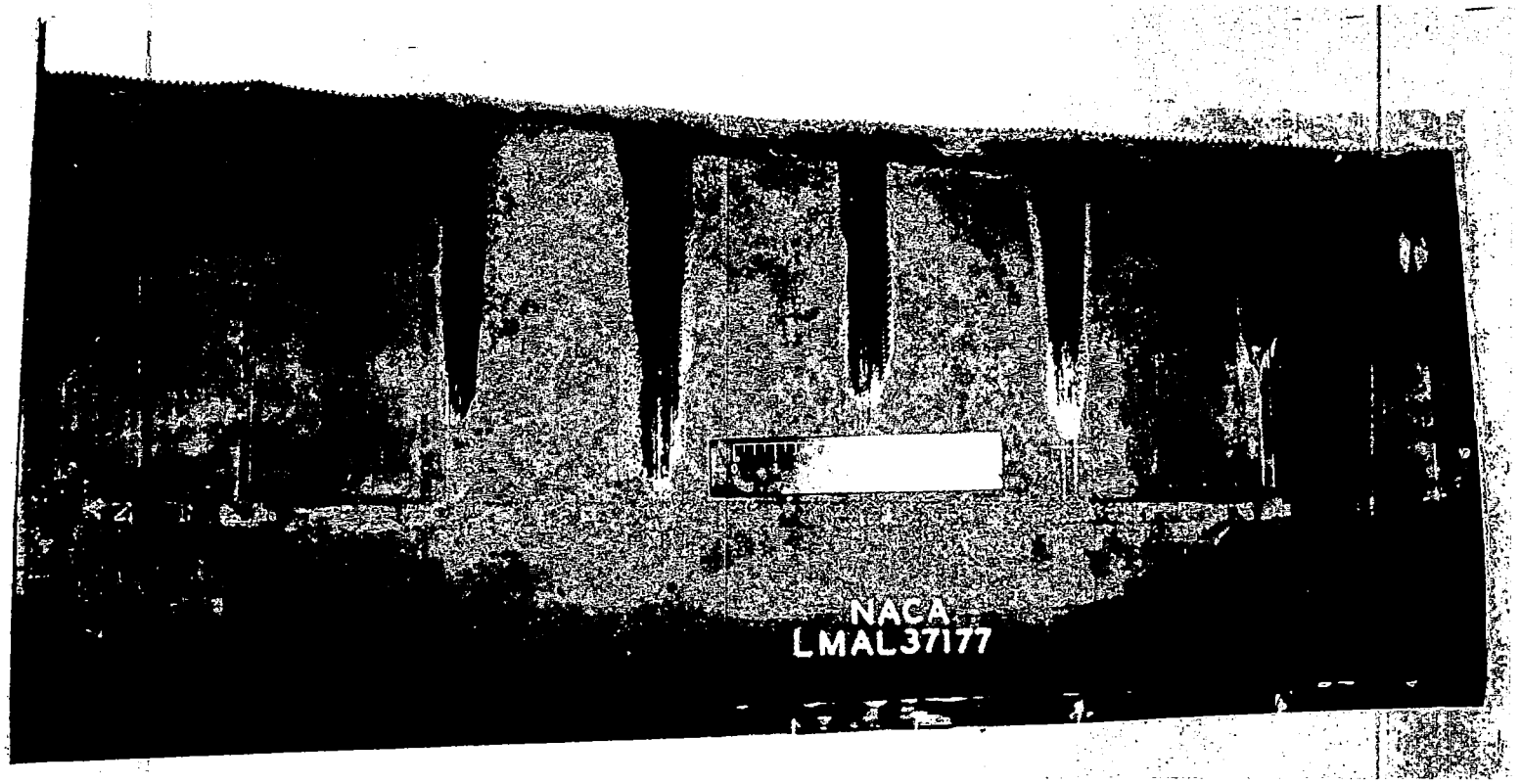

(a) Upper surface upon completion of tests.

Figure 4.- Photograph of YR-4A No. 6 helicopter test specimen.

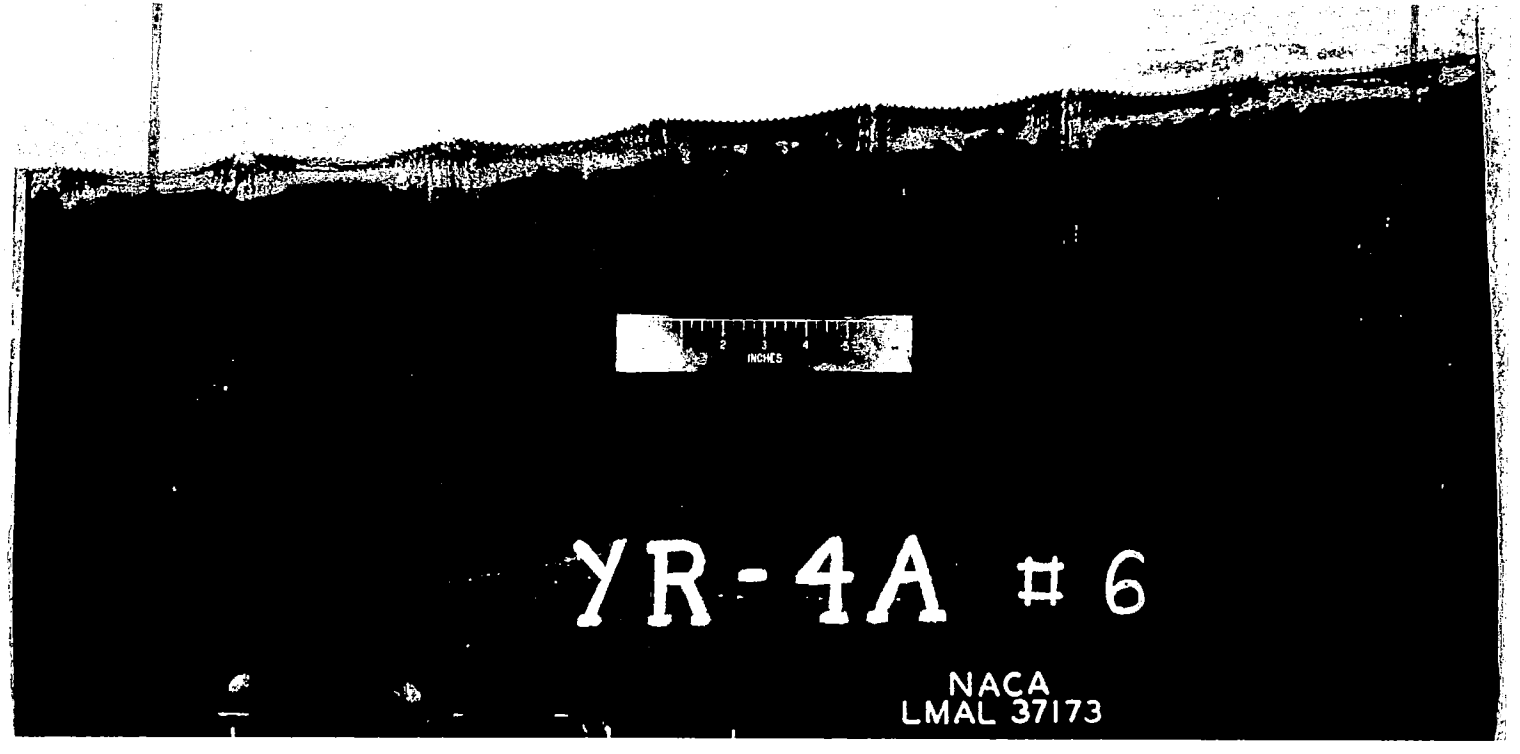

(b) Lower surface upon completion of tests.

Figure 4.- Concluded.

Upper surface upon completion of tests.

Figure 5.- Photograph of YR-4A No. 10 helicopter test specimen.

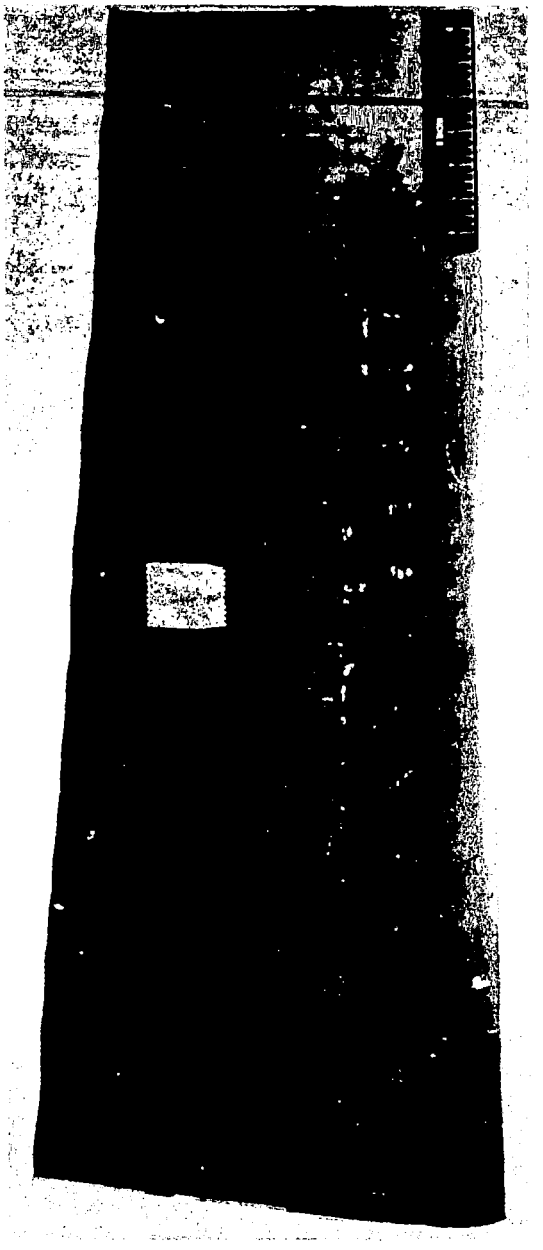

(a) Upper surface upon completion of tests.

Figure 6.- Photograph of YR-4A No. 10 (smooth forward portion) helicopter test specimen.

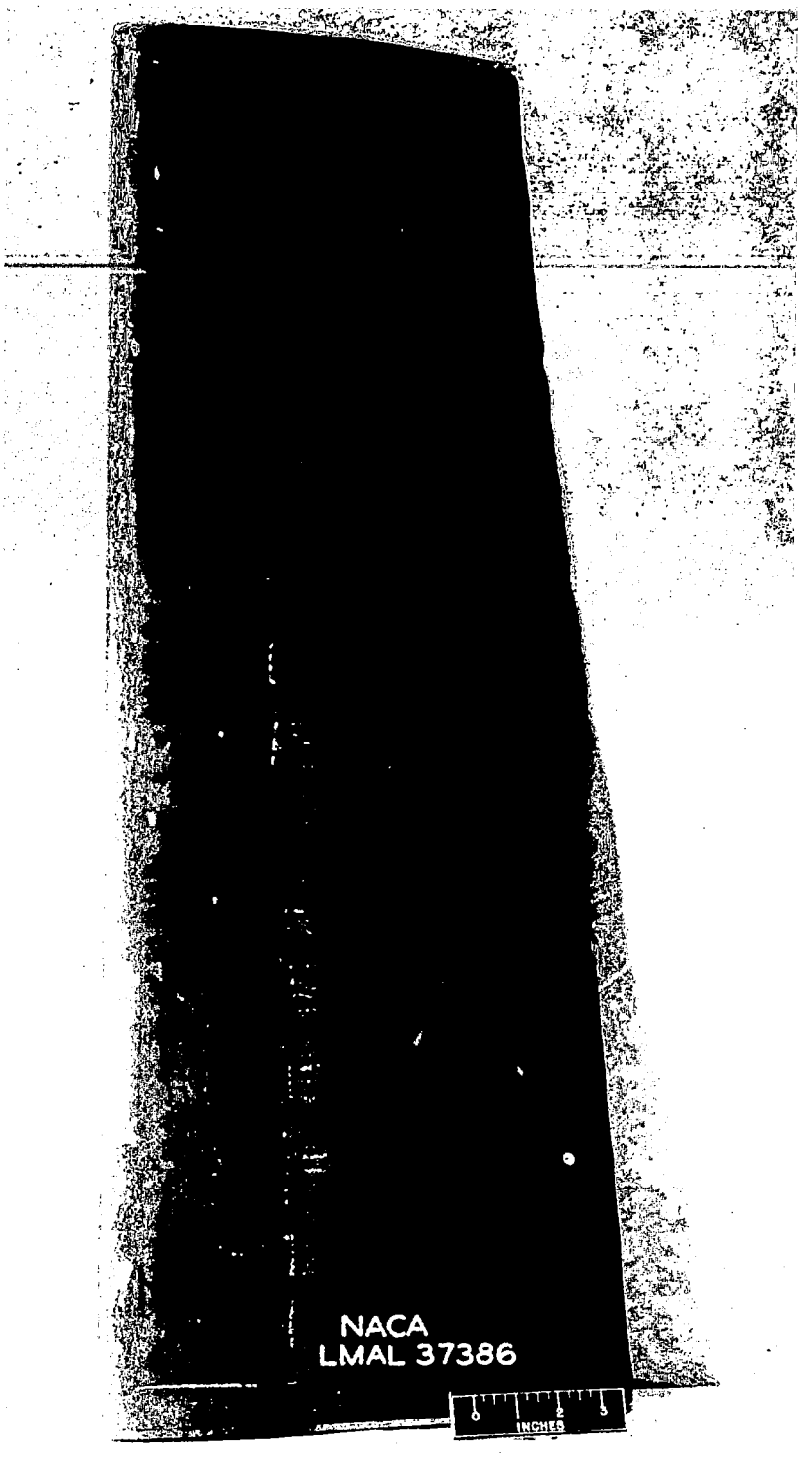

(b) Lower surface upon completion of tests.

Figure 6.- Concluded.

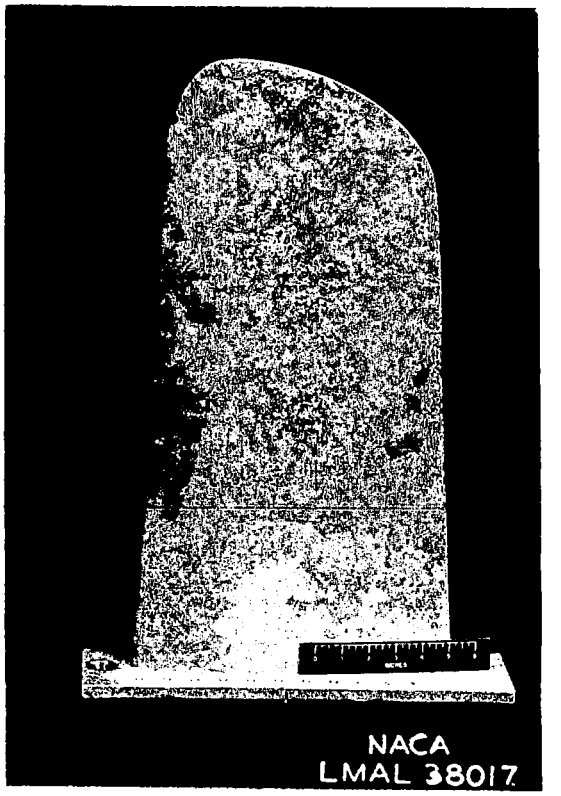

Lower surface upon completion of tests.

Figure 7.- Photograph of XR-6 No. 2 tip section.

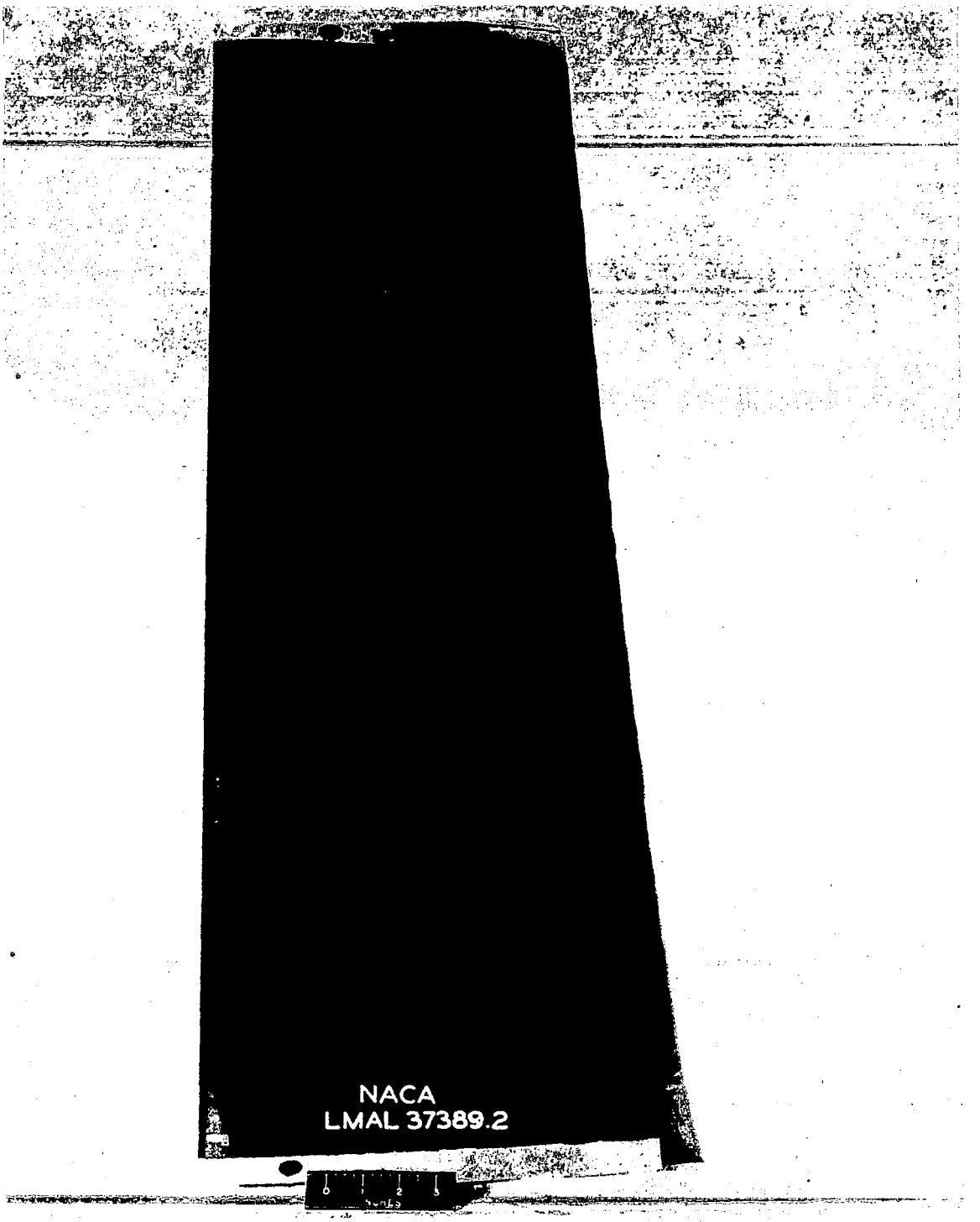

Lower surface upon completion of tests.

Figure 8.- Photograph of XR-6 No. 5 helicopter test specimen.

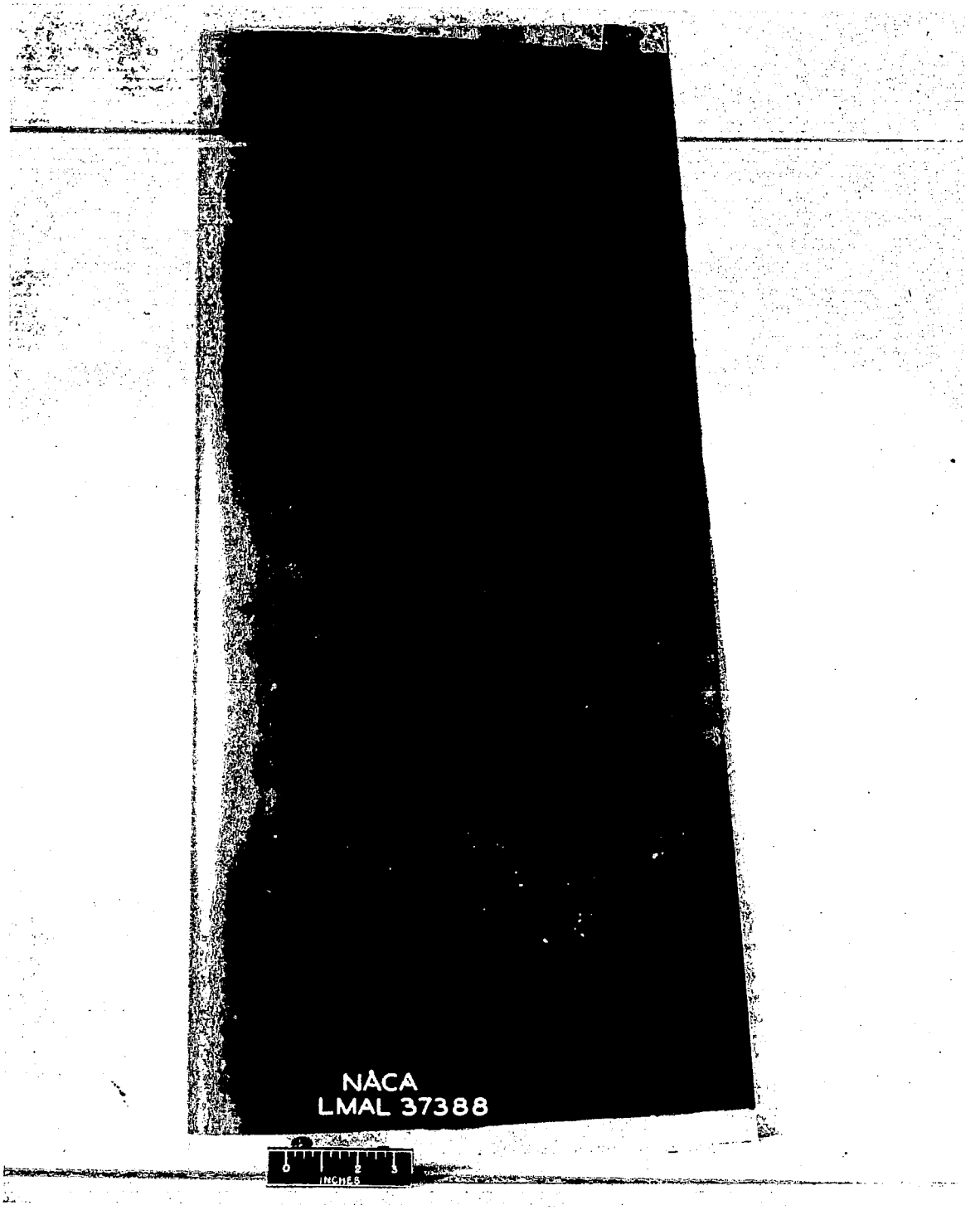

Lower surface upon completion of tests.

Figure 9.- Photograph of XR-6 No. 7 helicopter test specimen.

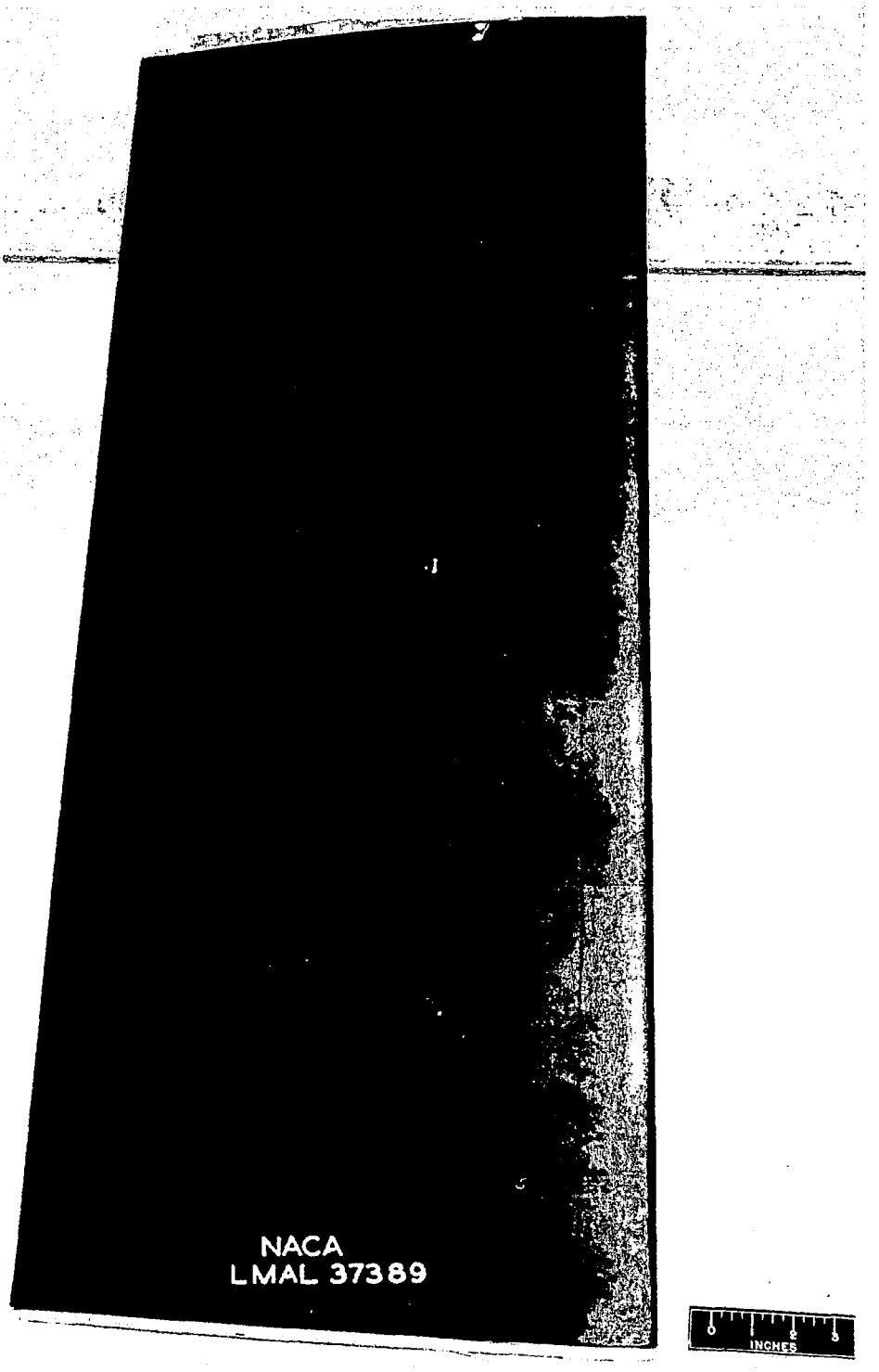

(a) Upper surface upon completion of tests.

Figure 10.- Photograph of XR-5(a) helicopter test specimen.

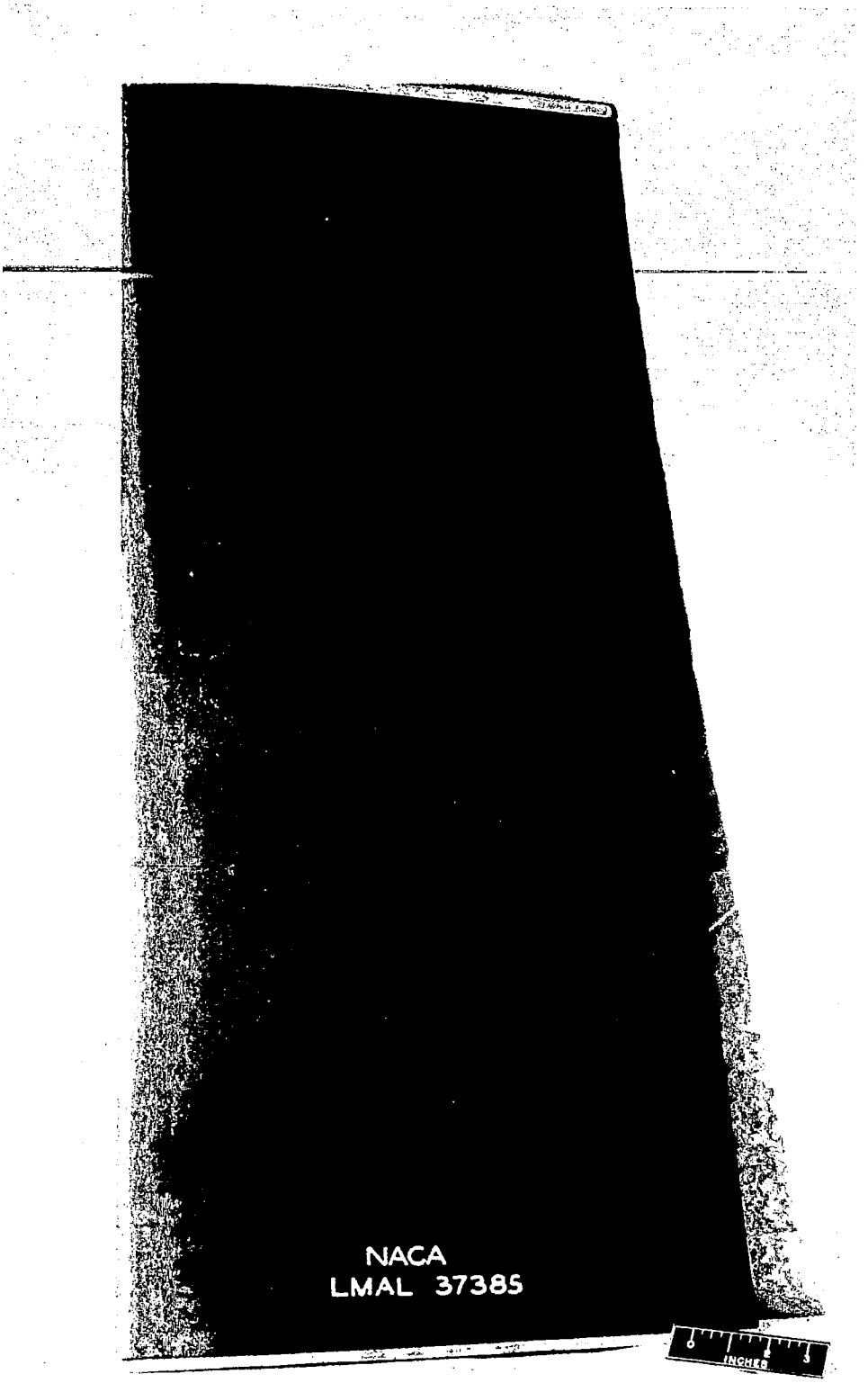

(b) Lower surface upon completion of tests.

Figure 10.- Concluded.

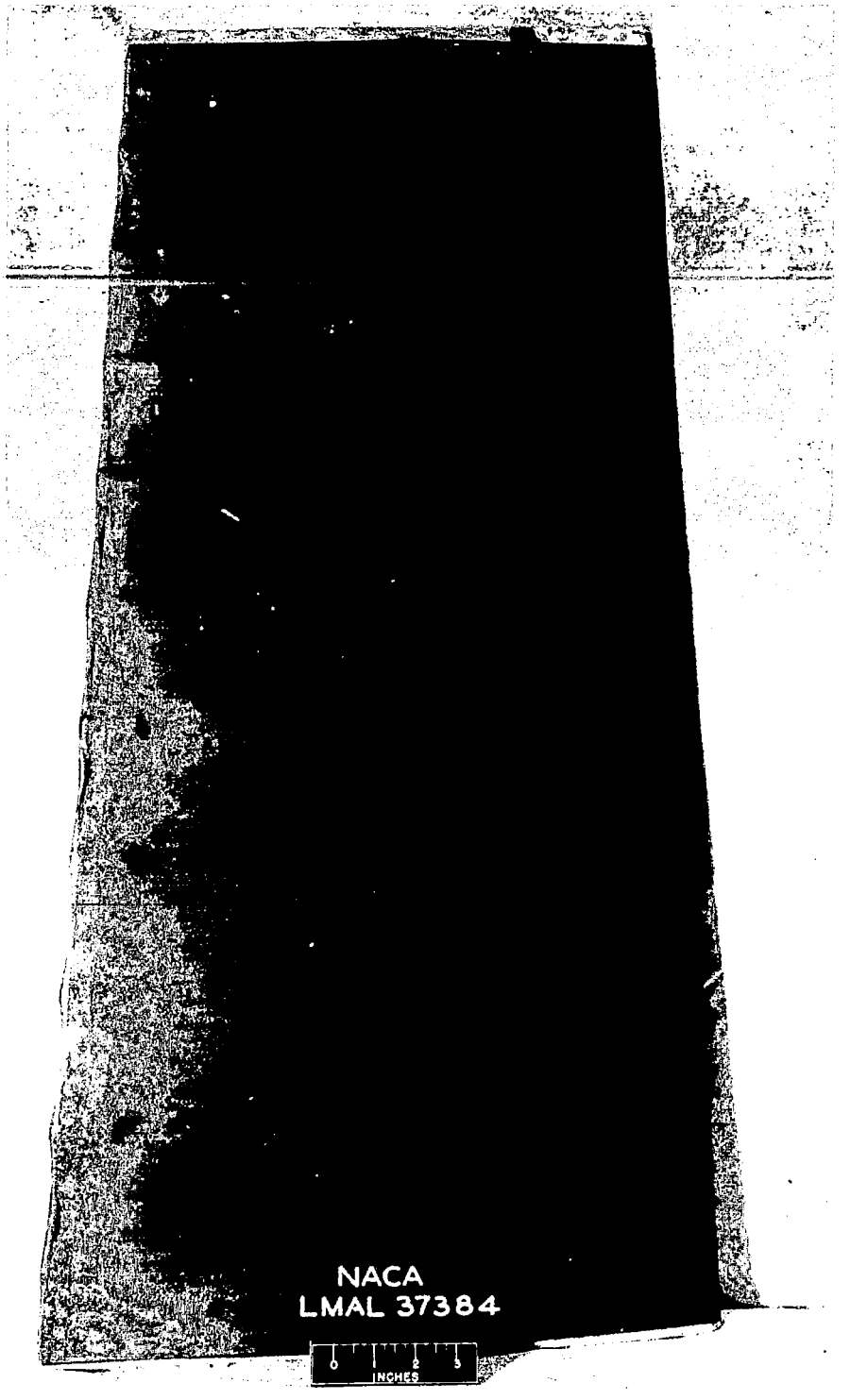

(a) Upper surface upon completion of tests.

Figure 11.- Photograph of XR-5(b) helicopter test specimen.

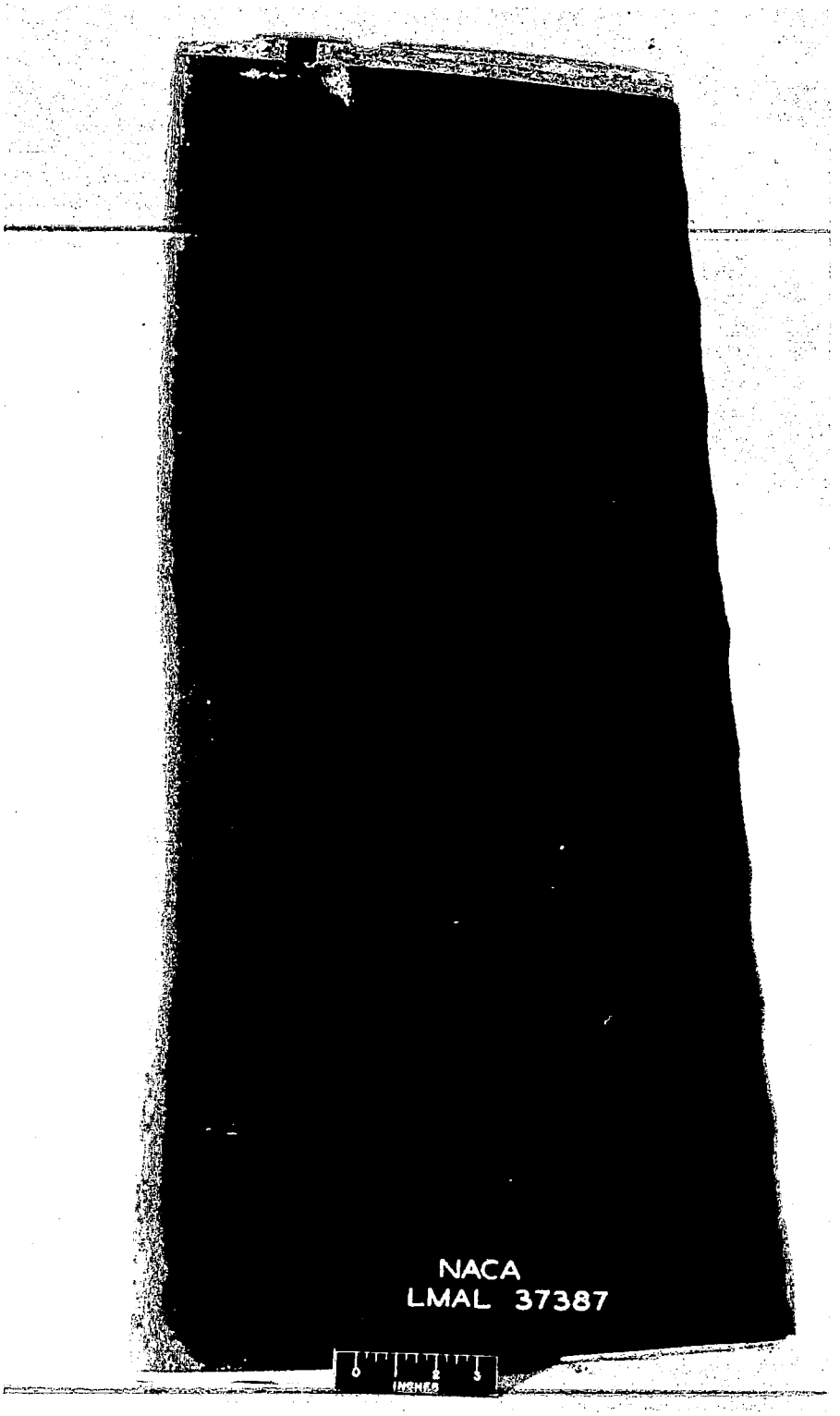

(b) Lower surface upon completion of tests.

Figure 11.- Concluded.

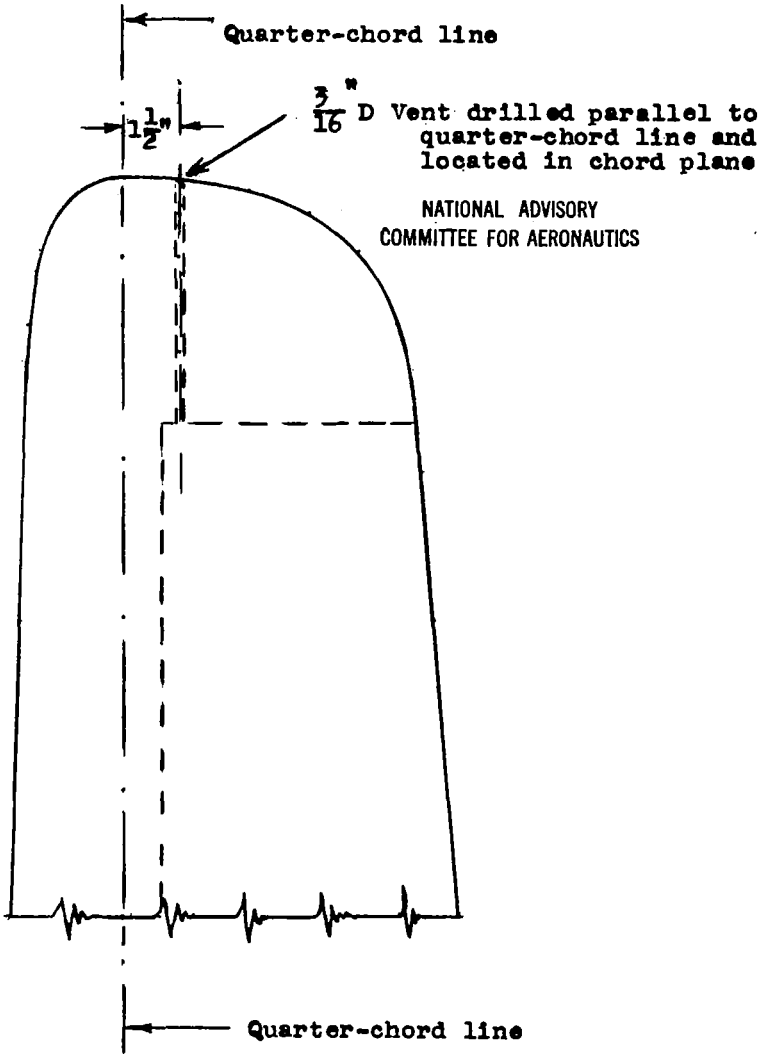

Figure 12.- Location of tip vent on YR-4A No. 1 blade tip section.

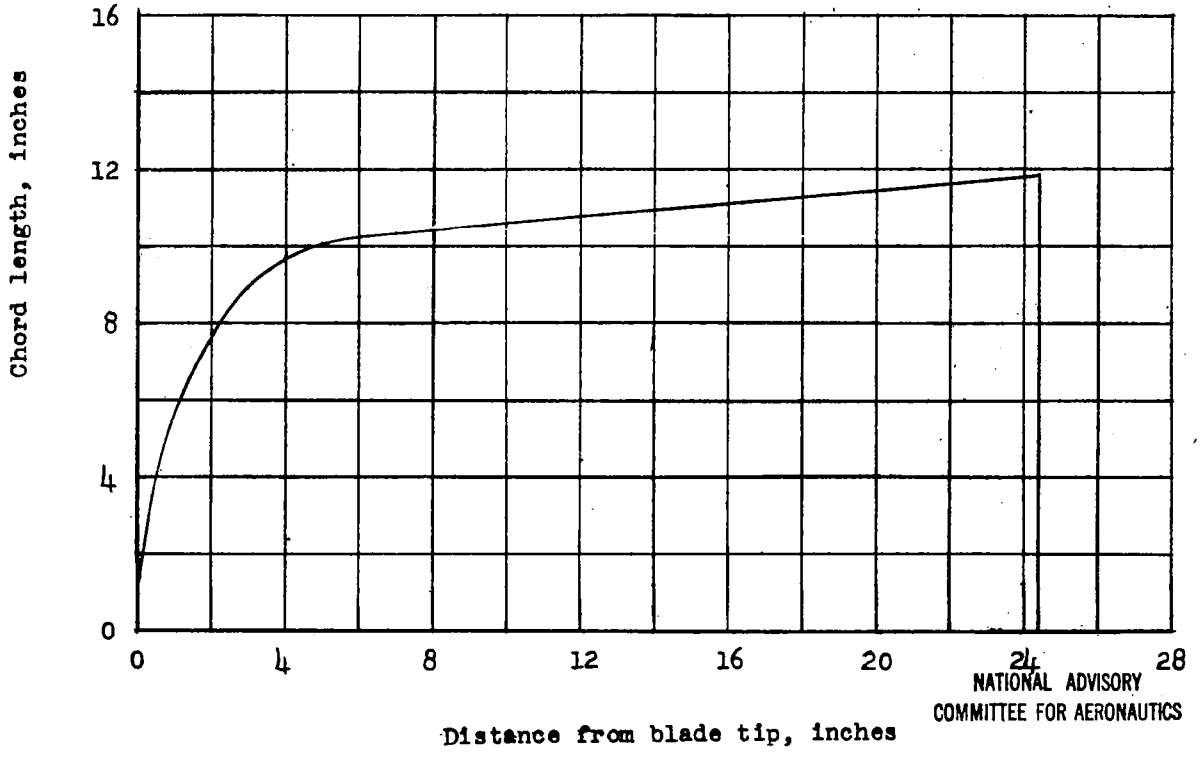

Figure 13.- Variation of chord along span of YR-4A No. 1 and XR-6 No. 2 blade tip section.

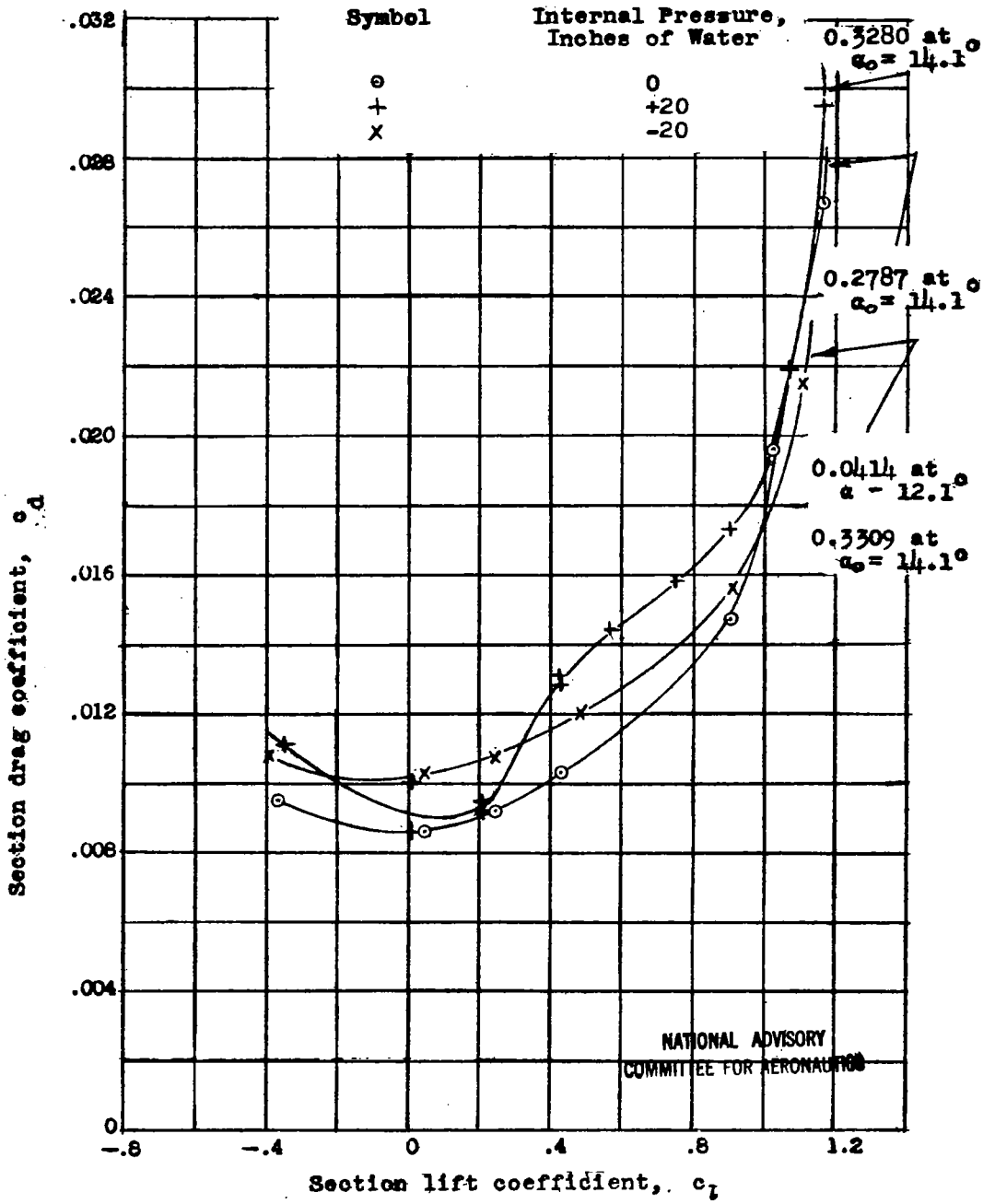

(a) Drag coefficient versus lift coefficient.

Figure 14.- Aerodynamic data for the YR-4A No. 3 Helicopter test section. R = .91 × 10^6, M = .131.

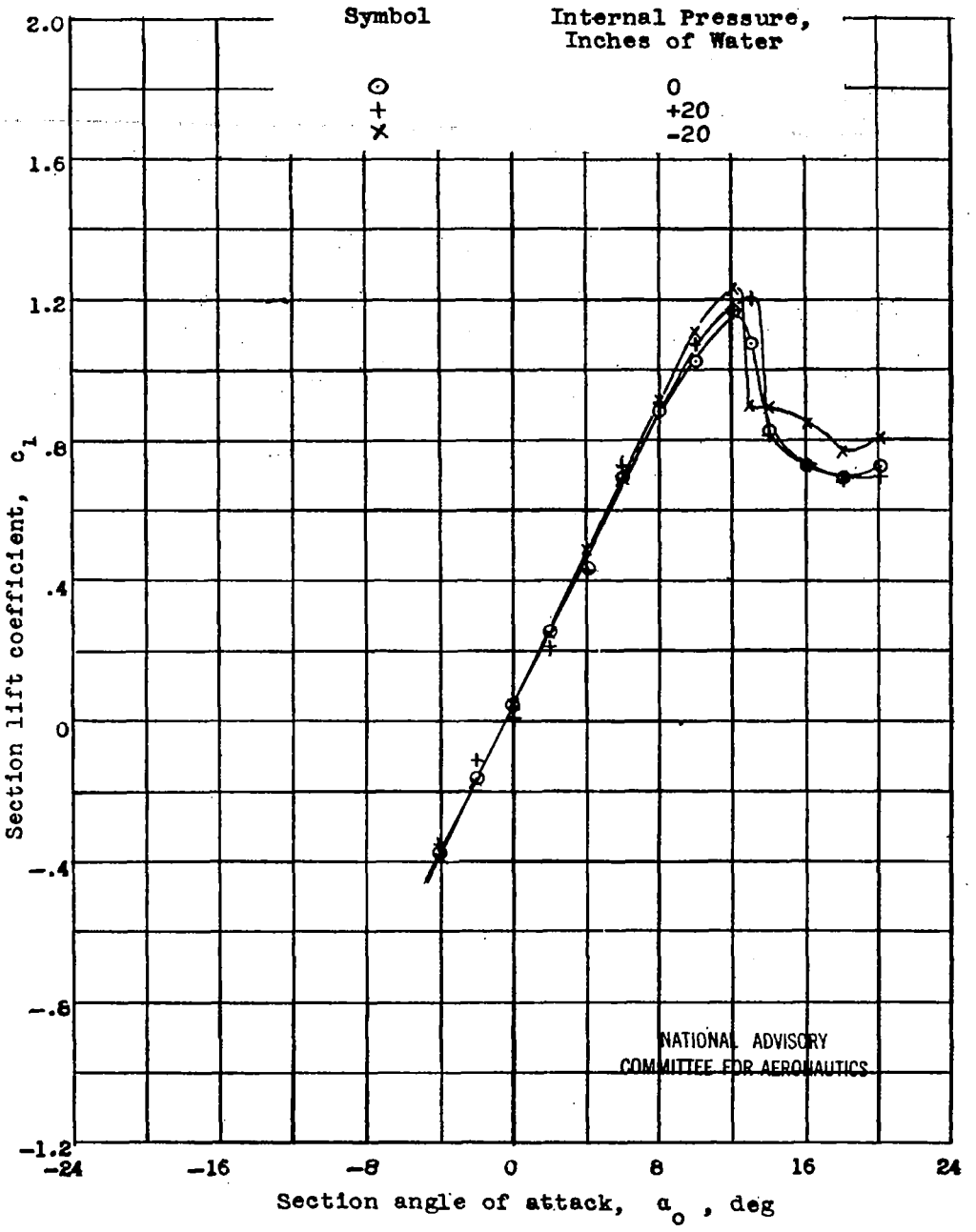

(b) Lift coefficient versus angle of attack.

Figure 14.- Continued.

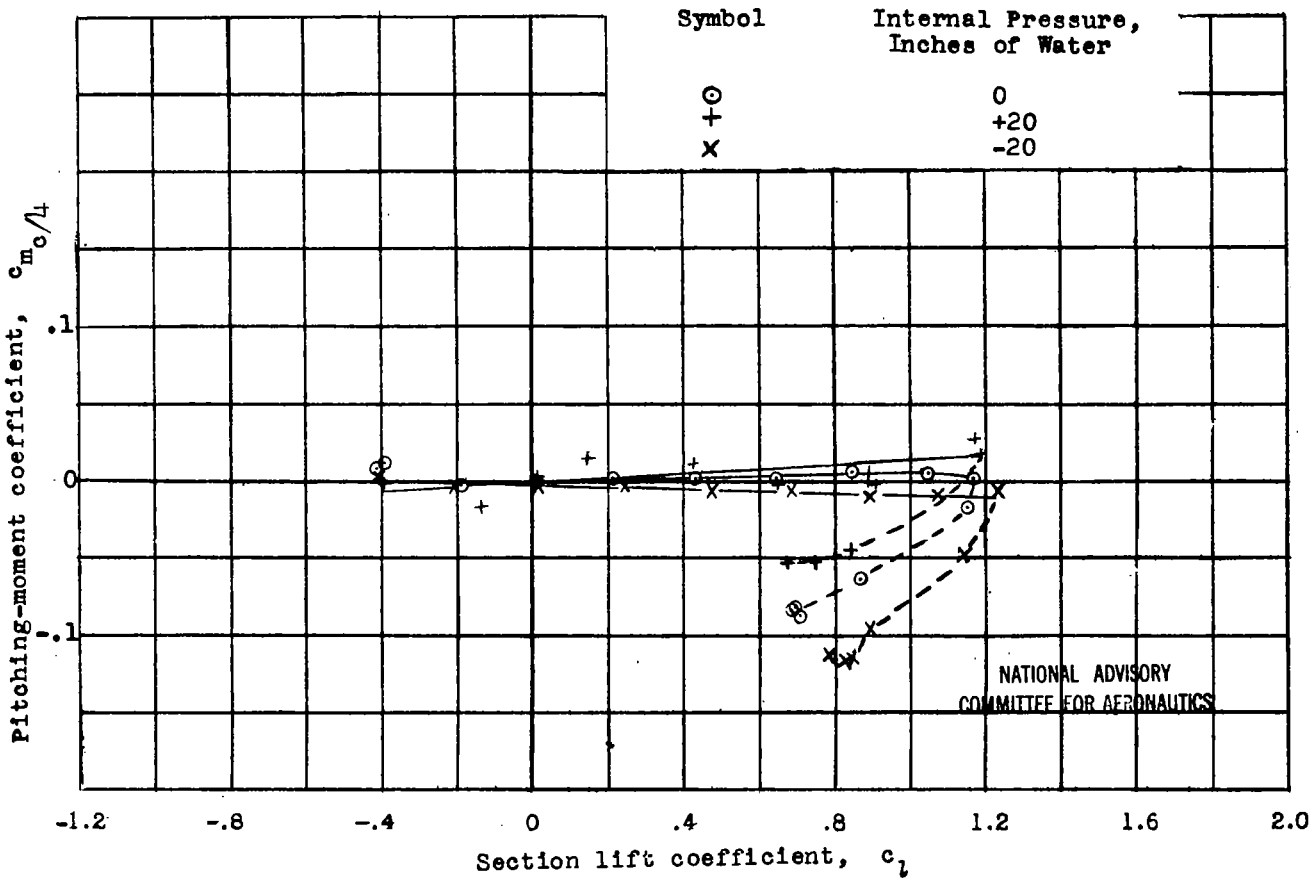

(c) Pitching-moment coefficient about quarter-chord point versus lift coefficient.

Figure 14.- Continued.

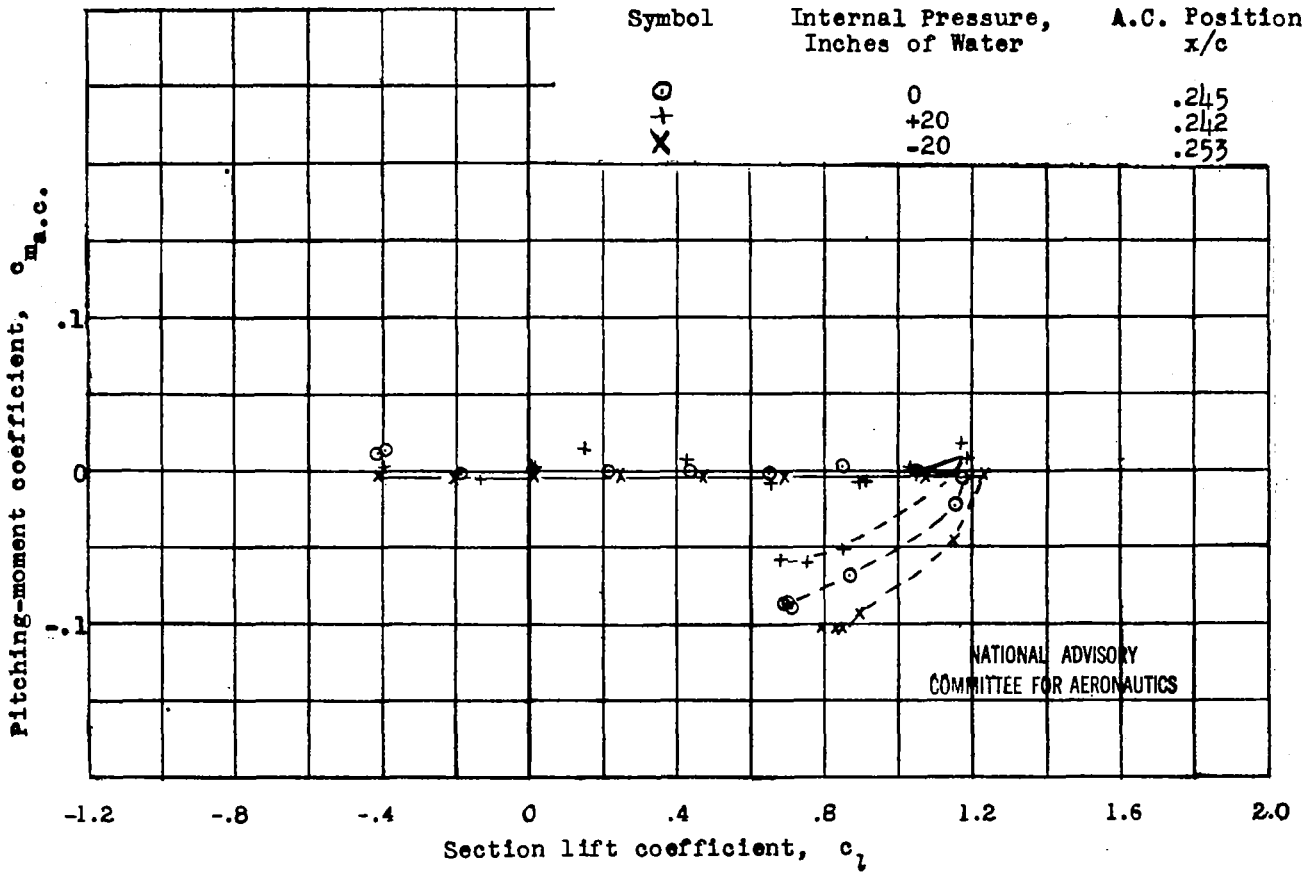

(d) Pitching-moment coefficient about aerodynamic centers versus lift coefficient.

Figure 14 .- Concluded.

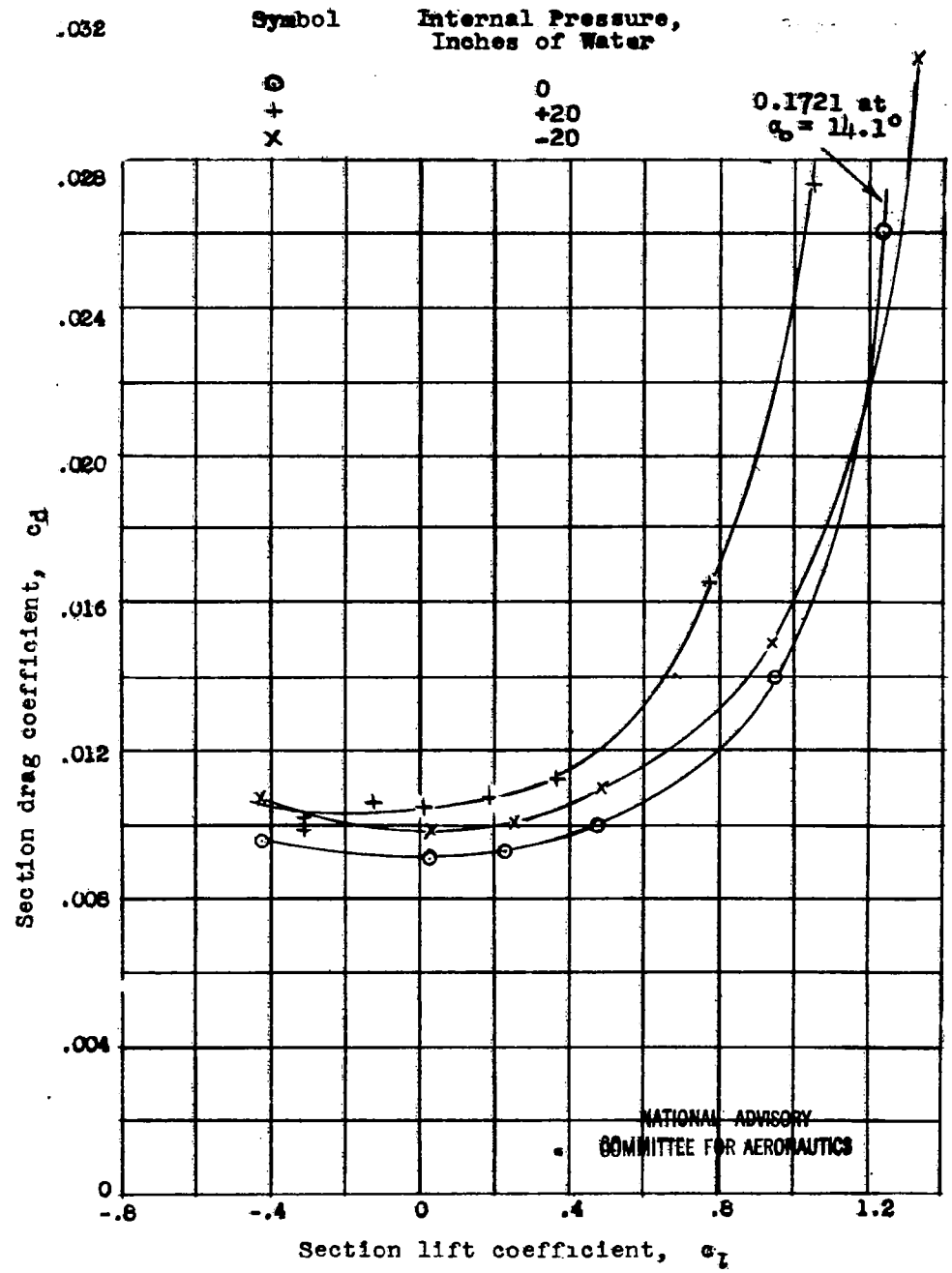

(a) Drag coefficient versus lift coefficient

Figure 45.- Aerodynamic data for the YR-4A No. 3 Helicopter test section. $R = 1.84 \times 10^6$, $M = 0.262$.

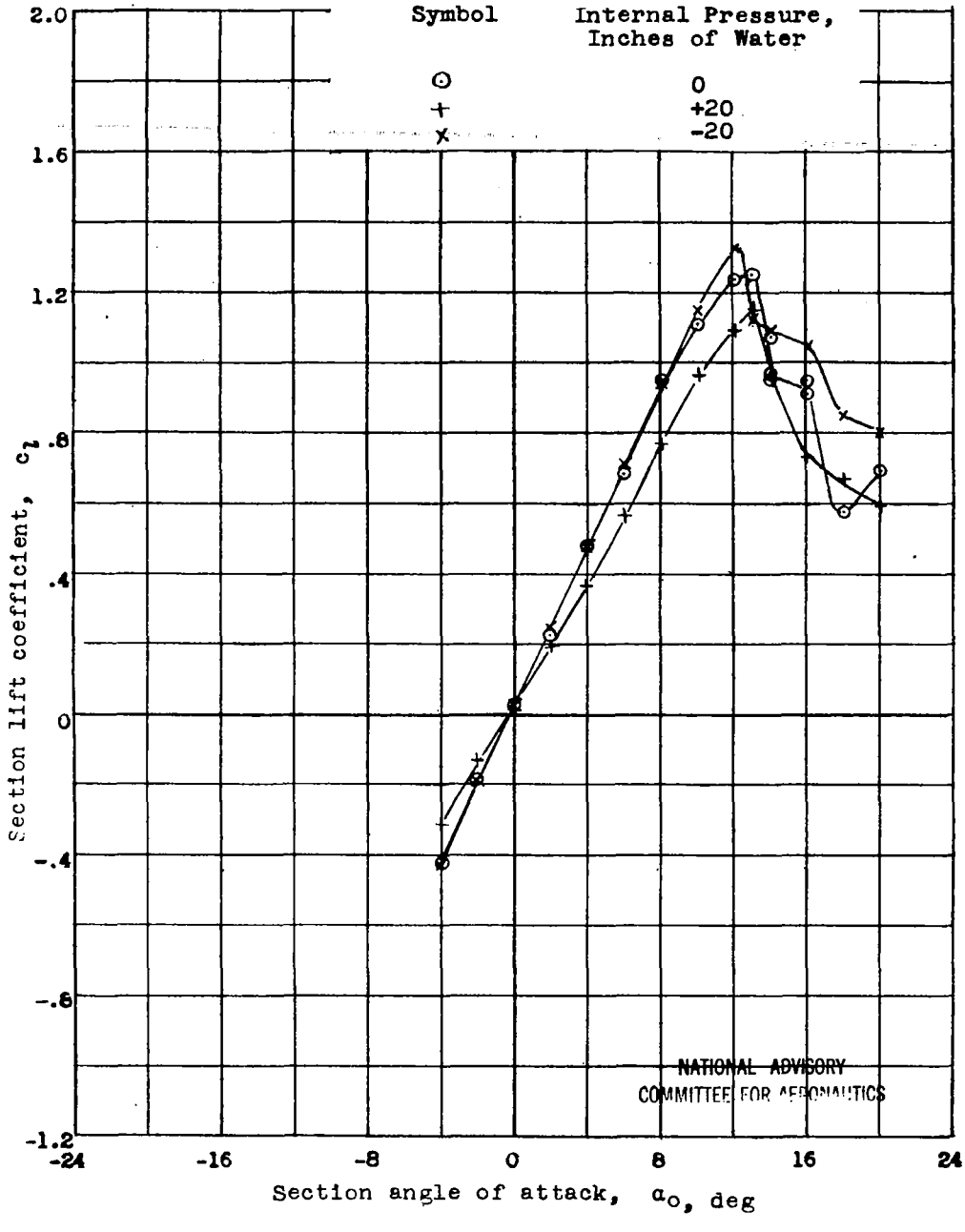

(b) Lift coefficient versus angle of attack.

Figure 15.- Continued.

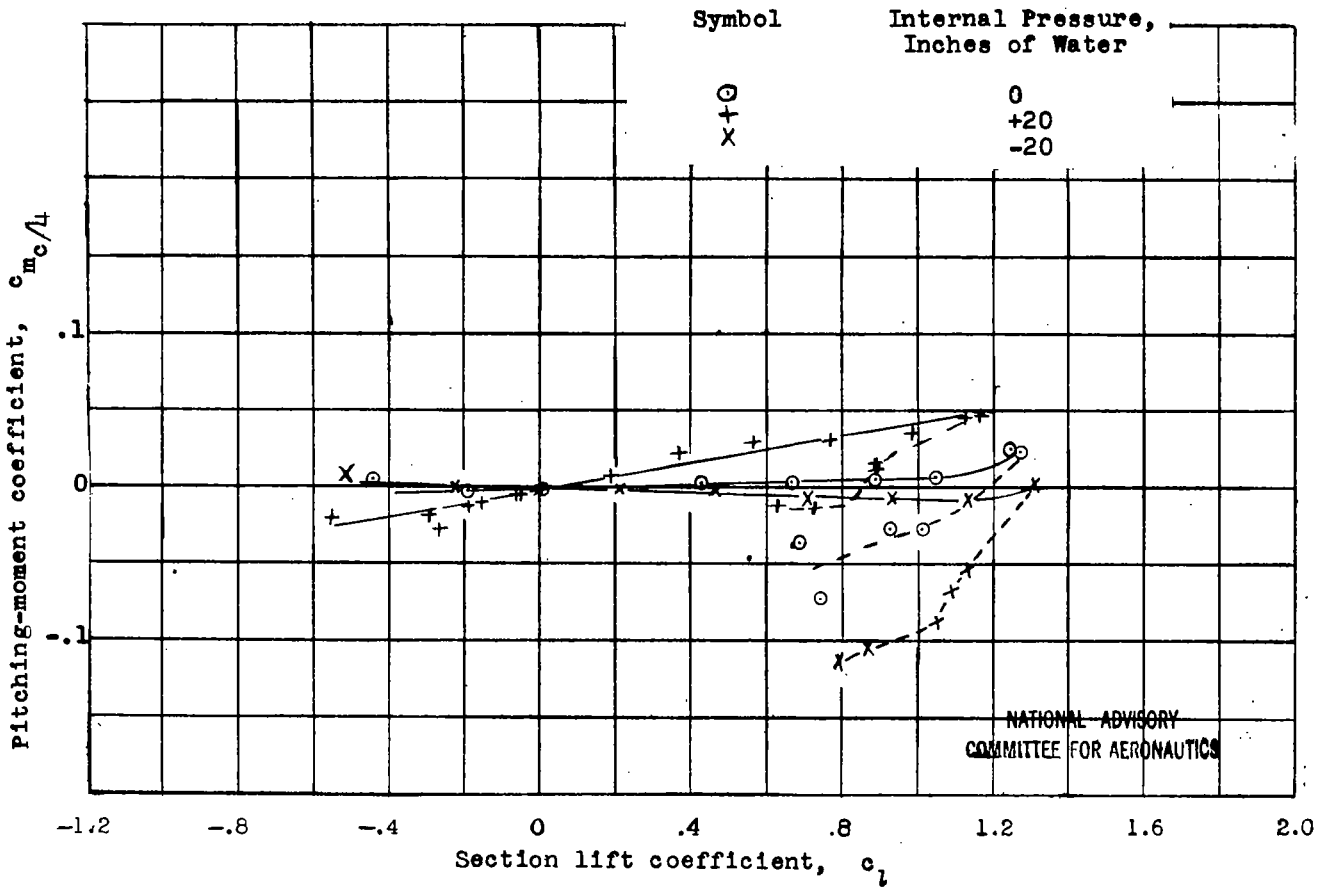

(c) Pitching-moment coefficient about quarter-chord point versus lift coefficient

Figure 15.- Continued.

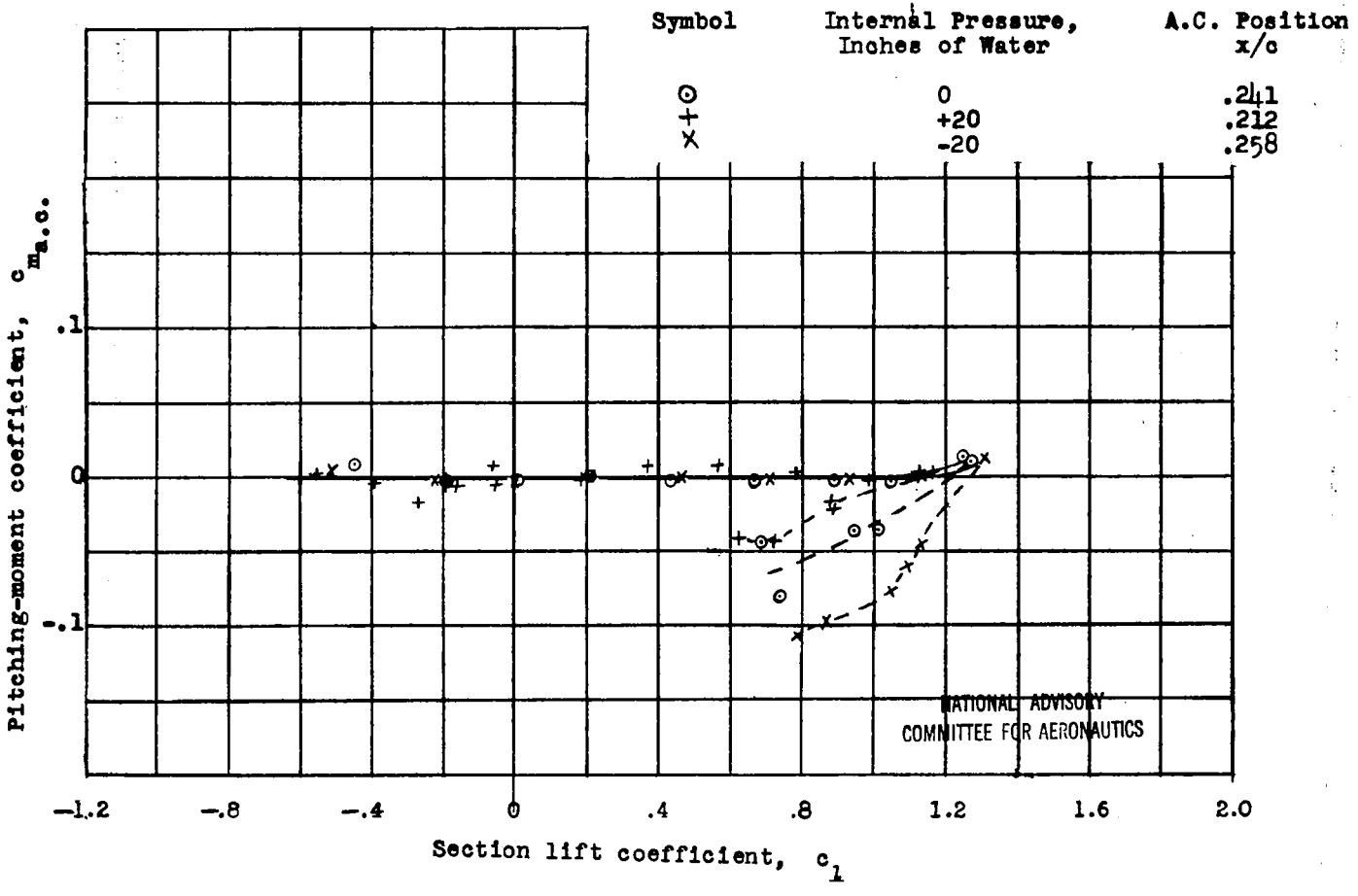

(d) Pitching-moment coefficient about aerodynamic centers versus lift coefficient

Figure 15.- Concluded.

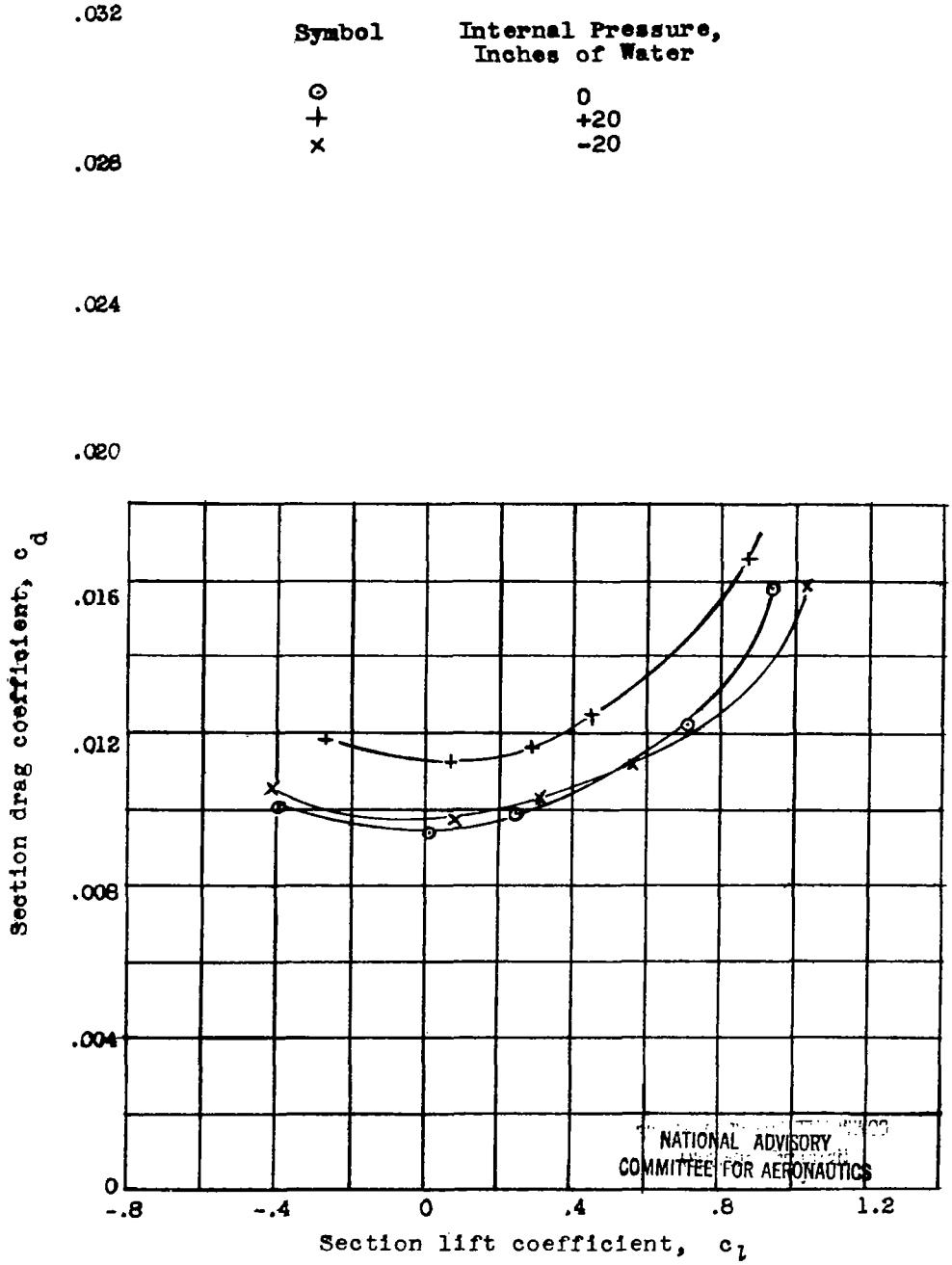

(a) Drag coefficient versus lift coefficient

Figure 16.- Aerodynamic data for the YR-4A No. 3 Helicopter test section. $R = 2.58 \times 10^6$, $M = 0.375$.

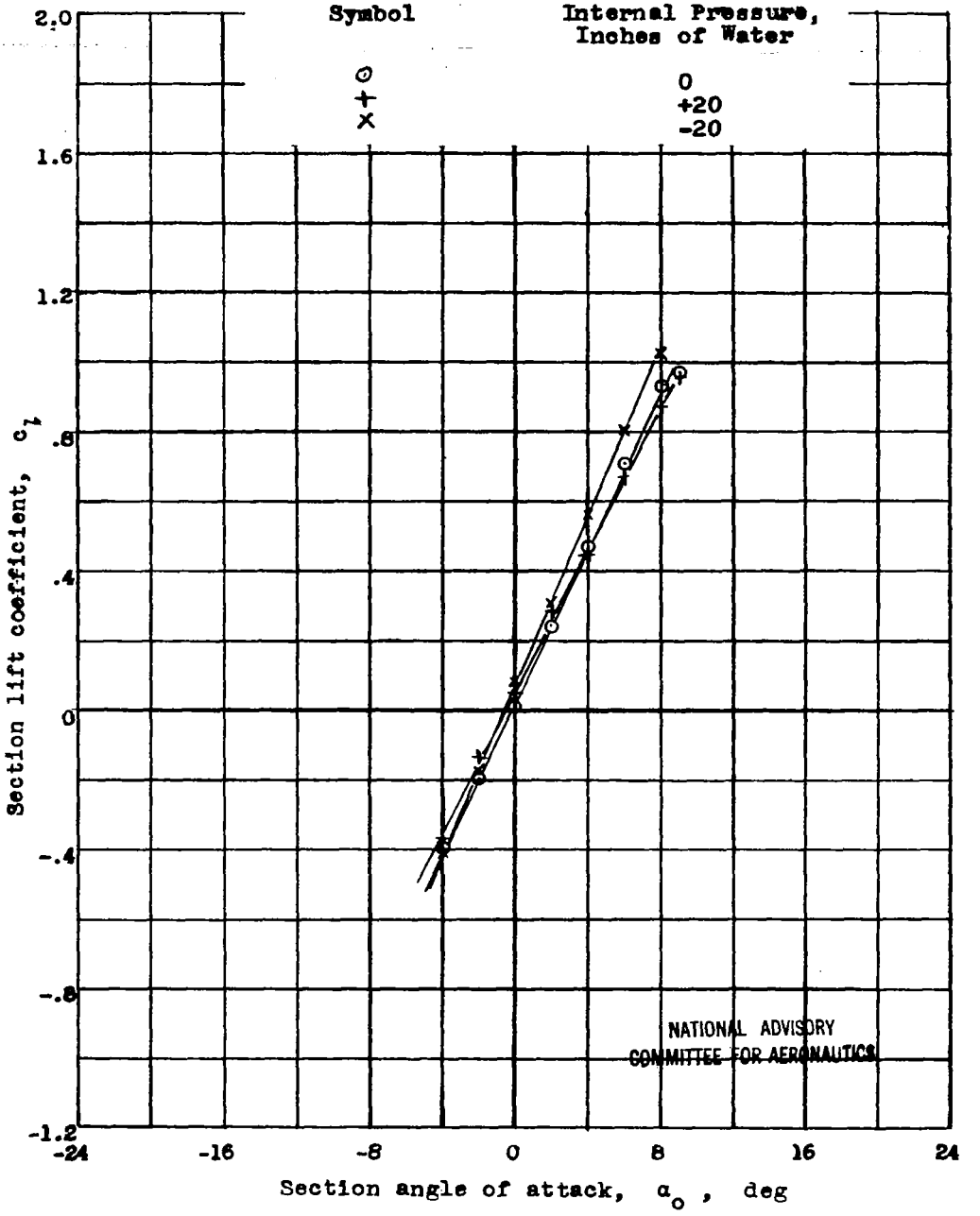

(b) Lift coefficient versus angle of attack.

Figure 16.- Continued.

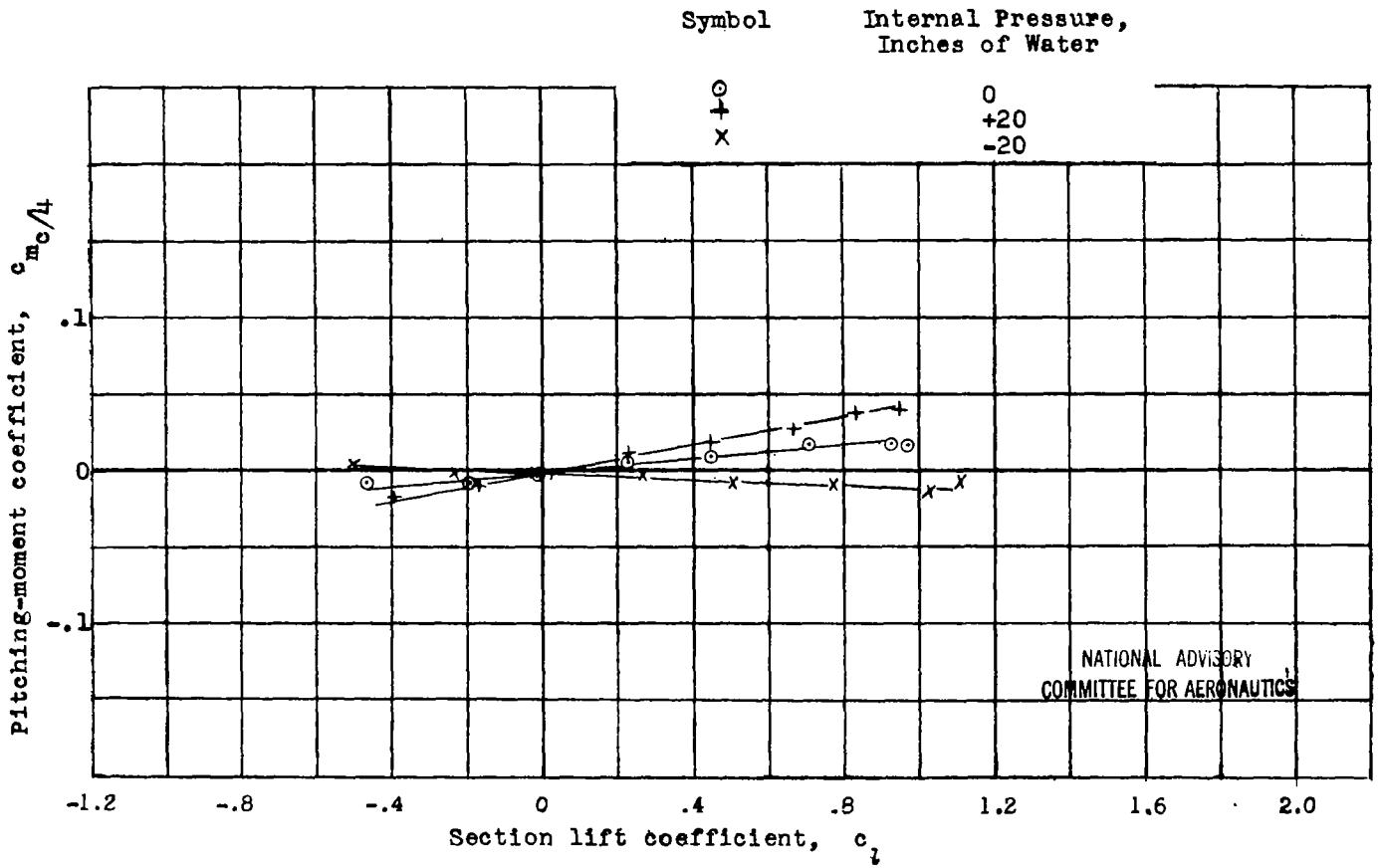

(c) Pitching-moment coefficient about quarter-chord point versus lift coefficient

Figure 6.- Continued.

Symbol	Internal Pressure, Inches of Water	A.C. Position x/c
⊙	0	.227
+	+20	.206
x	-20	.262

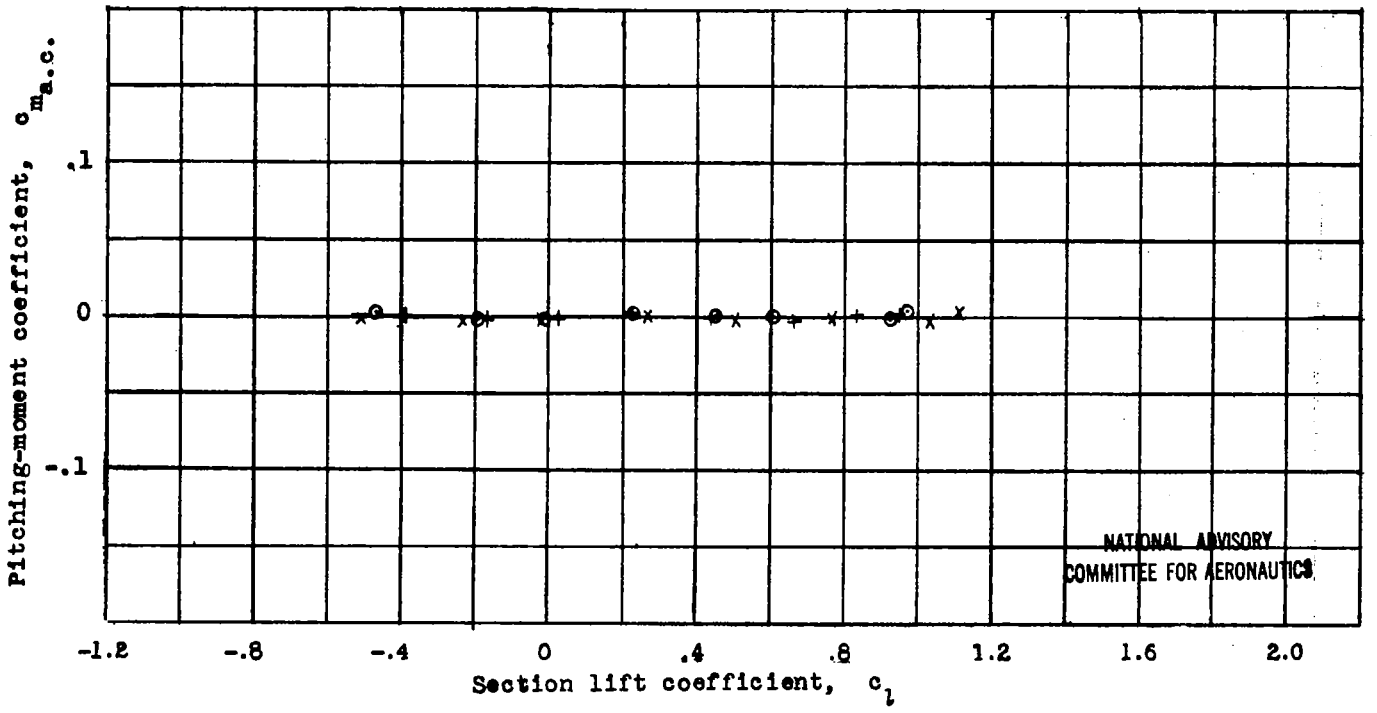

(d) Pitching-moment coefficient about aerodynamic centers versus lift coefficient

Figure 16.- Concluded.

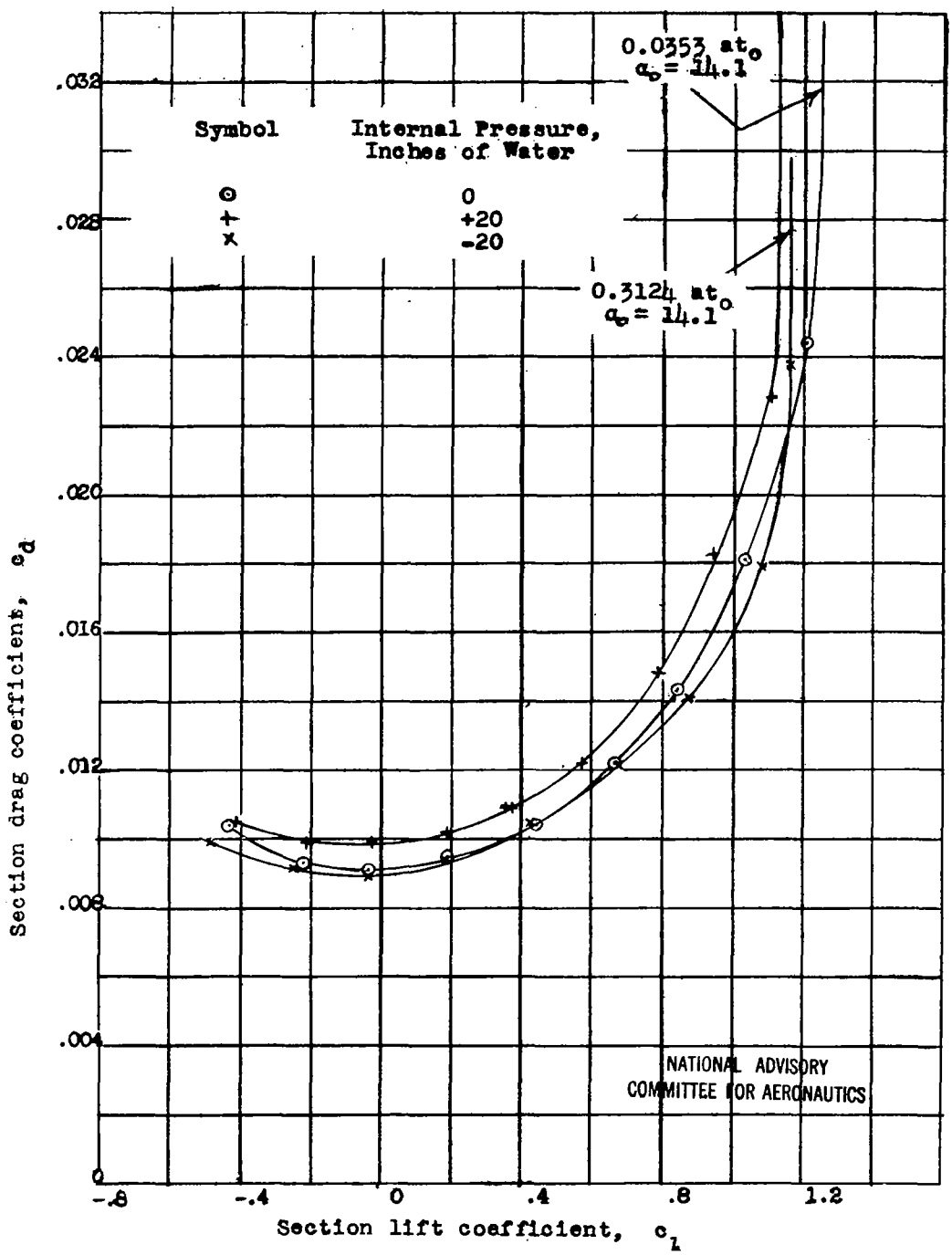

(a) Drag coefficient versus lift coefficient

Figure 17.- Aerodynamic data for the YR-4A No. 6 Helicopter test section. R = 1.72 × 10^6, M = 0.181.

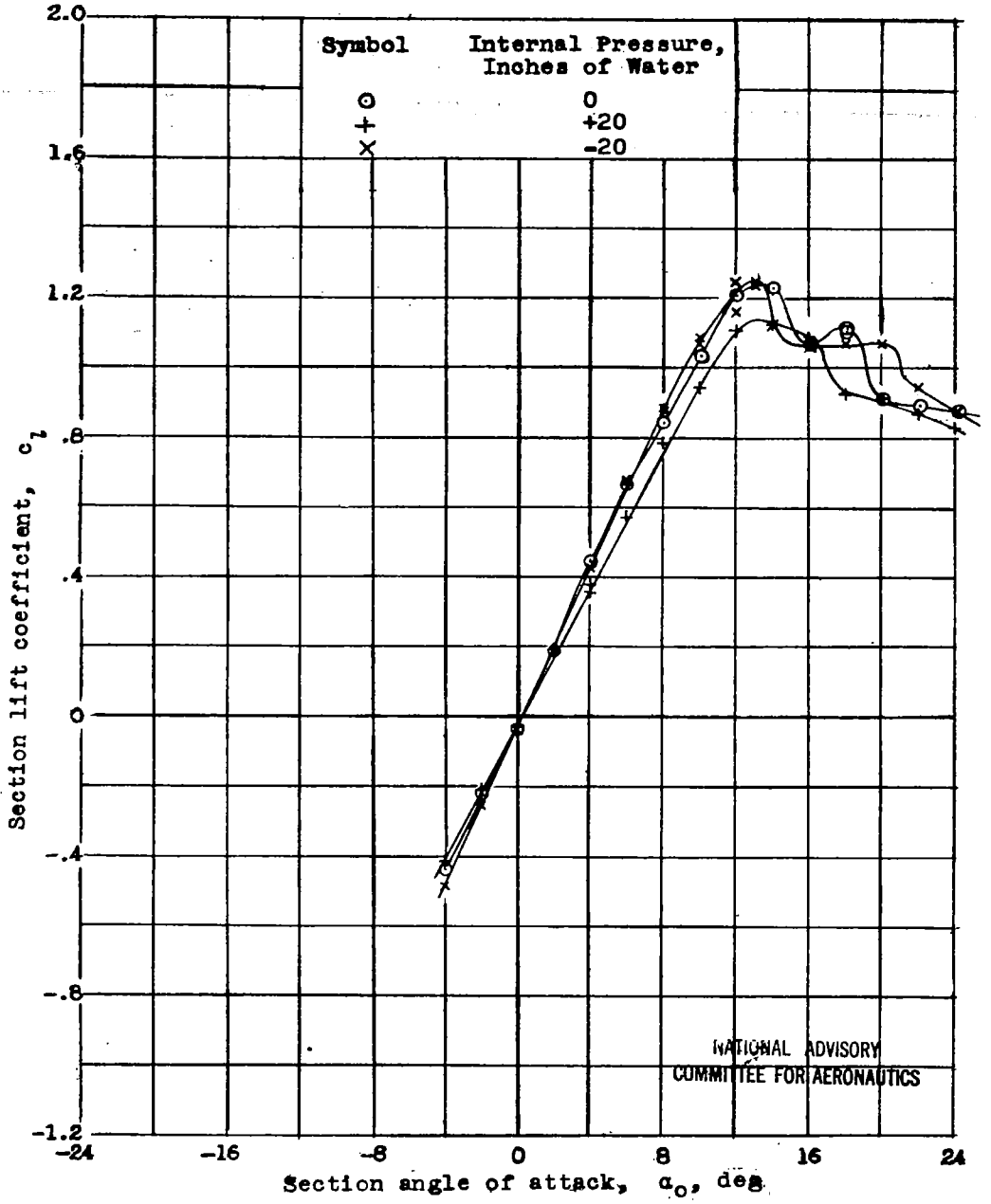

(b) Lift coefficient versus angle of attack

Figure 7 .- Continued.

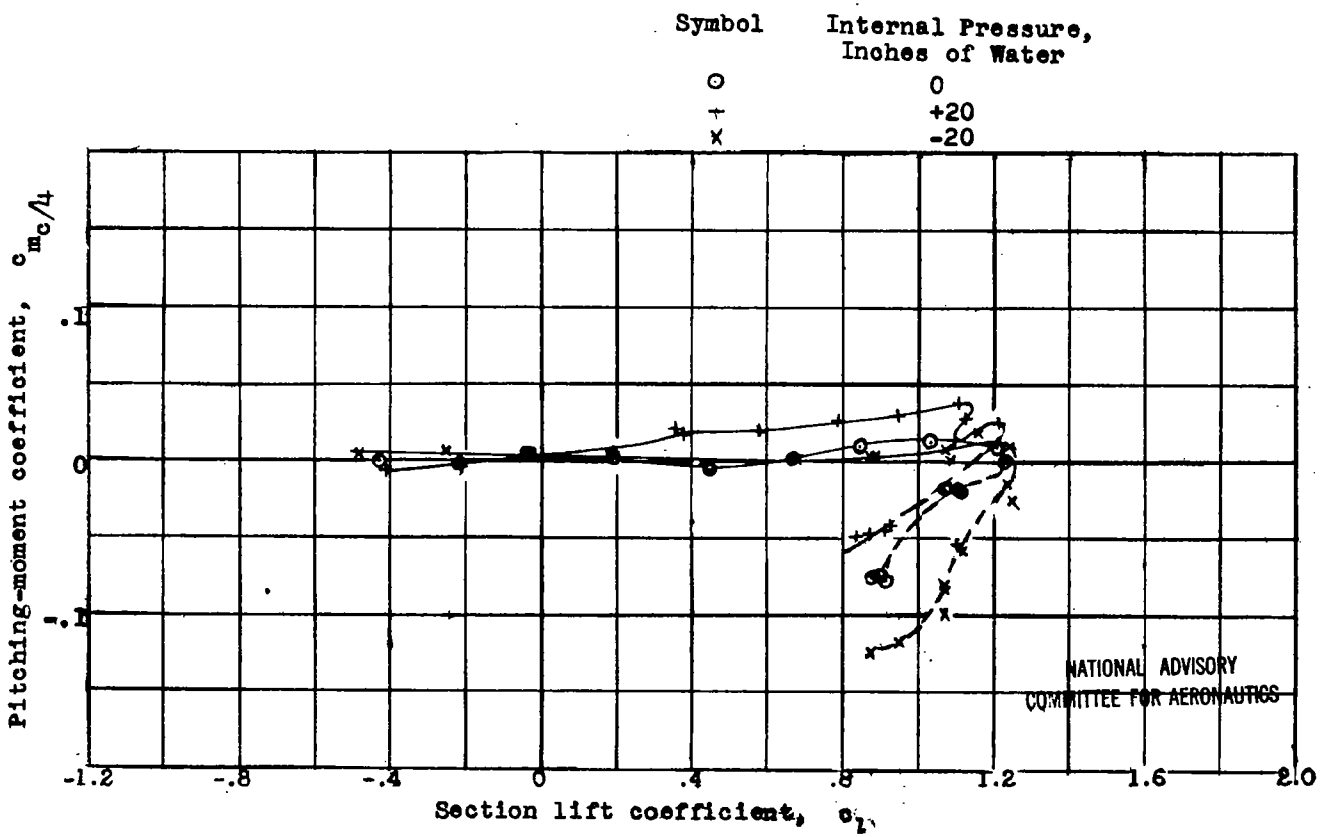

(c) Pitching-moment coefficient about quarter-chord veraus lift coefficient

Figure 17.- Continued.

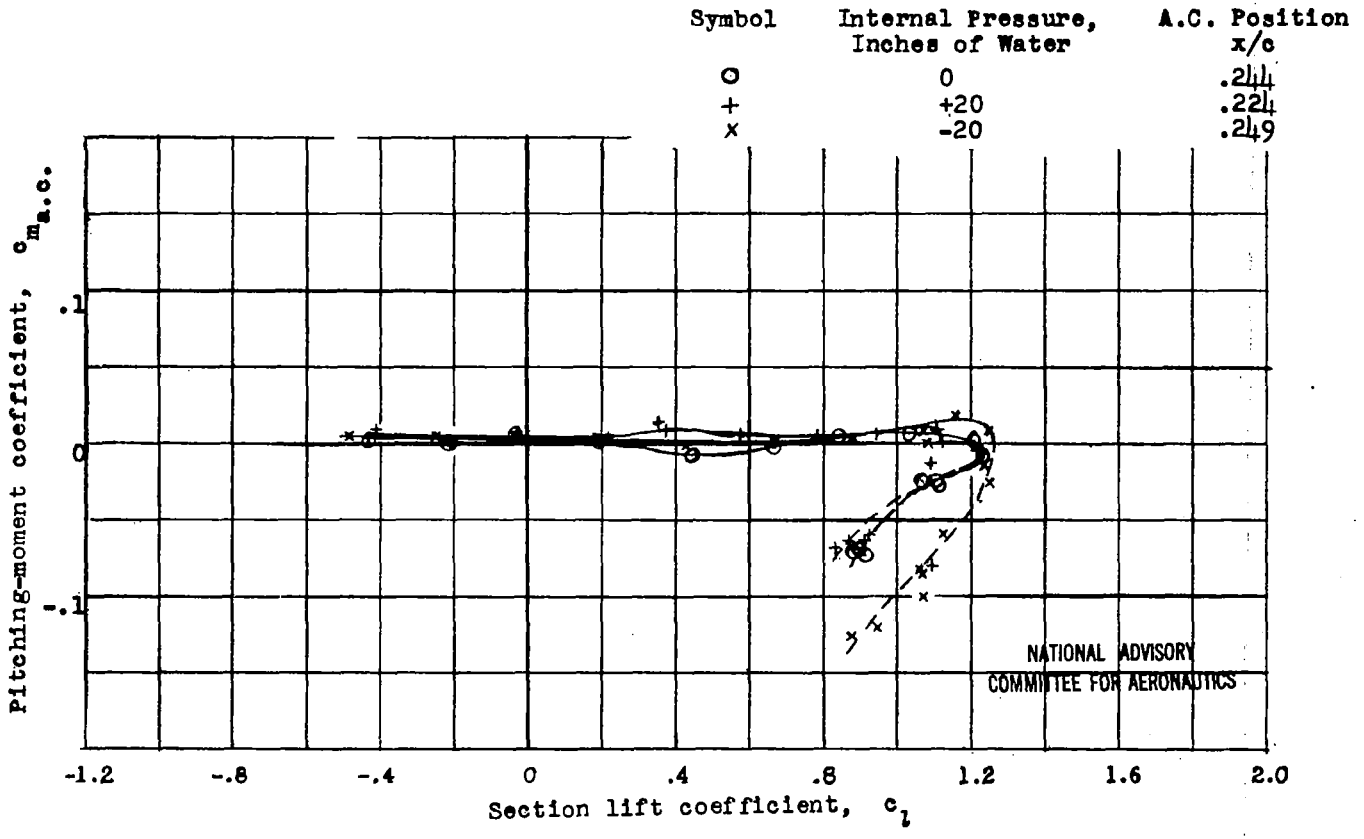

(d) Pitching-moment coefficient about aerodynamic center versus lift coefficient

Figure 17.- Concluded.

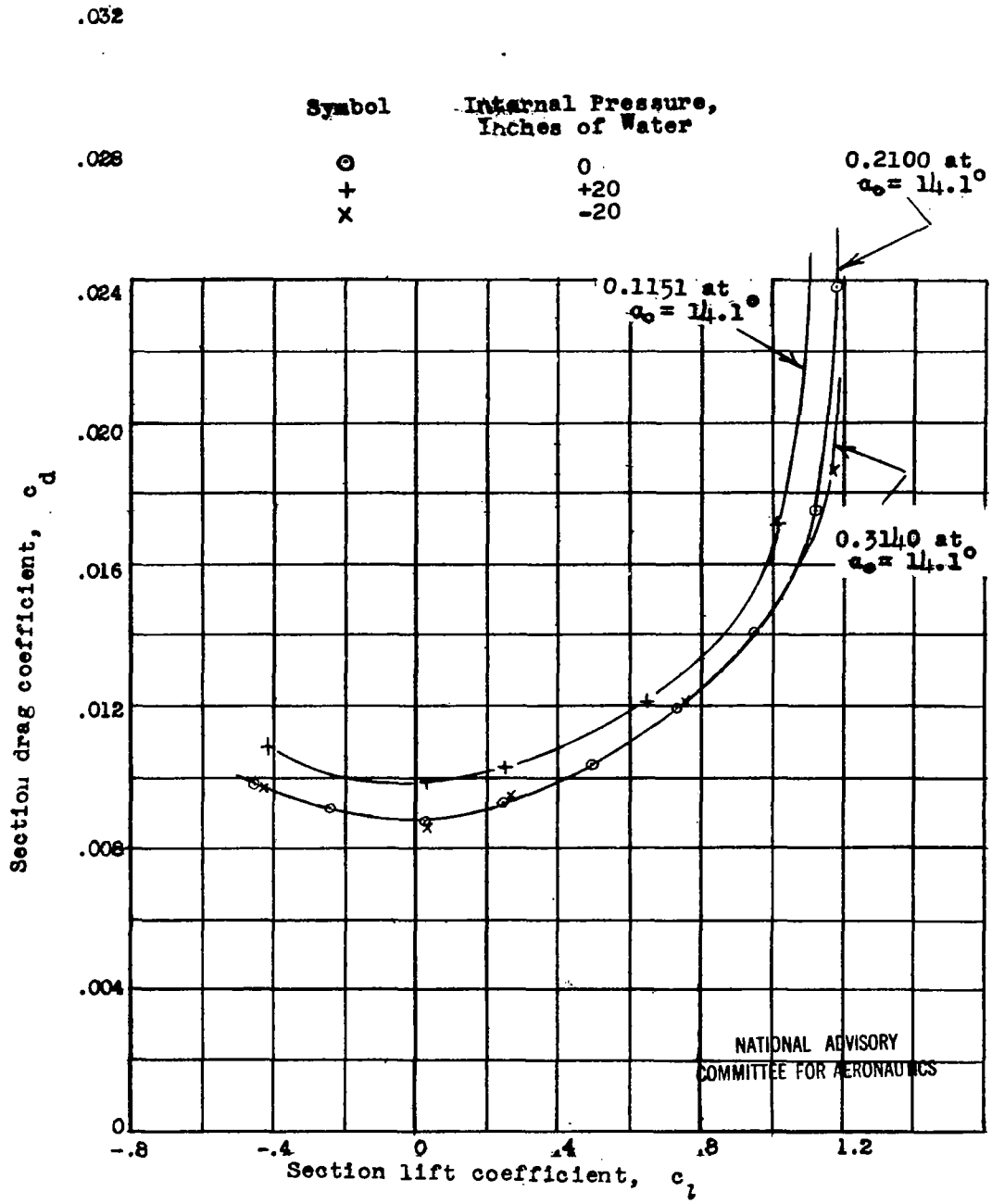

(a) Drag coefficient versus lift coefficient

Figure 18.- Aerodynamic data for the YR-4A No. 6 Helicopter test section. $R = 2.42 \times 10^6$, $M = 0.262$.

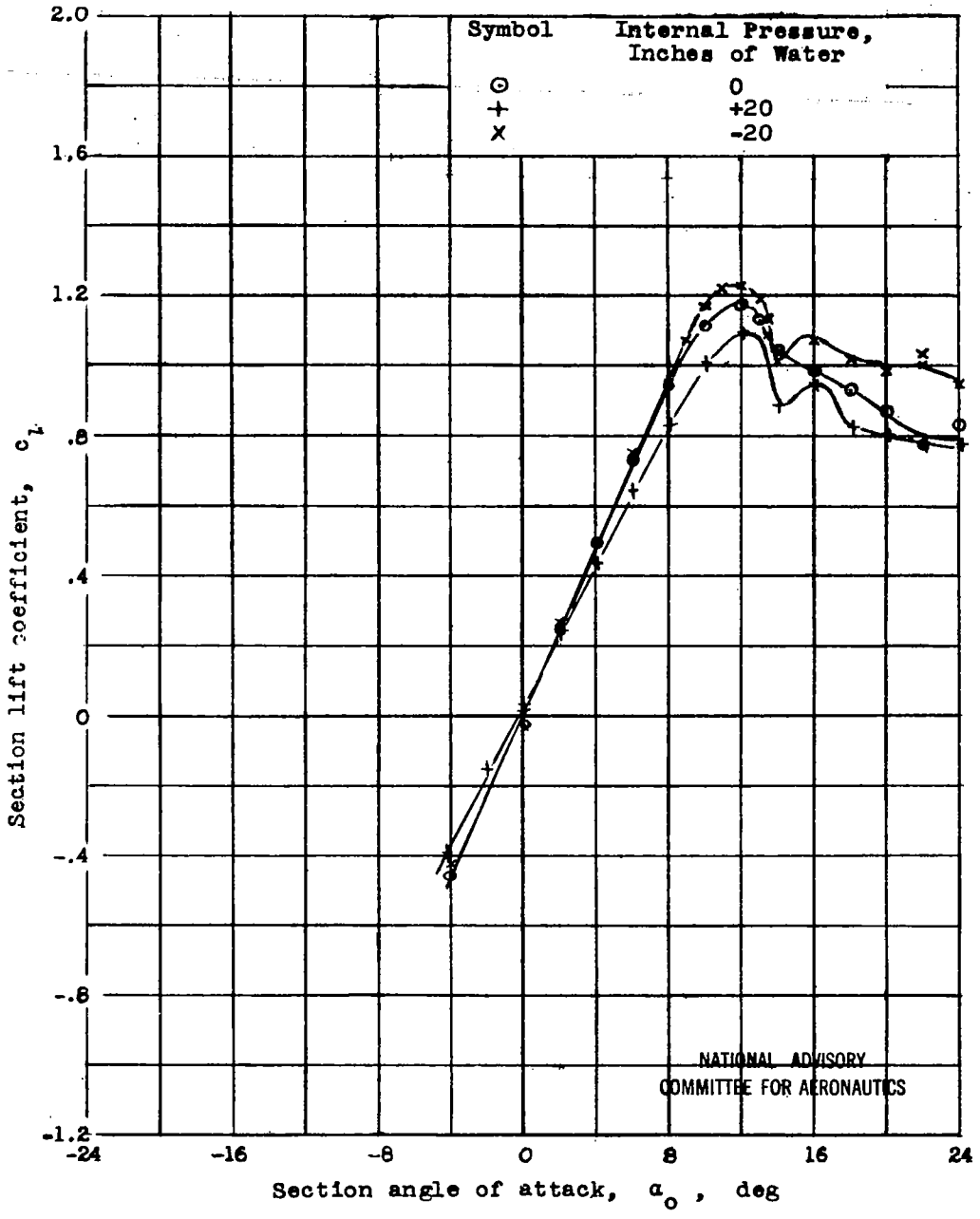

(b) Lift versus angle of attack

Figure 18 .- Continued.

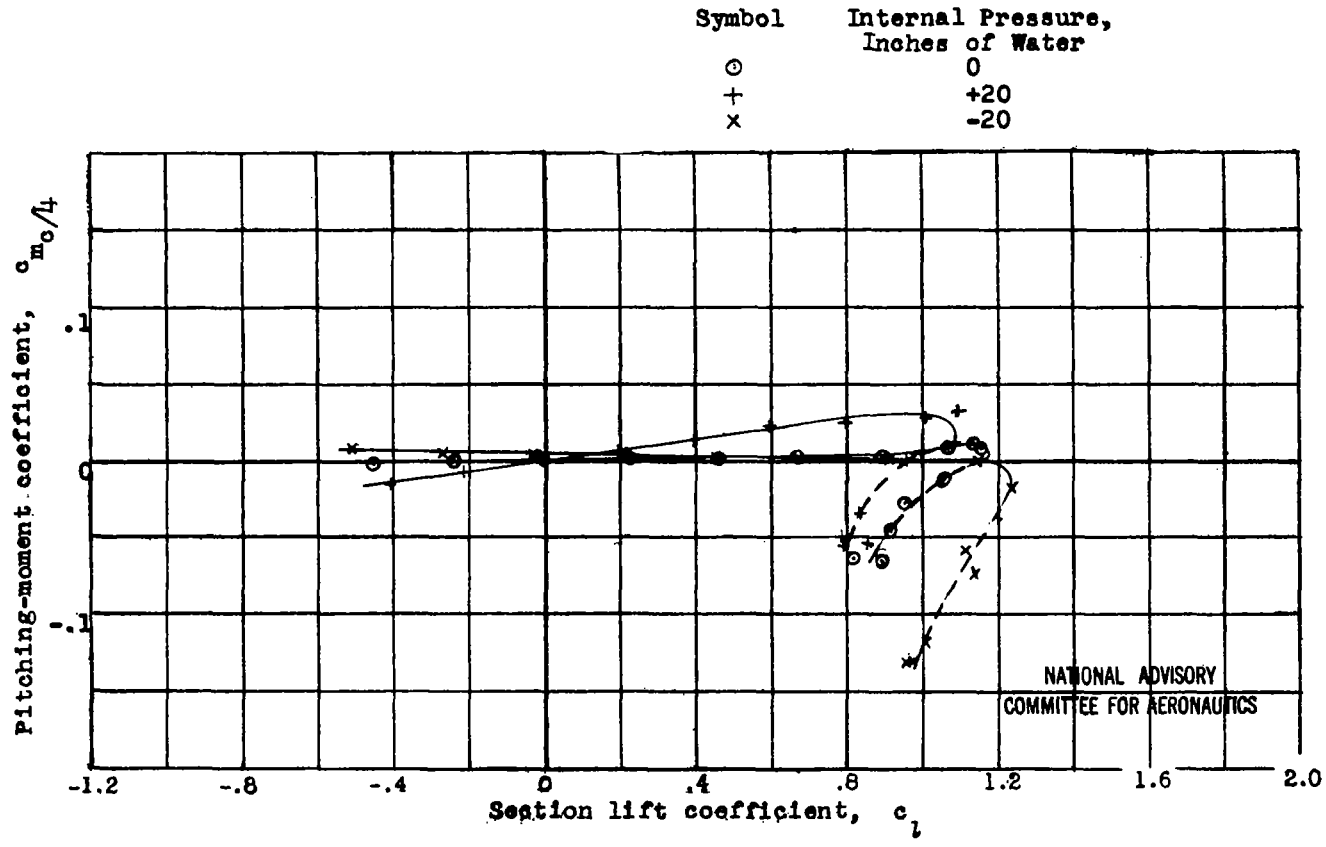

(c) Pitching-moment coefficient about quarter-chord versus lift coefficient.

Figure 18.- Continued.

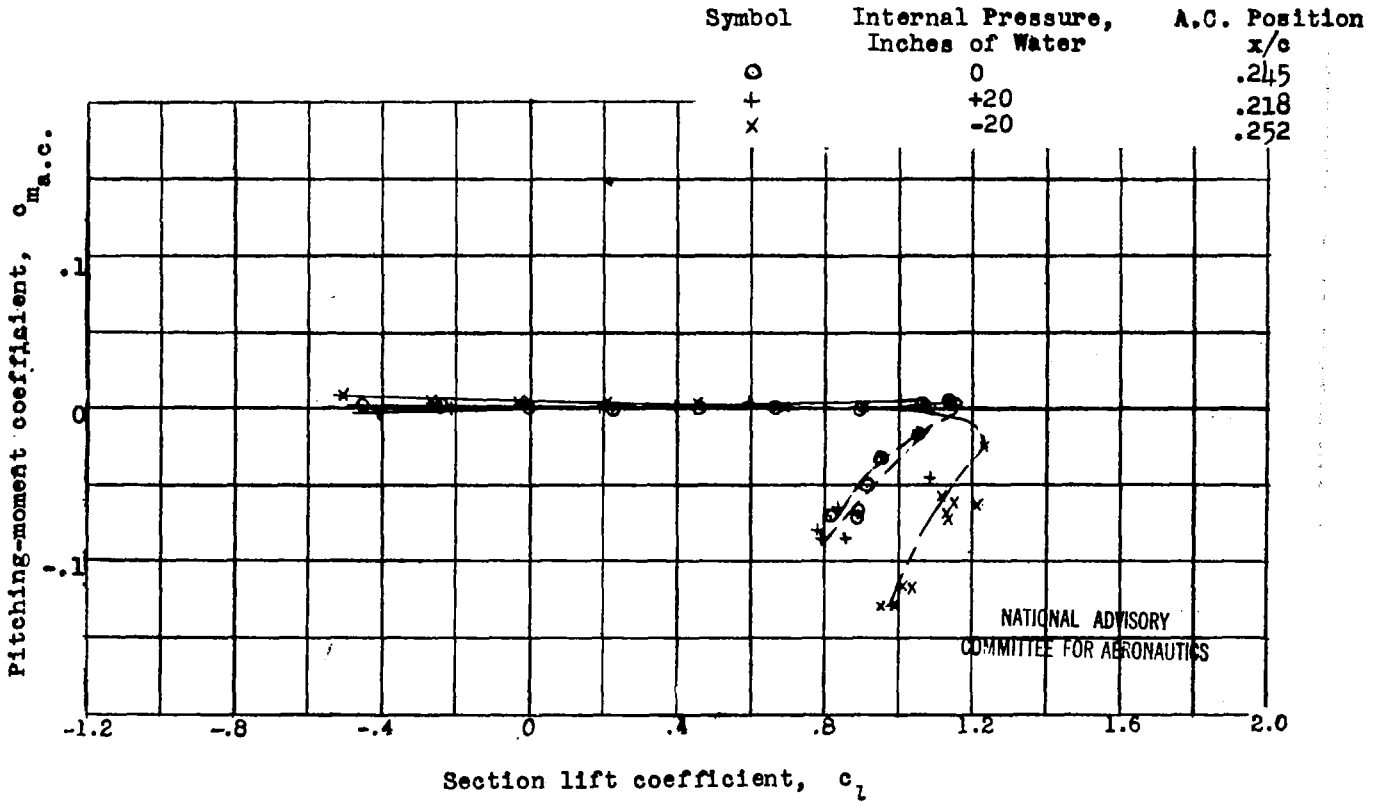

(d) Pitching-moment coefficient about aerodynamic center versus lift coefficient

Figure 18 .- Concluded.

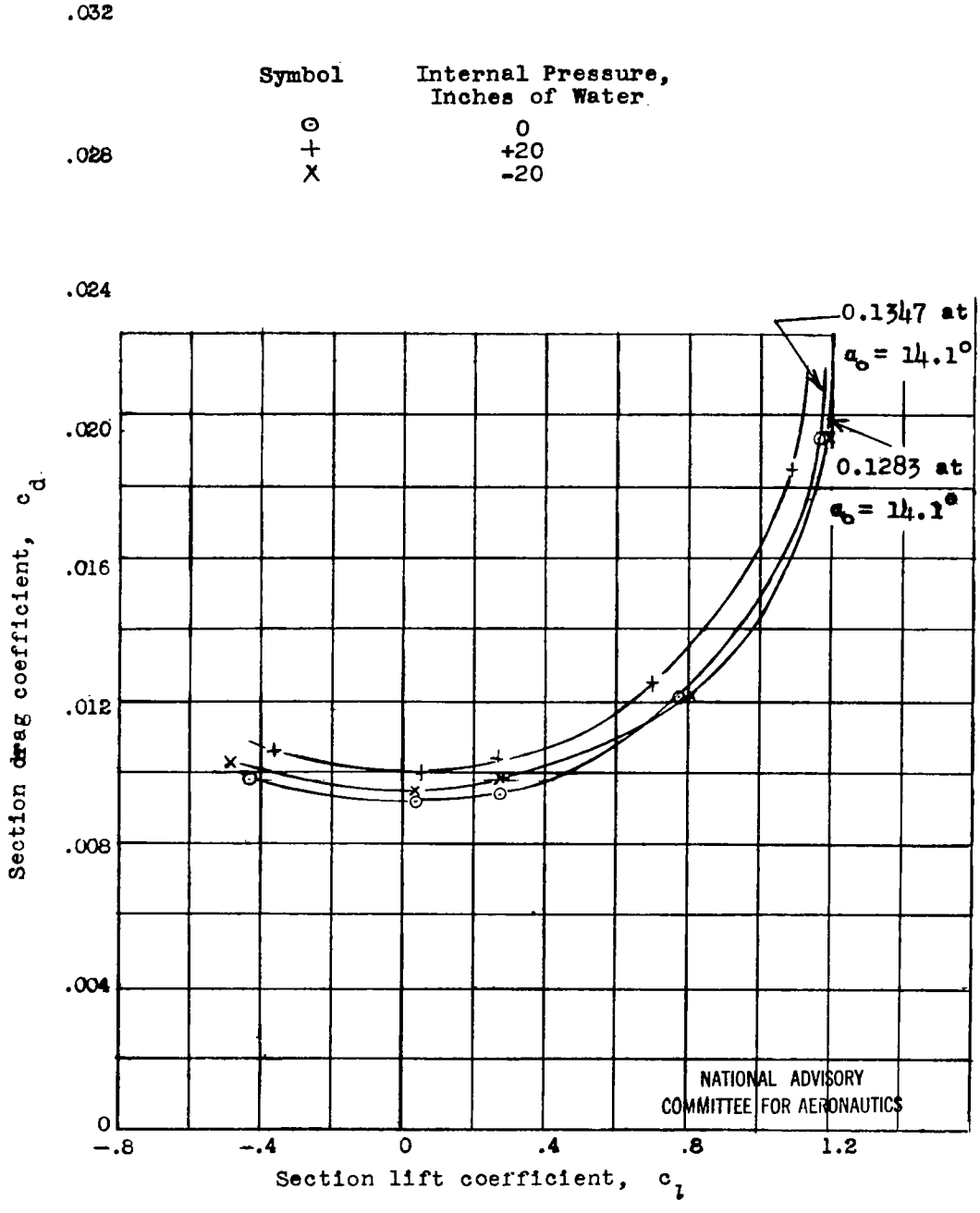

(a) Drag coefficient versus lift coefficient

Figure 19.- Aerodynamic data for the YR-4A No. 6 Helicopter test section. $R = 2.93 \times 10^6$, $M = 0.322$.

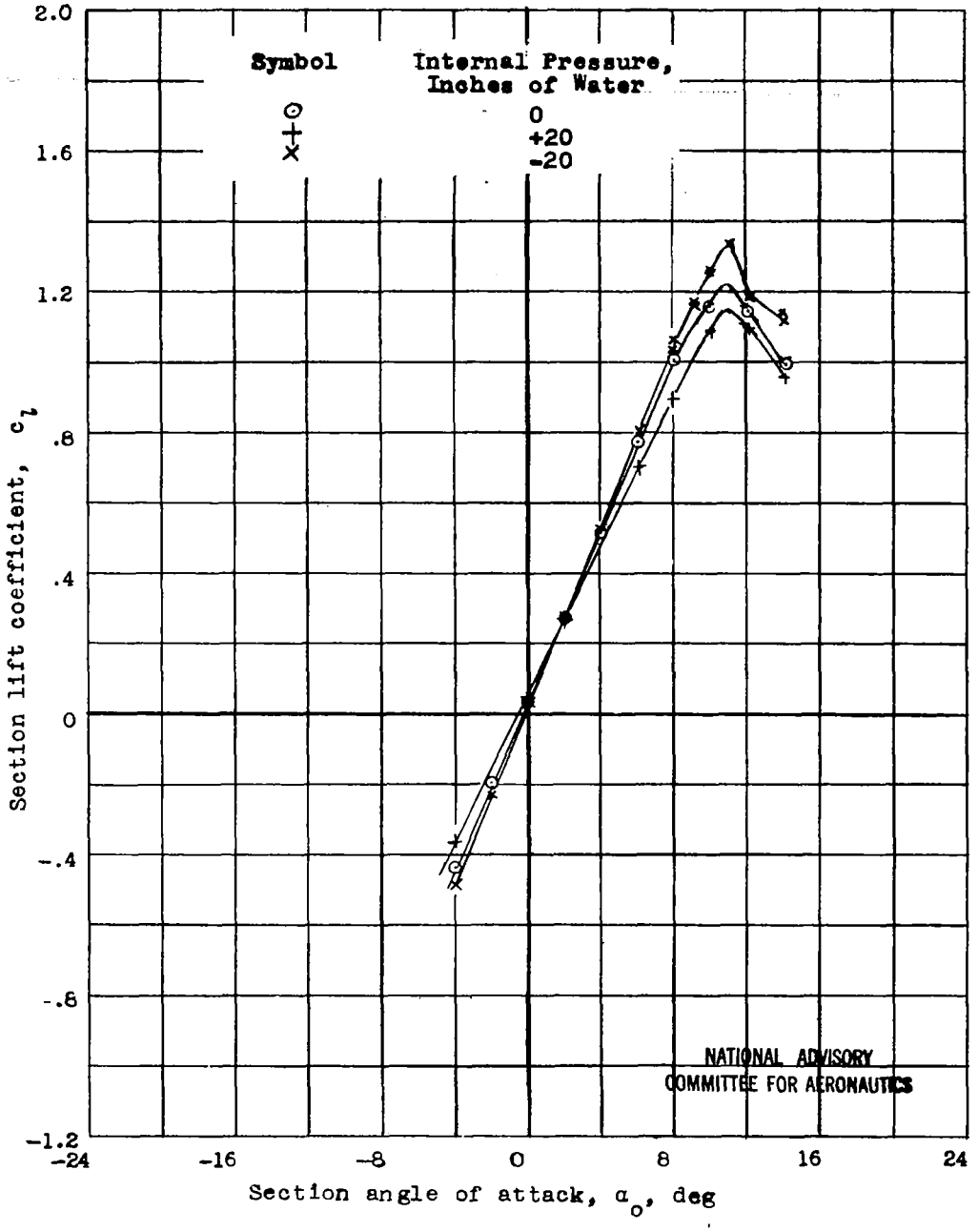

(b) Lift versus angle of attack

Figure 19.- Continued.

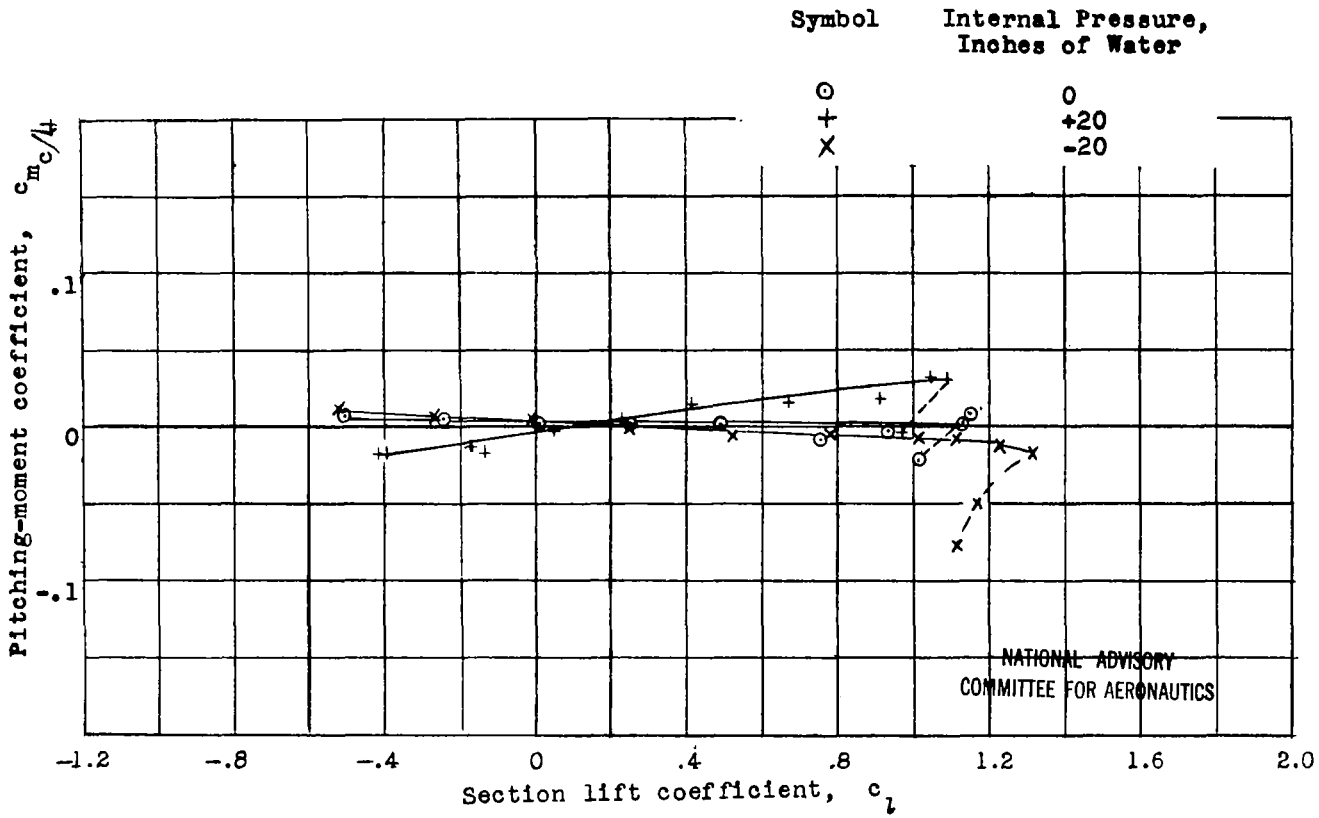

(c) Pitching-moment coefficient about quarter-chord versus lift coefficient

Figure 19.- Continued.

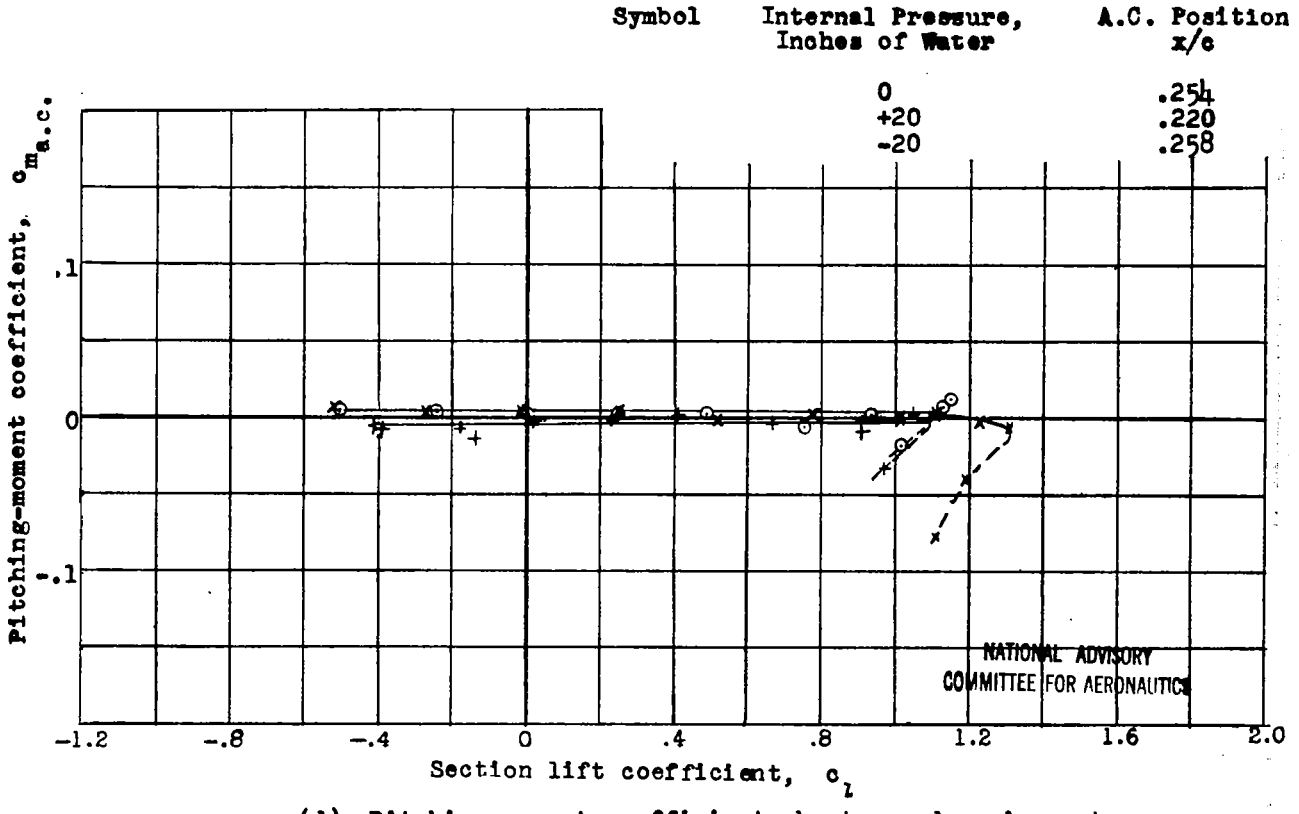

(d) Pitching-moment coefficient about aerodynamic center versus lift coefficient

Figure 19.- Concluded.

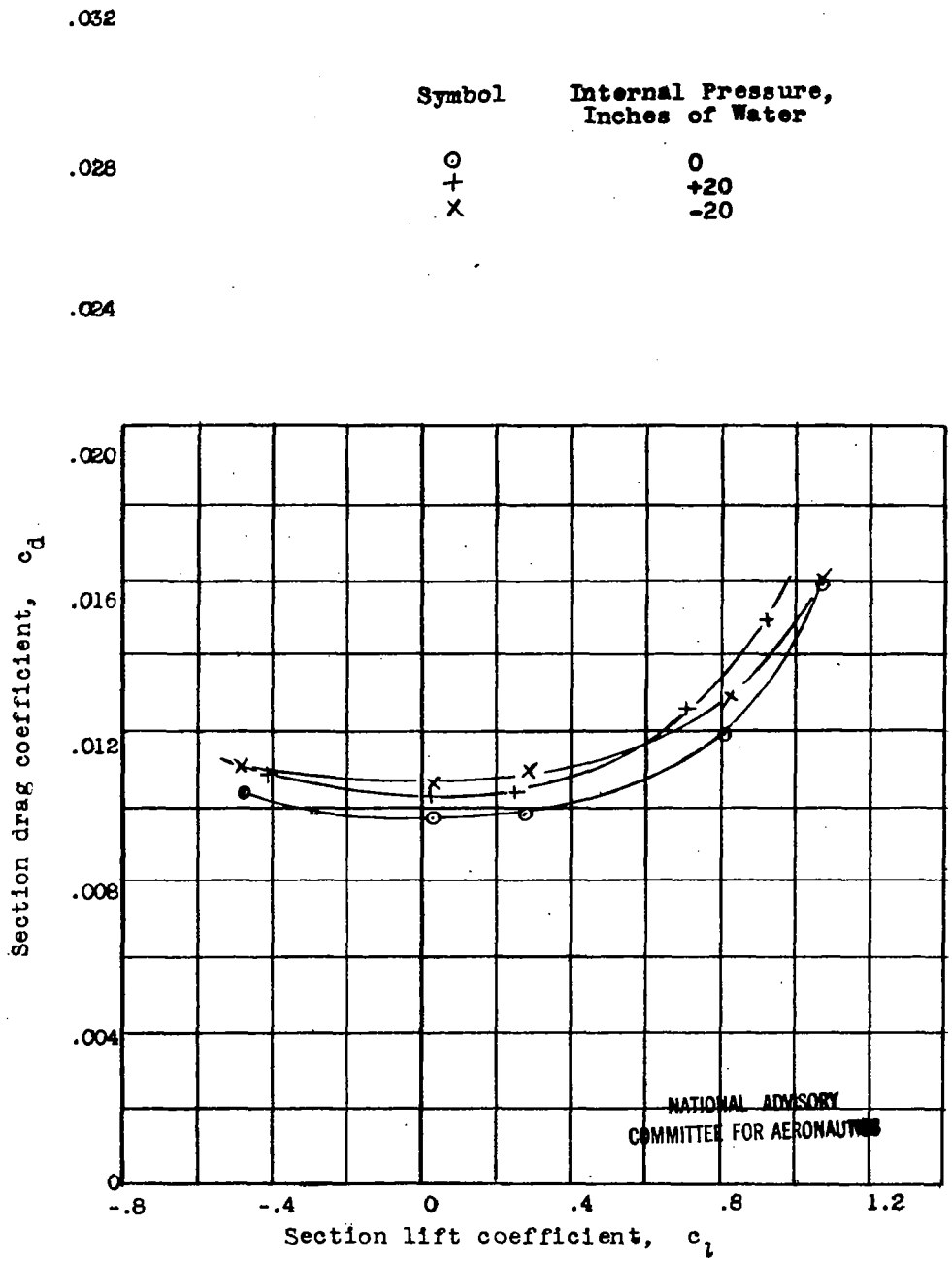

(a) Drag coefficient versus lift coefficient

Figure 20.- Aerodynamic data for the YR-4A No. 6 Helicopter test section. $R = 3.20 \times 10^6$, $M = 0.366$.

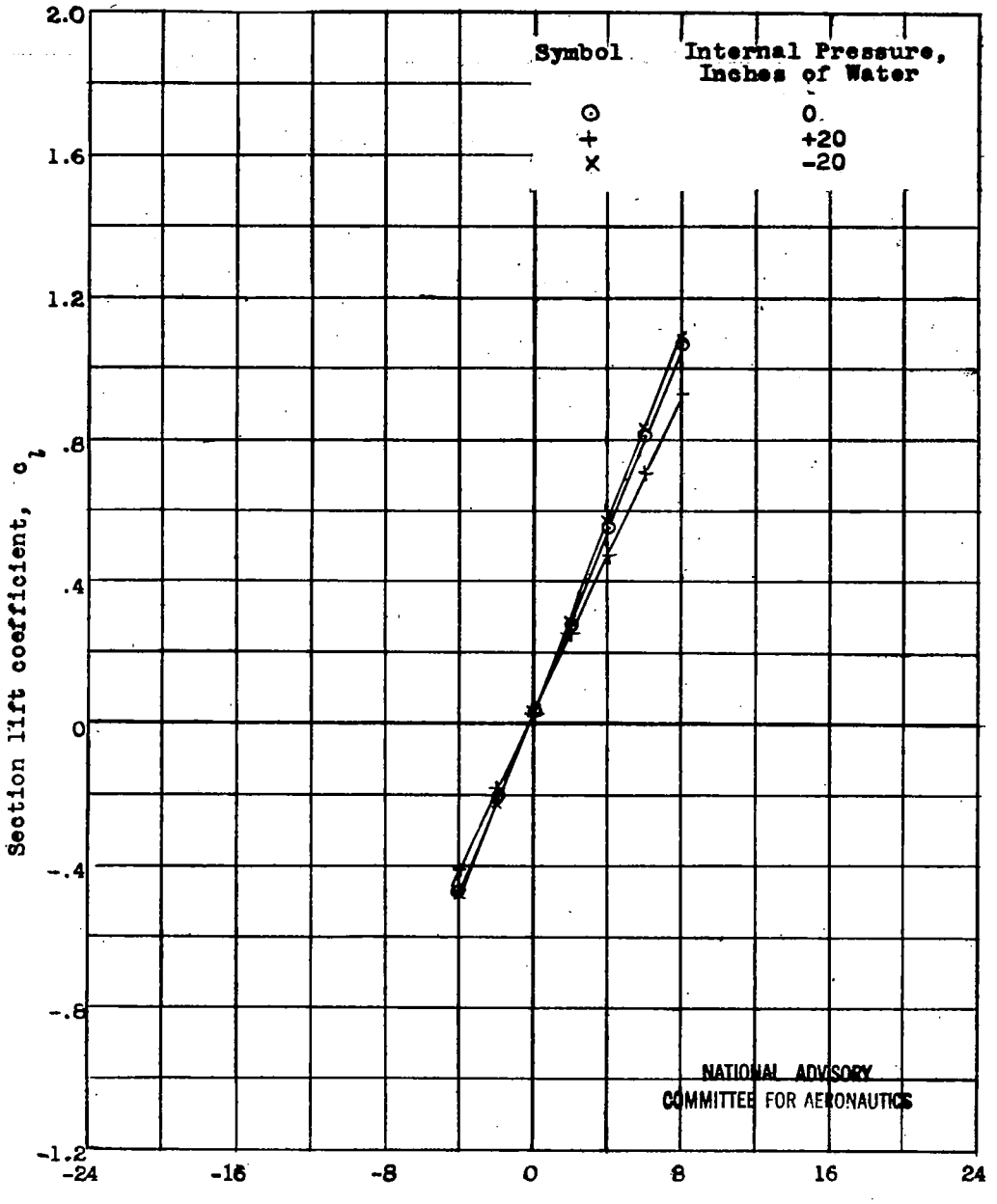

(b) Lift versus angle of attack

Figure 20.- Continued.

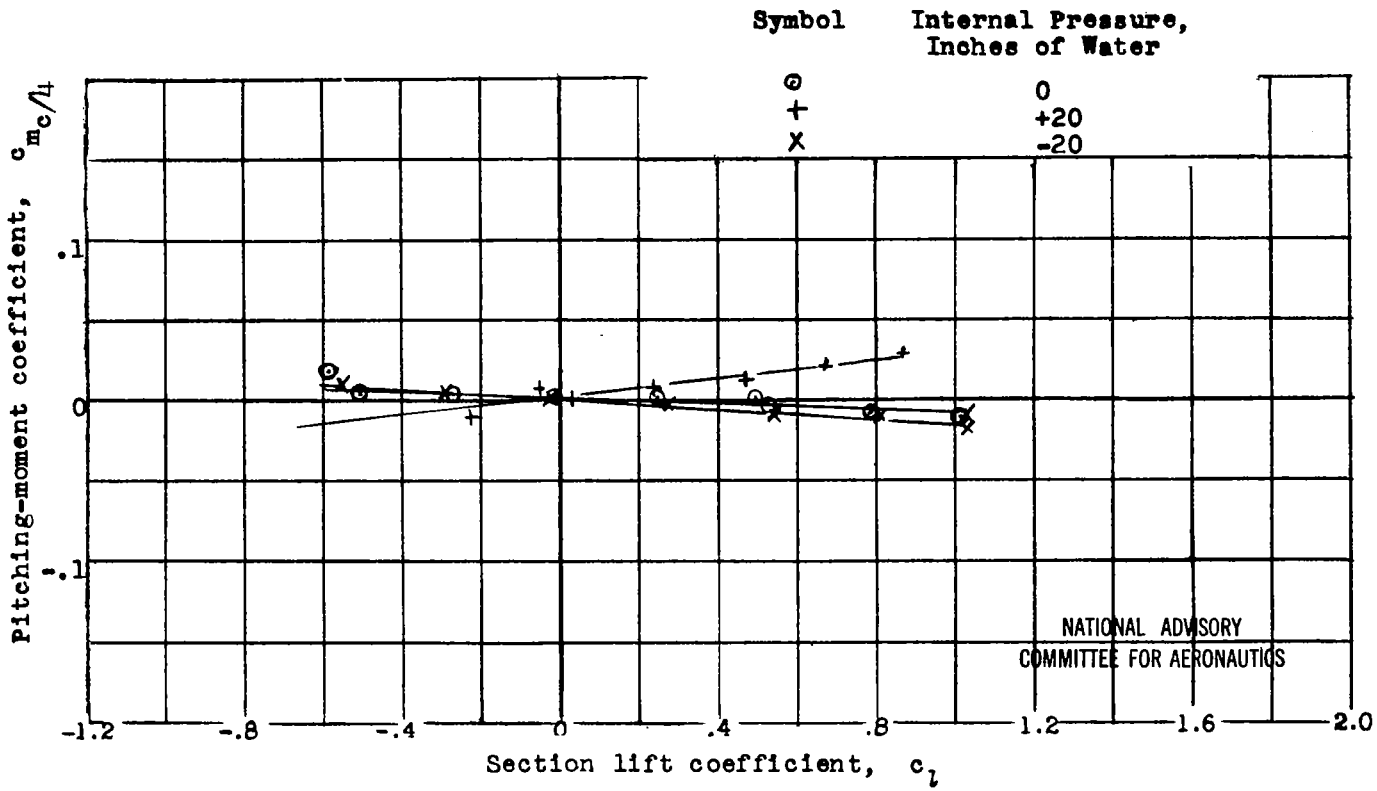

(c) Pitching-moment coefficient about quarter-chord point

Figure 20.- Continued.

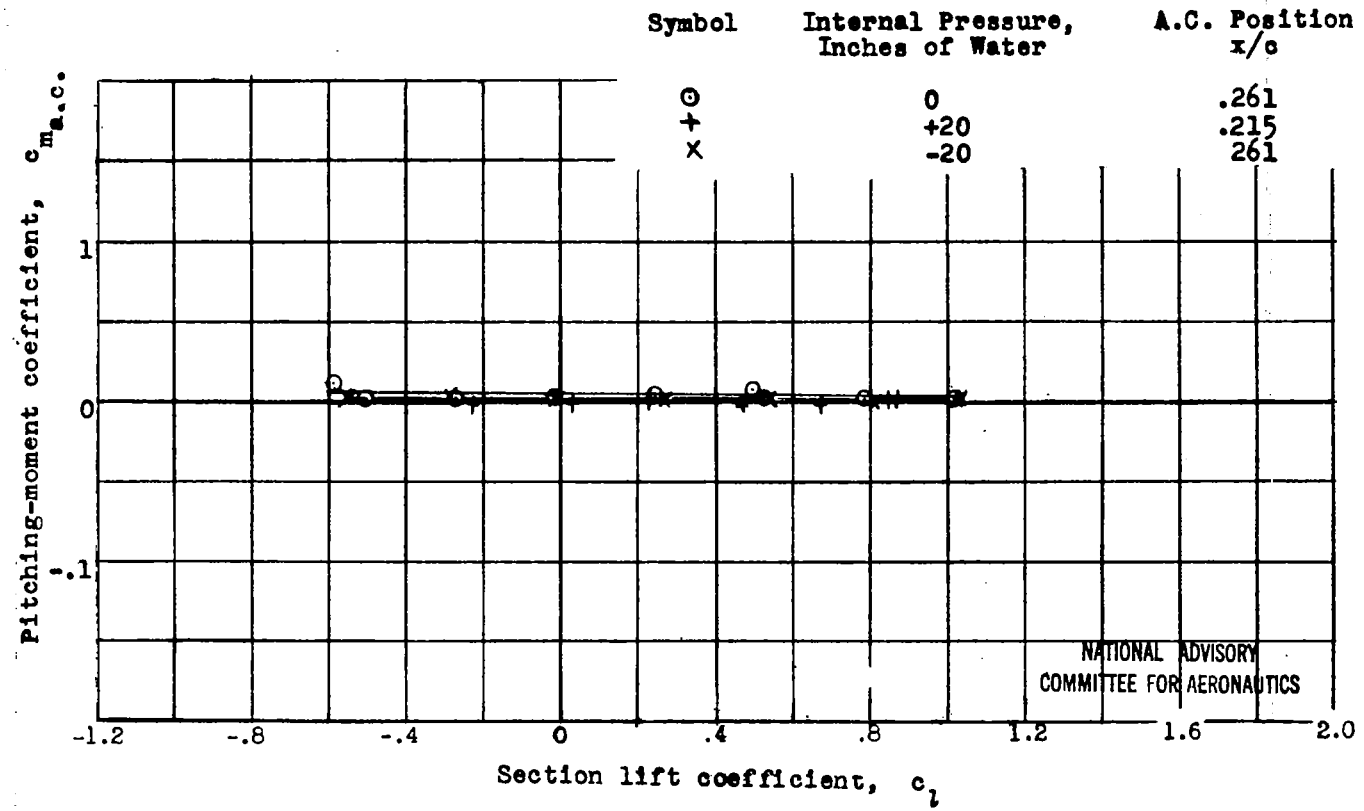

(d) Pitching-moment coefficient about aerodynamic center versus lift coefficient

Figure 20.- Concluded.

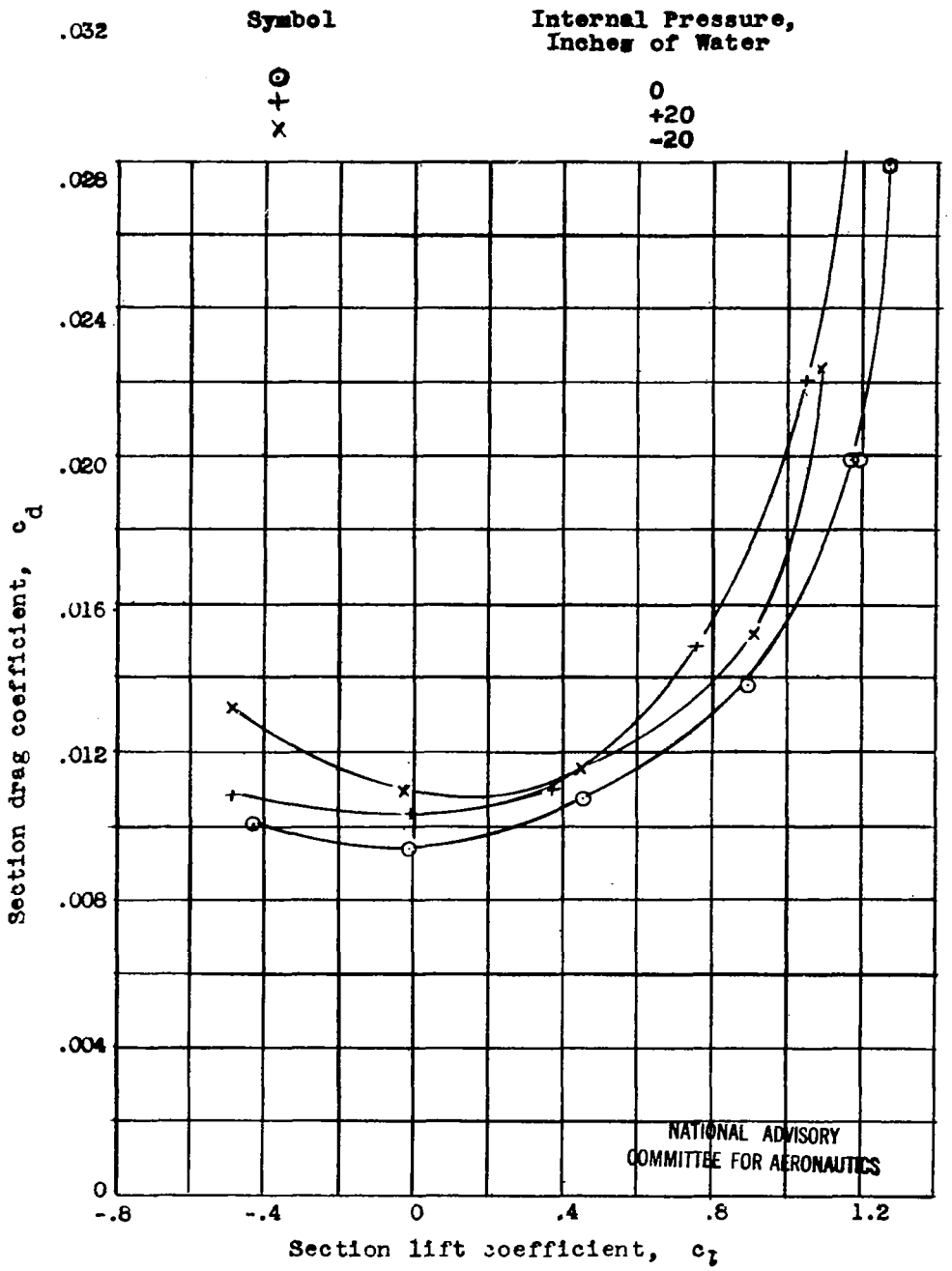

(a) Drag coefficient versus lift coefficient

Figure 21.- Aerodynamic data for the YR-4A No. 4 Helicopter test section. $R = 1.87 \times 10^6$, $M = 0.261$.

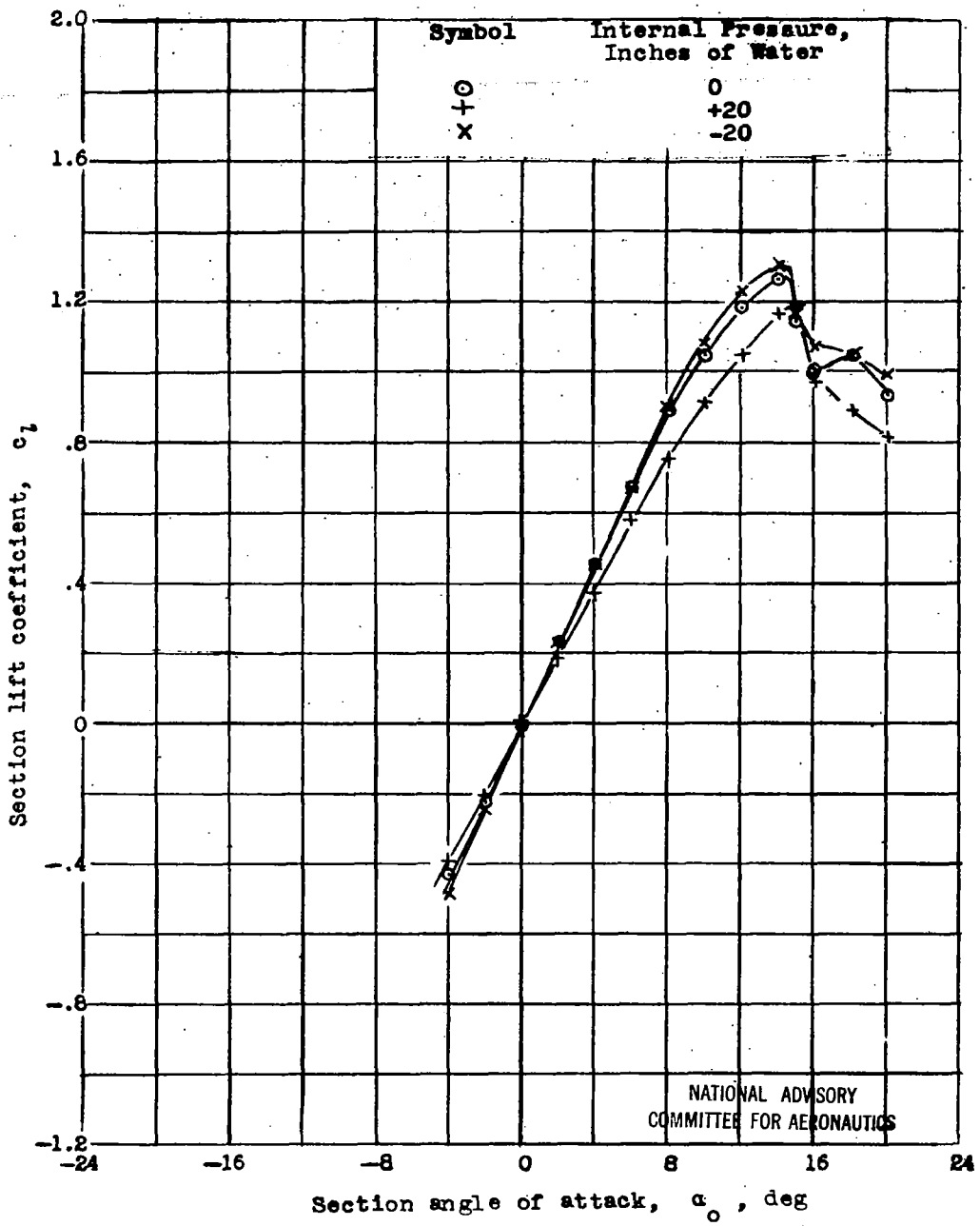

(b) Lift coefficient versus angle of attack

Figure 21.- Continued.

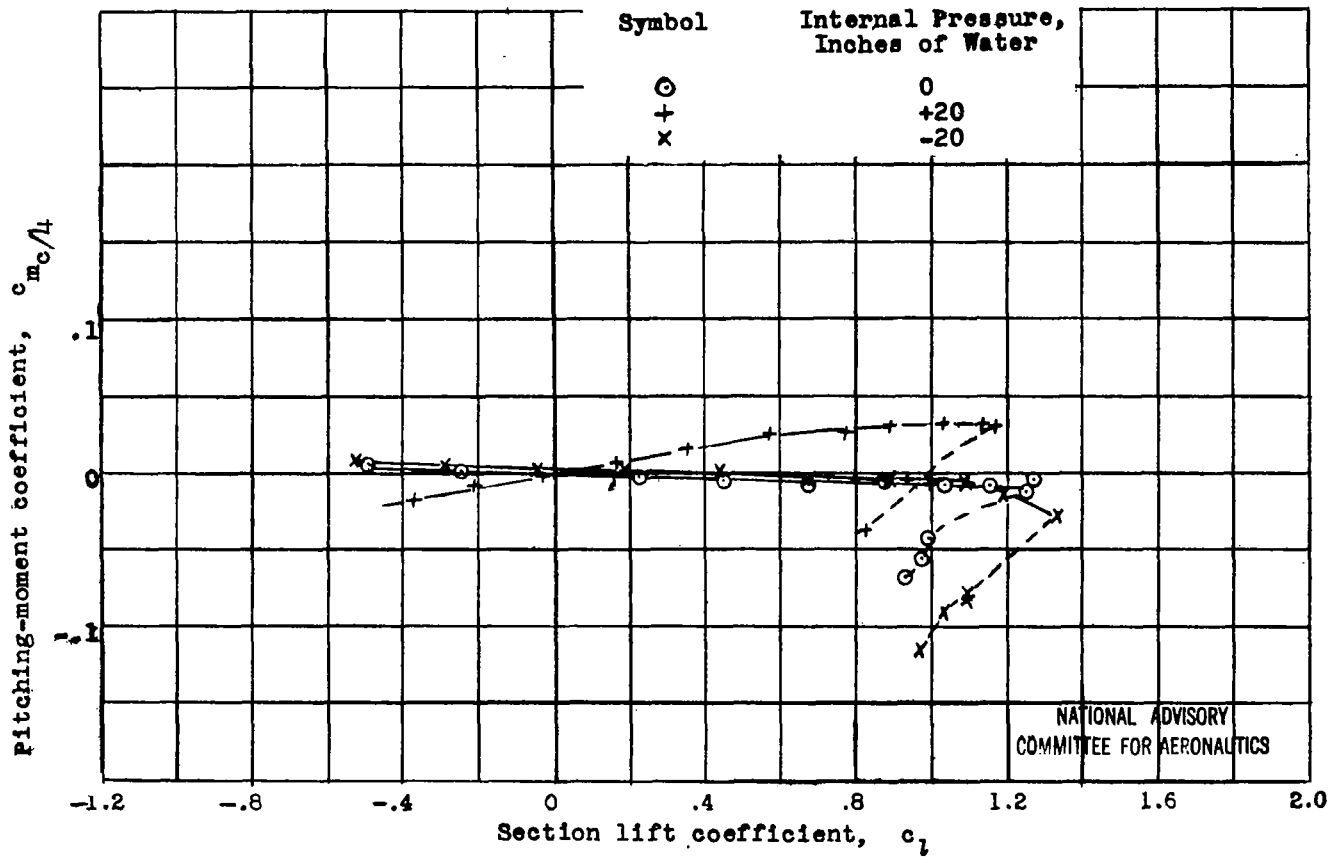

(c) Pitching-moment coefficient about quarter-chord point versus lift coefficient

Figure 21.- Continued.

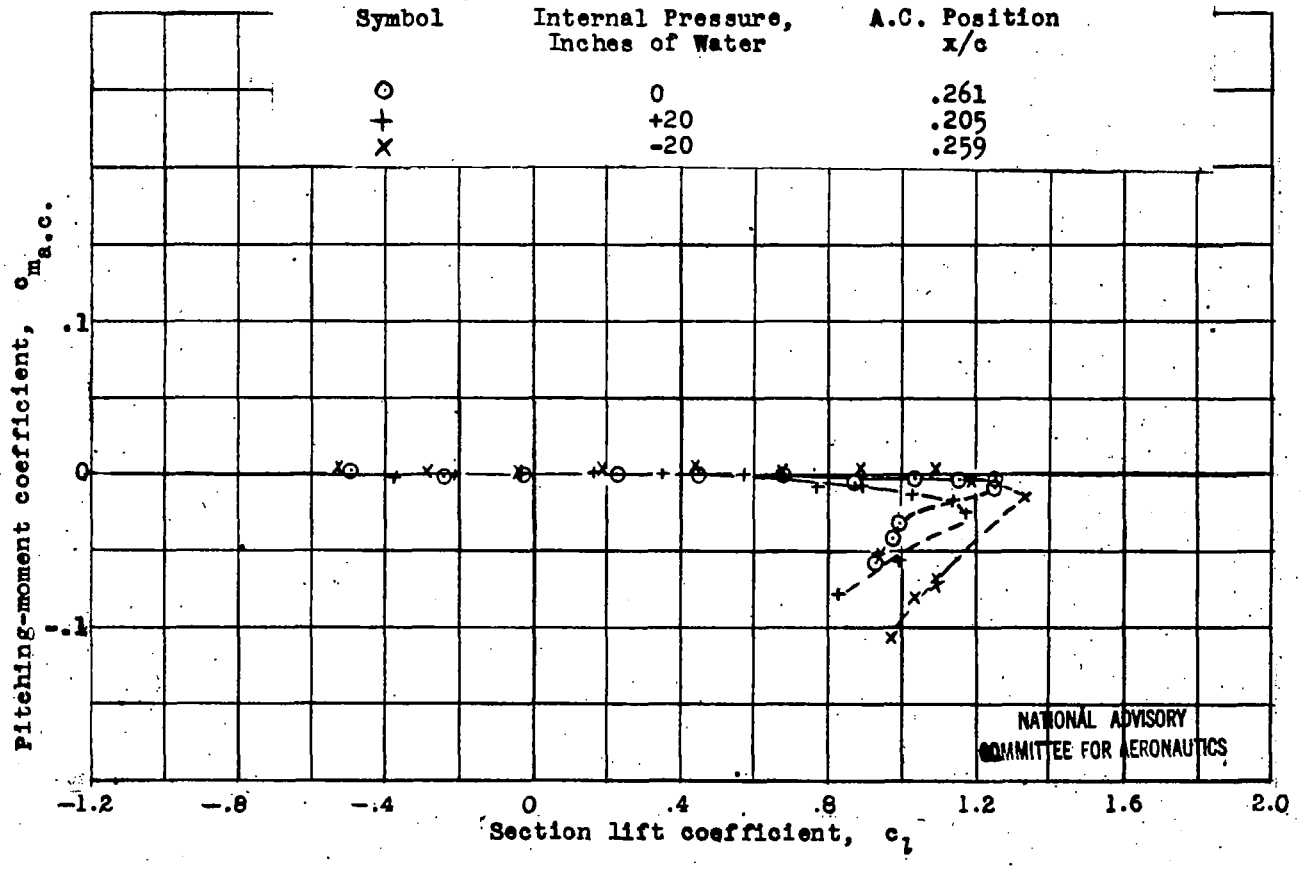

(d) Pitching-moment coefficients about aerodynamic centers versus lift coefficient.

Figure 21.- Concluded.

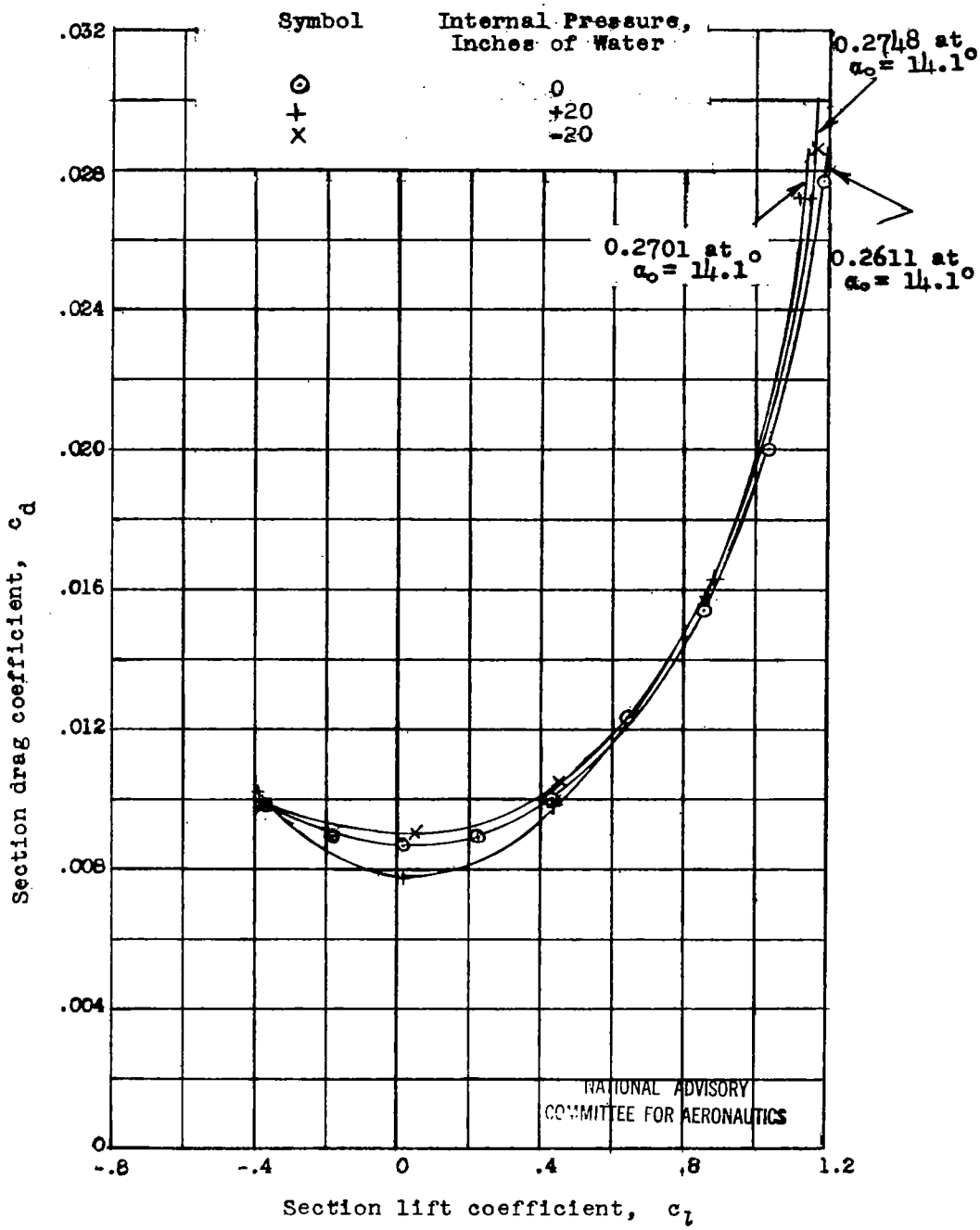

(a) Drag coefficient versus lift coefficient

Figure 22.- Aerodynamic characteristics of the YR-4A No. 10 Helicopter test section. R = .91 × 10^6, M = 0.131.

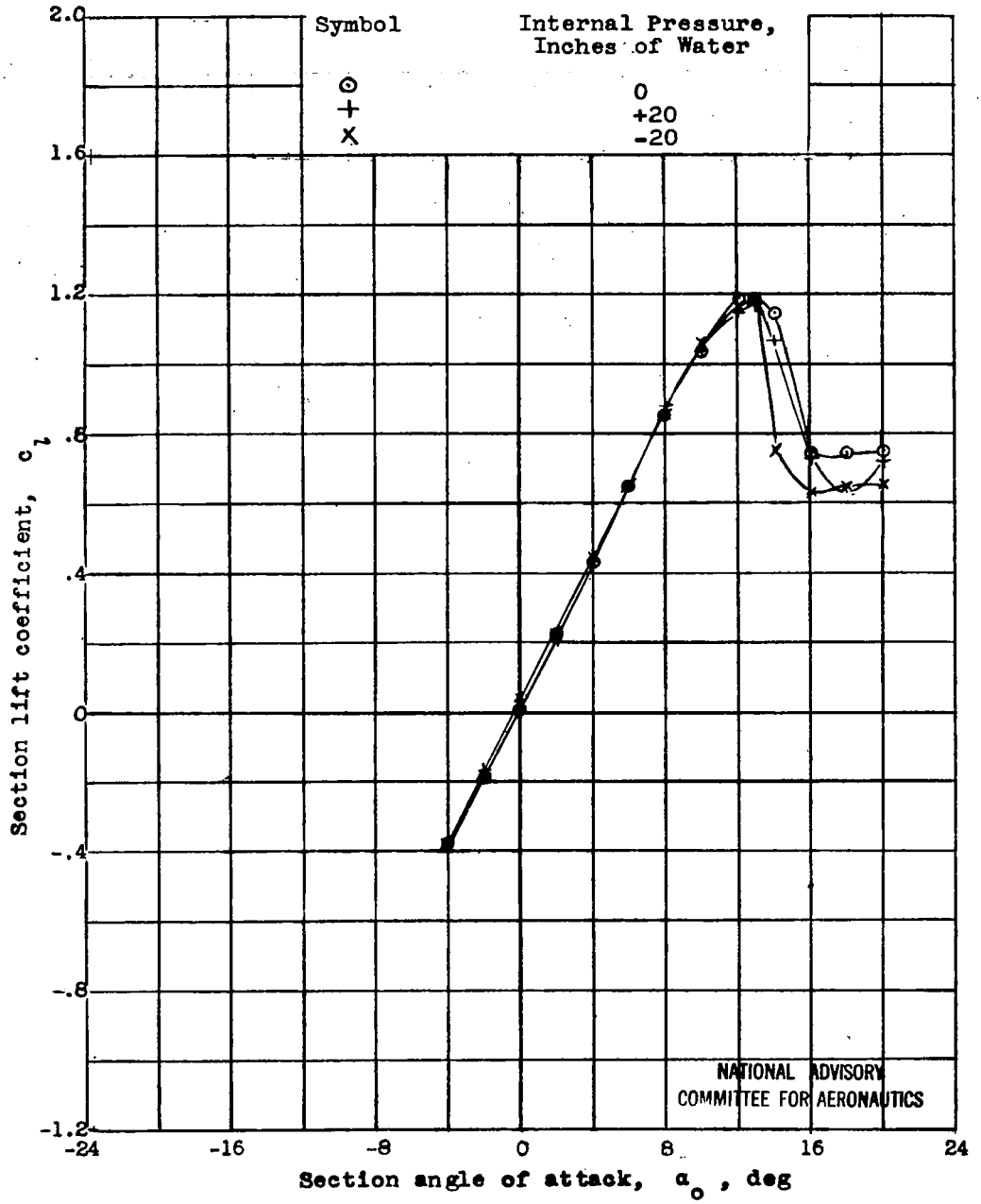

(b) Lift coefficient versus angle of attack

Figure 22.- Continued.

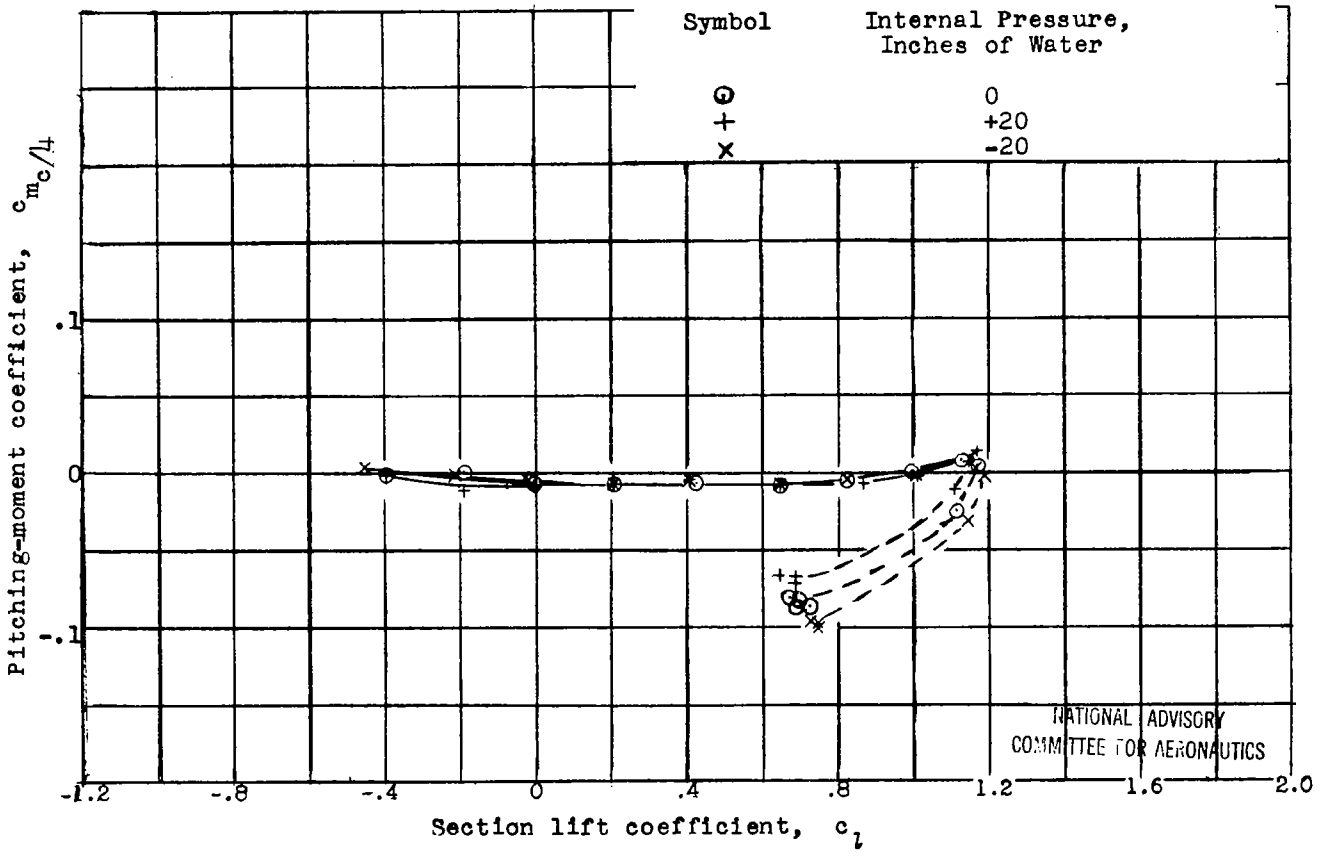

(c) Pitching-moment coefficient about quarter-chord point versus lift coefficient

Figure 22.- Concluded.

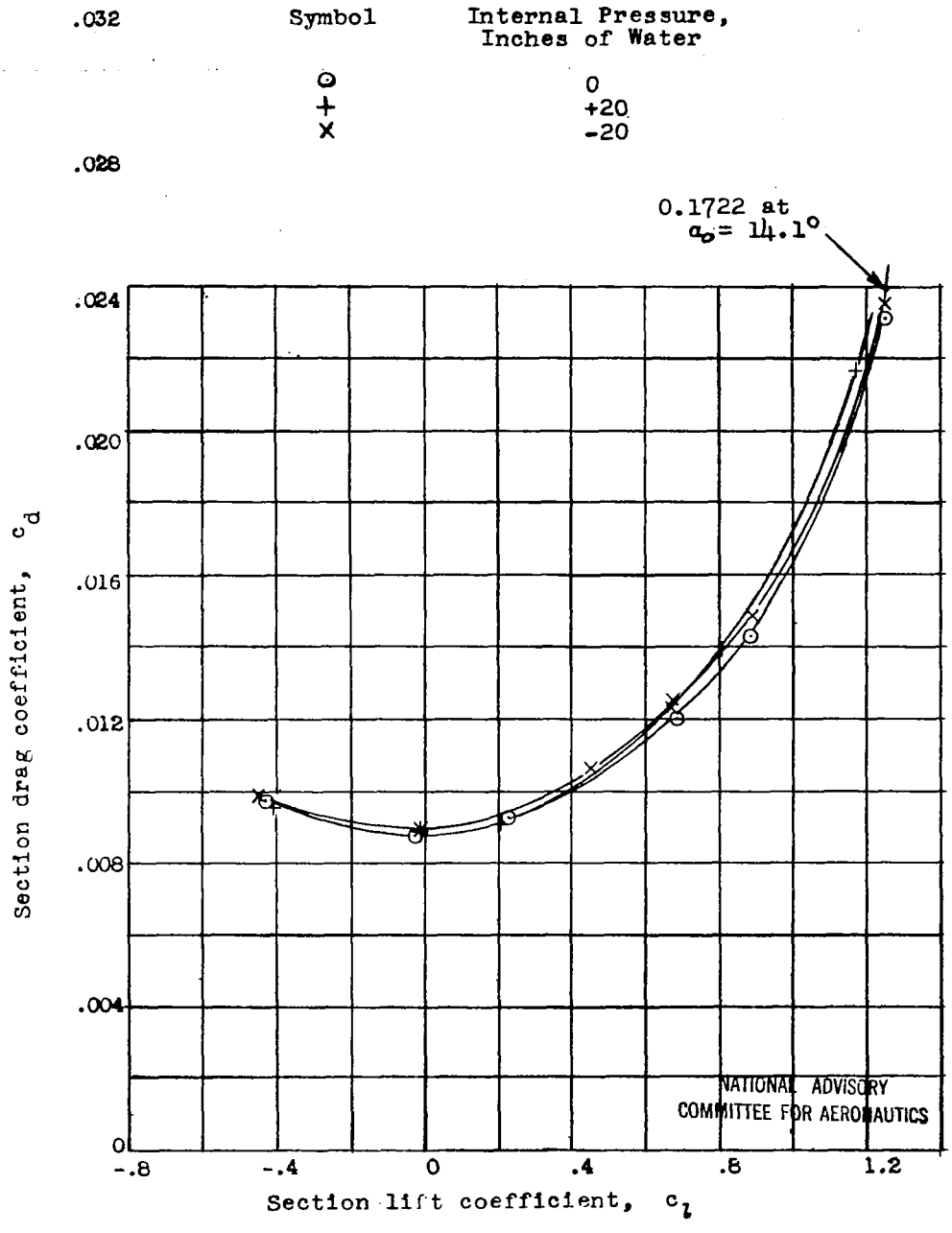

(a) Drag coefficient versus lift coefficient

Figure 23.- Aerodynamic data for the YR-4A No. 10 Helicopter test section. R = 1.84×10^6, M = 0.262.

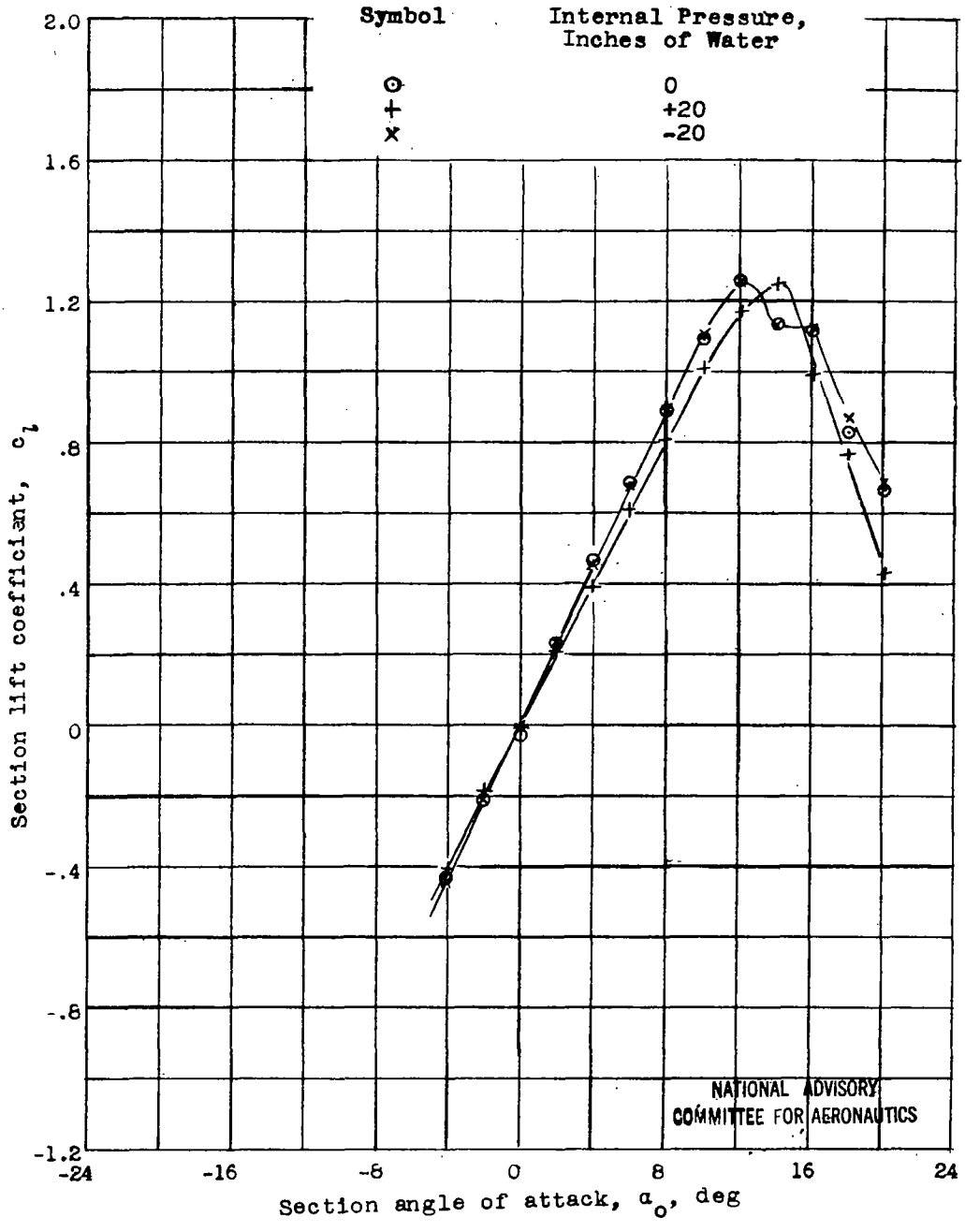

(b) Lift coefficient versus angle of attack

Figure 23.- Continued.

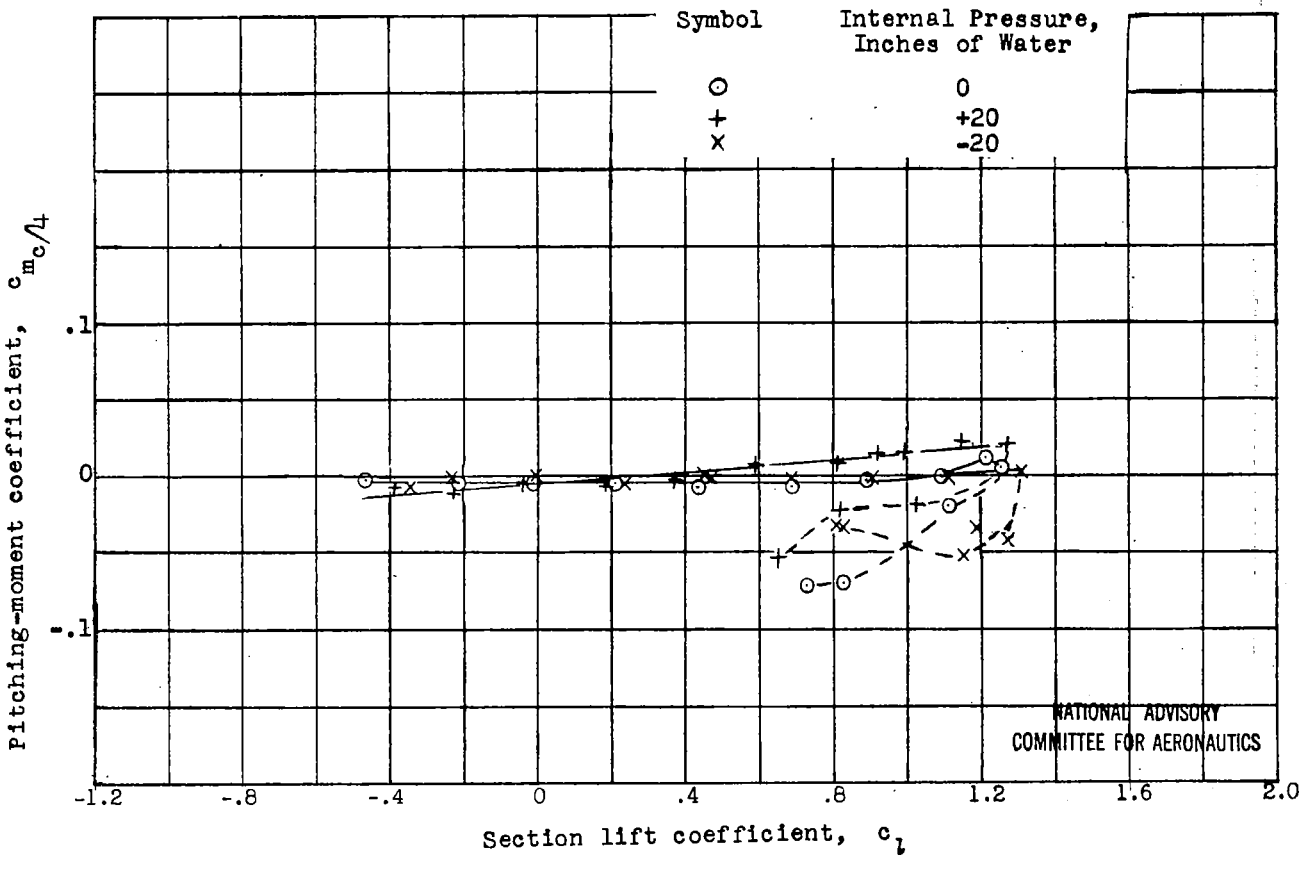

(c) Pitching-moment coefficient about quarter-chord point versus lift coefficient

Figure 23.- Continued.

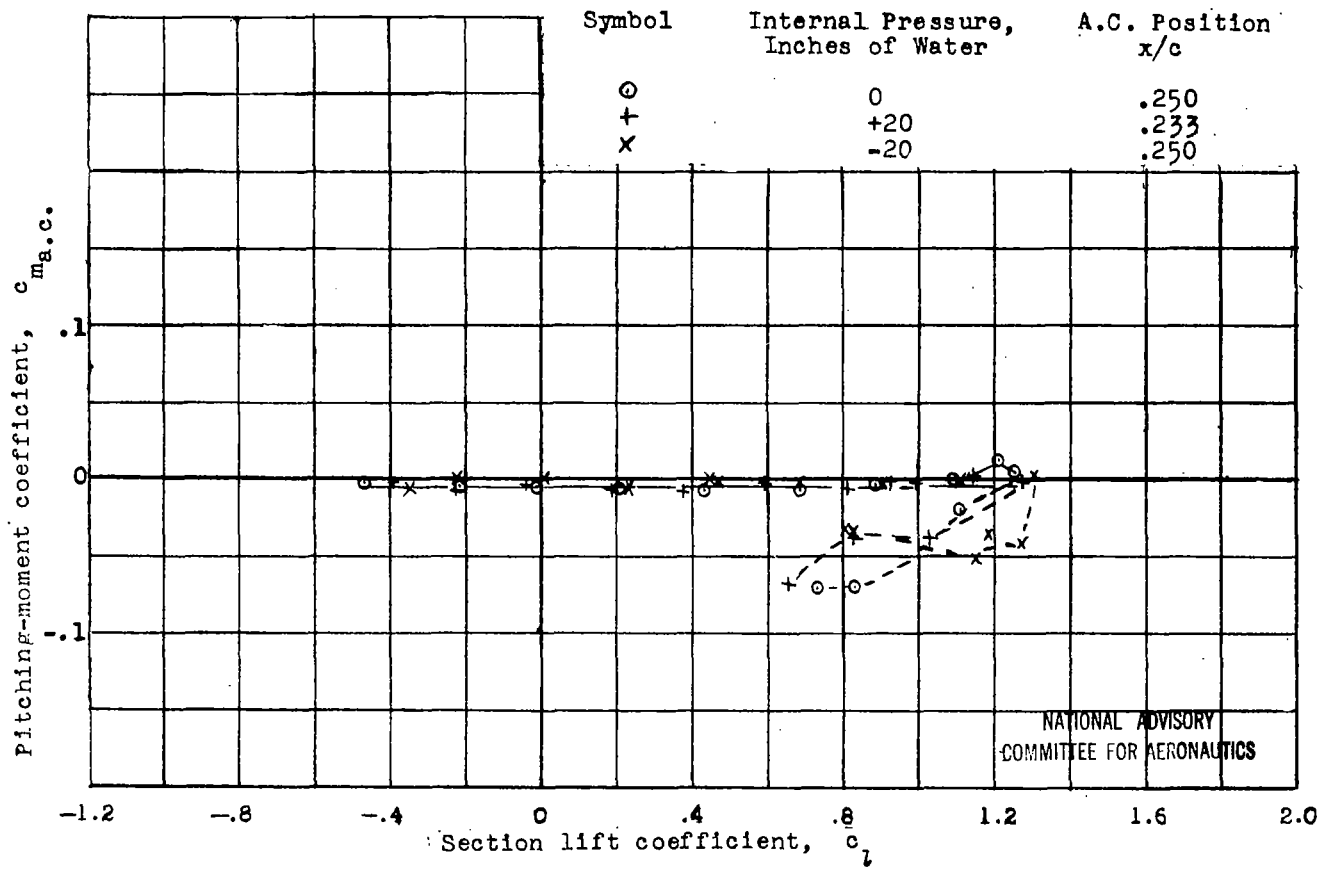

(d) Pitching-moment coefficient about aerodynamic centers versus lift coefficient

Figure 23.- Concluded.

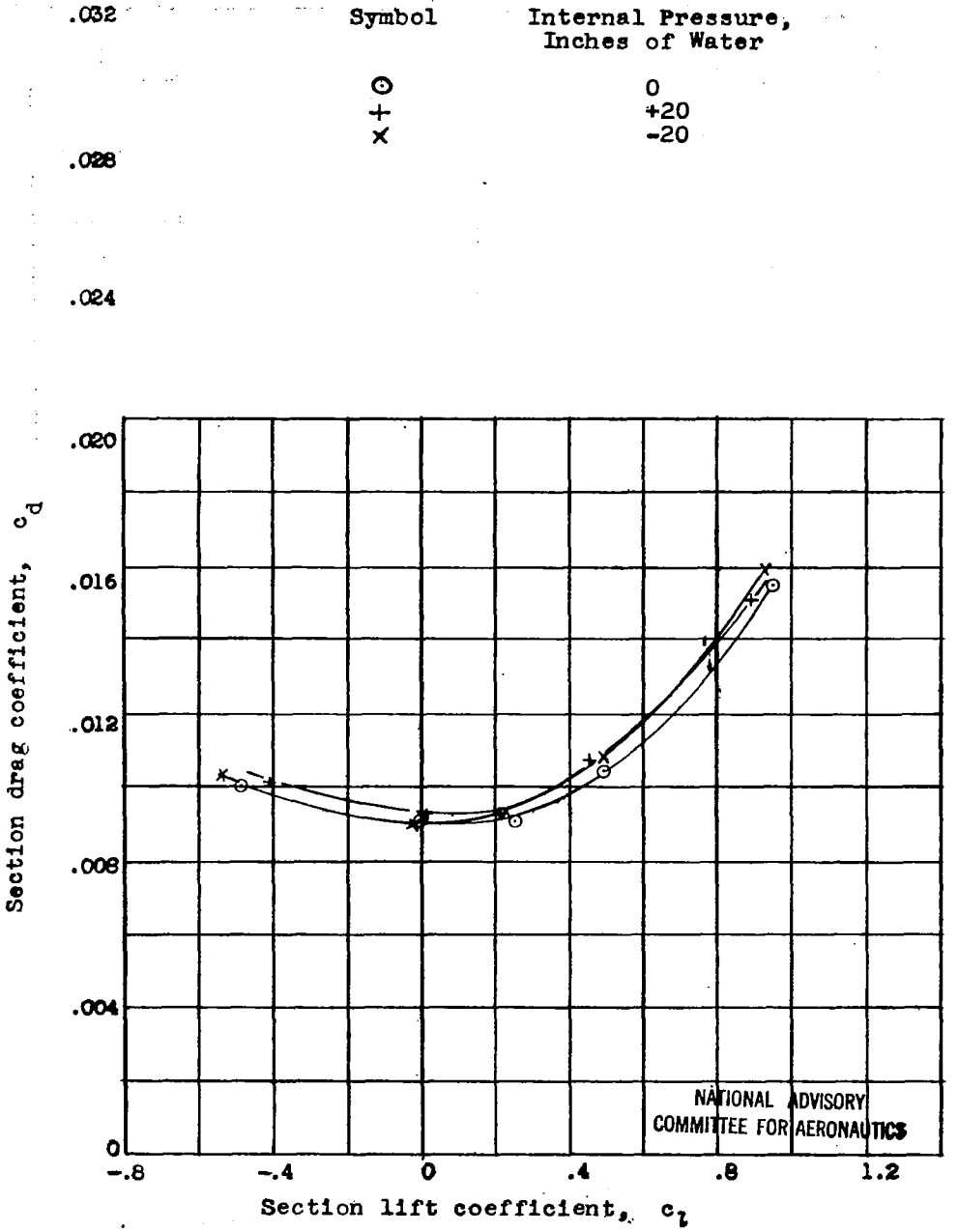

(a) Drag coefficient versus lift coefficient

Figure 24.- Aerodynamic characteristics of the YR-4A No. 10 Helicopter test section. $R = 2.59 \times 10^6$, $M = 0.376$.

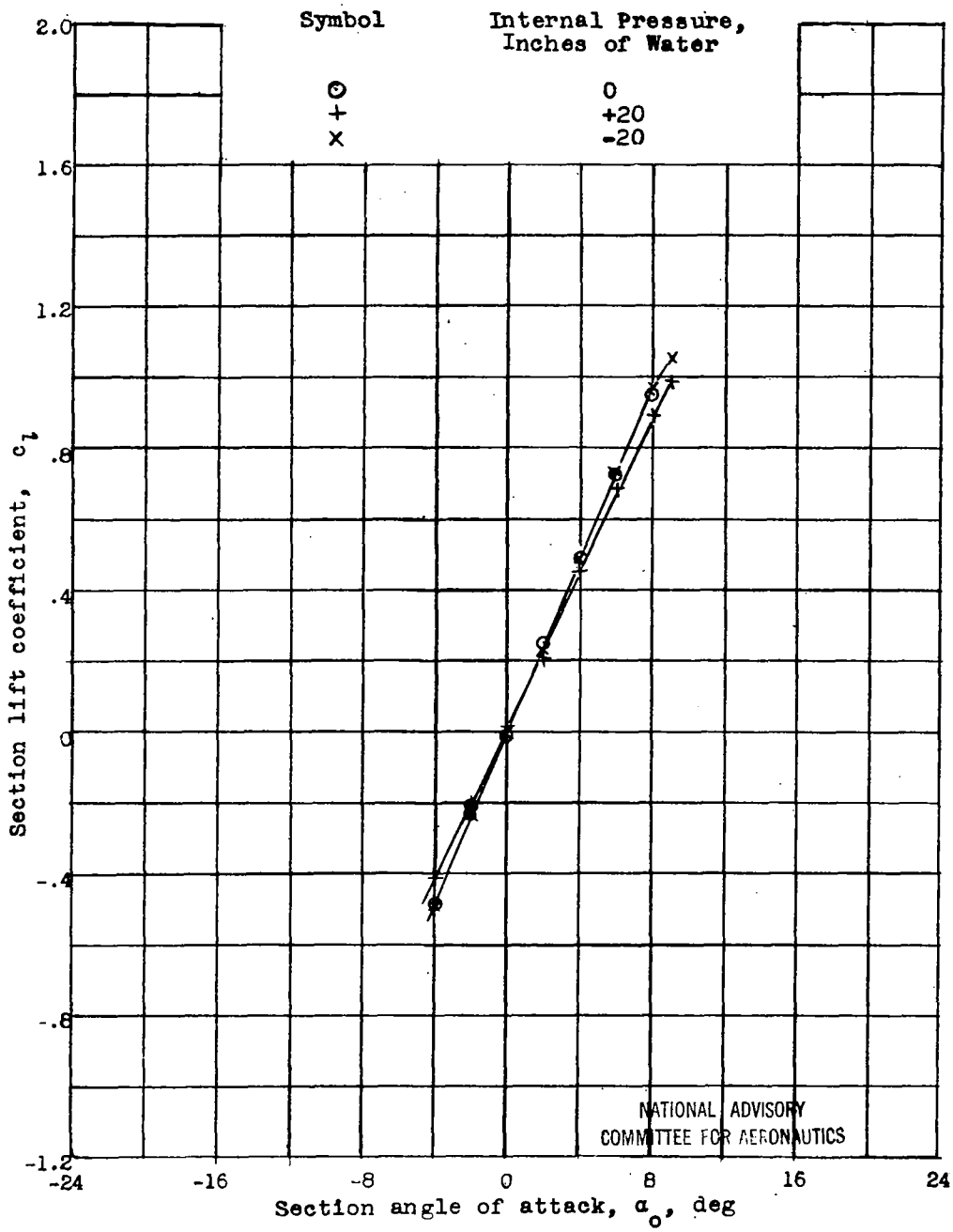

(b) Lift coefficient versus angle of attack

Figure 24.- Continued.

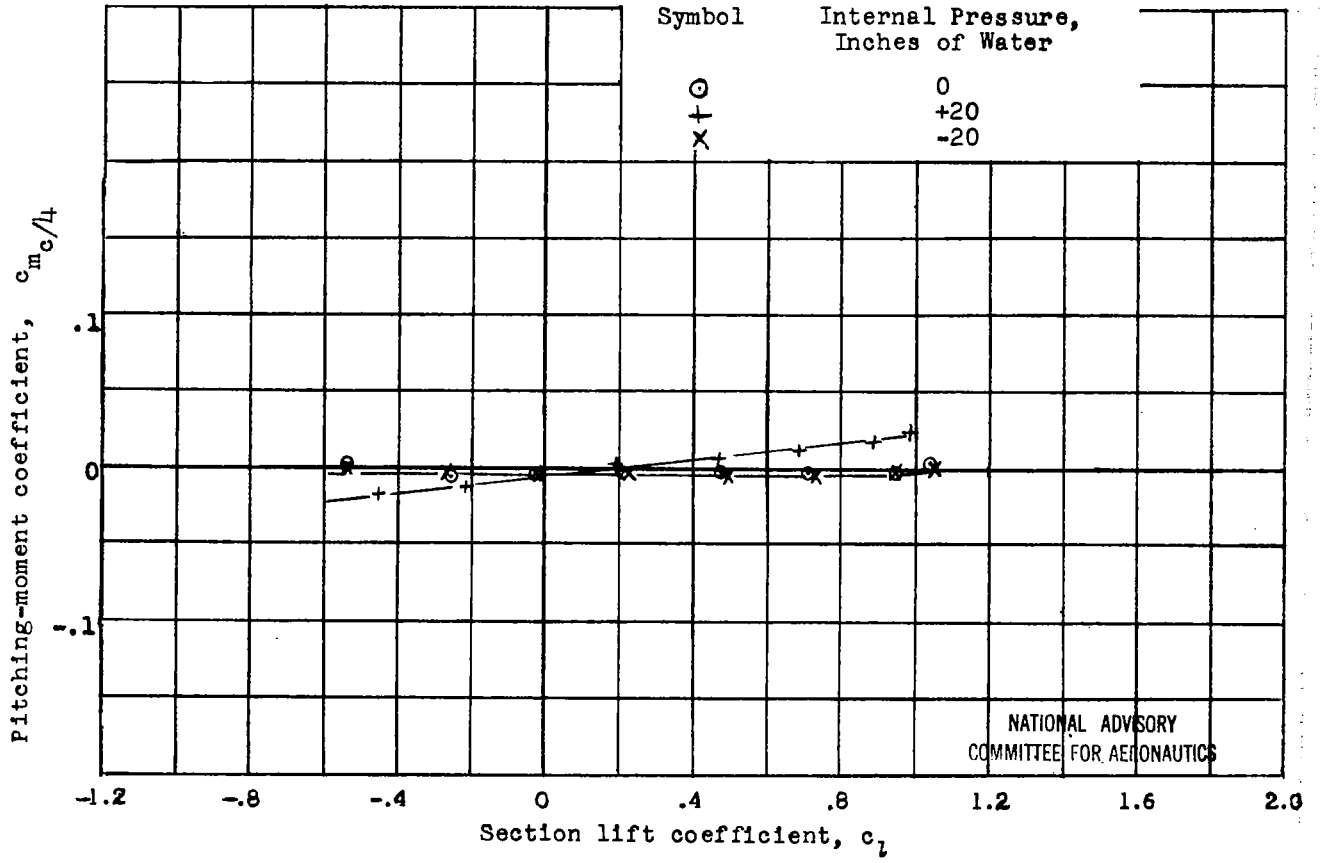

(c) Pitching-moment coefficient about quarter-chord point versus lift coefficient

Figure 24.- Continued.

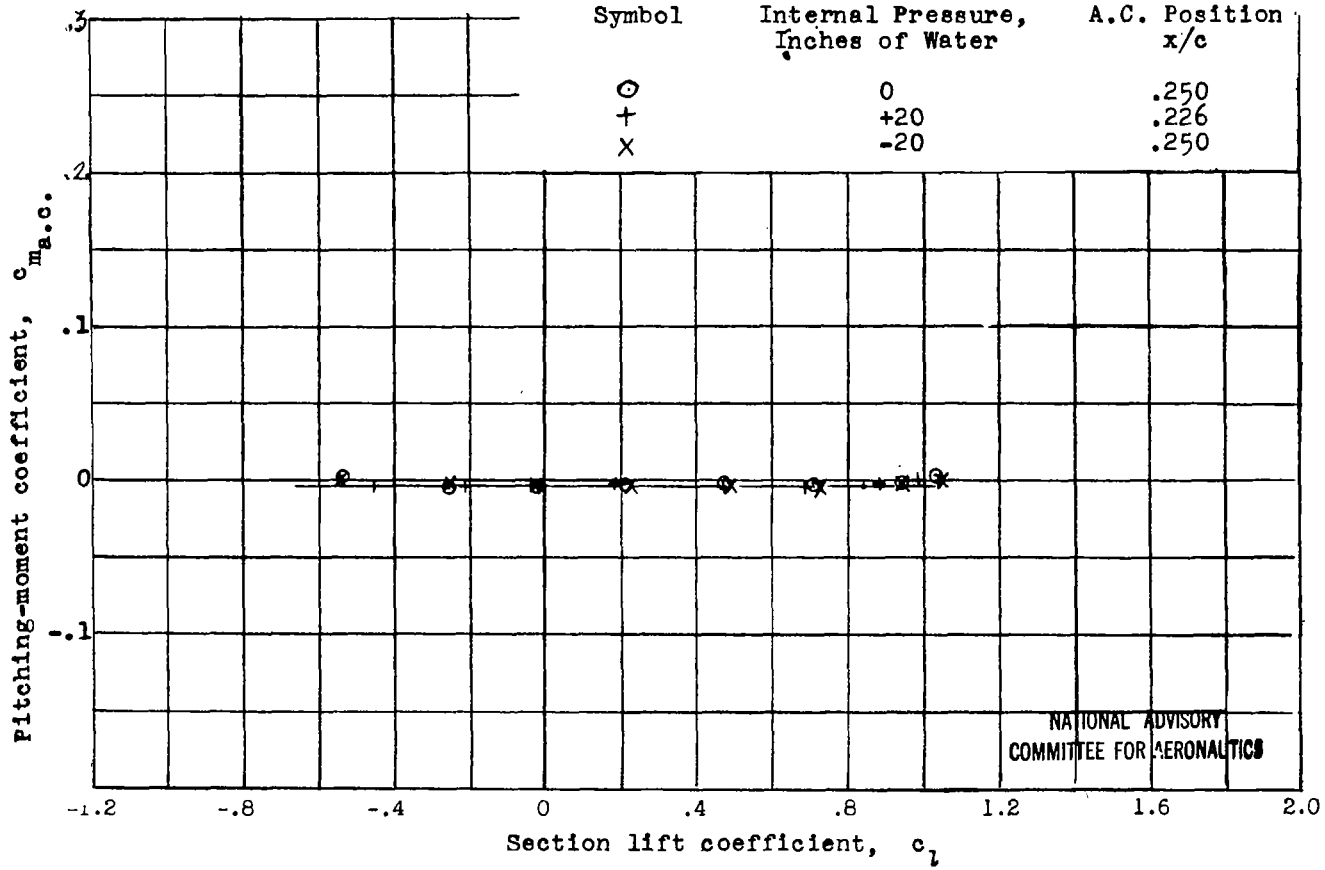

(d) Pitching-moment coefficient about aerodynamic centers versus lift coefficient.

Figure 24.- Concluded.

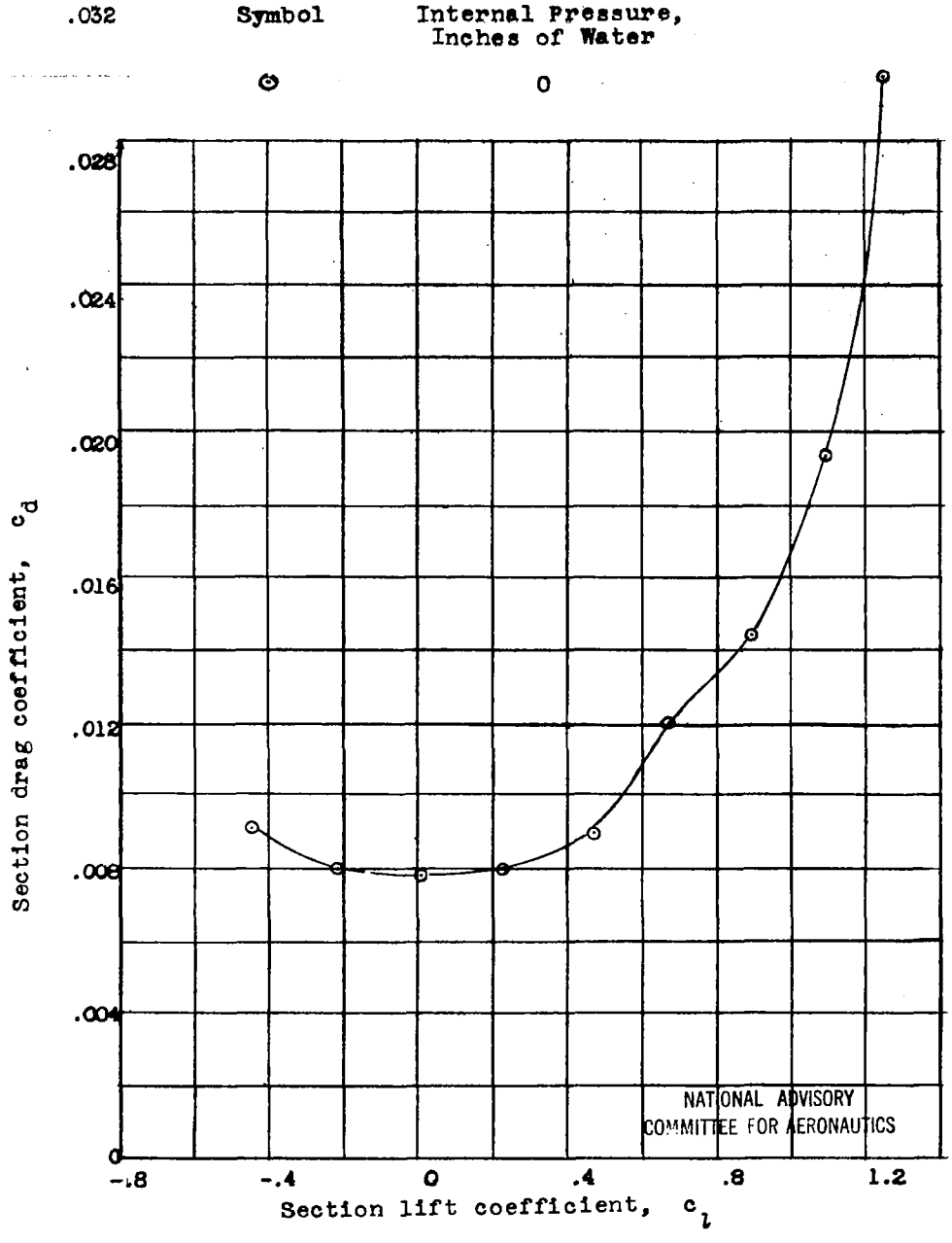

(a) Drag coefficient versus lift coefficient

Figure 25.- Aerodynamic data for the YR-4A No. 10 (Smooth Forward Portion) Helicopter test section. R = 1.84×10^6, M = 0.262.

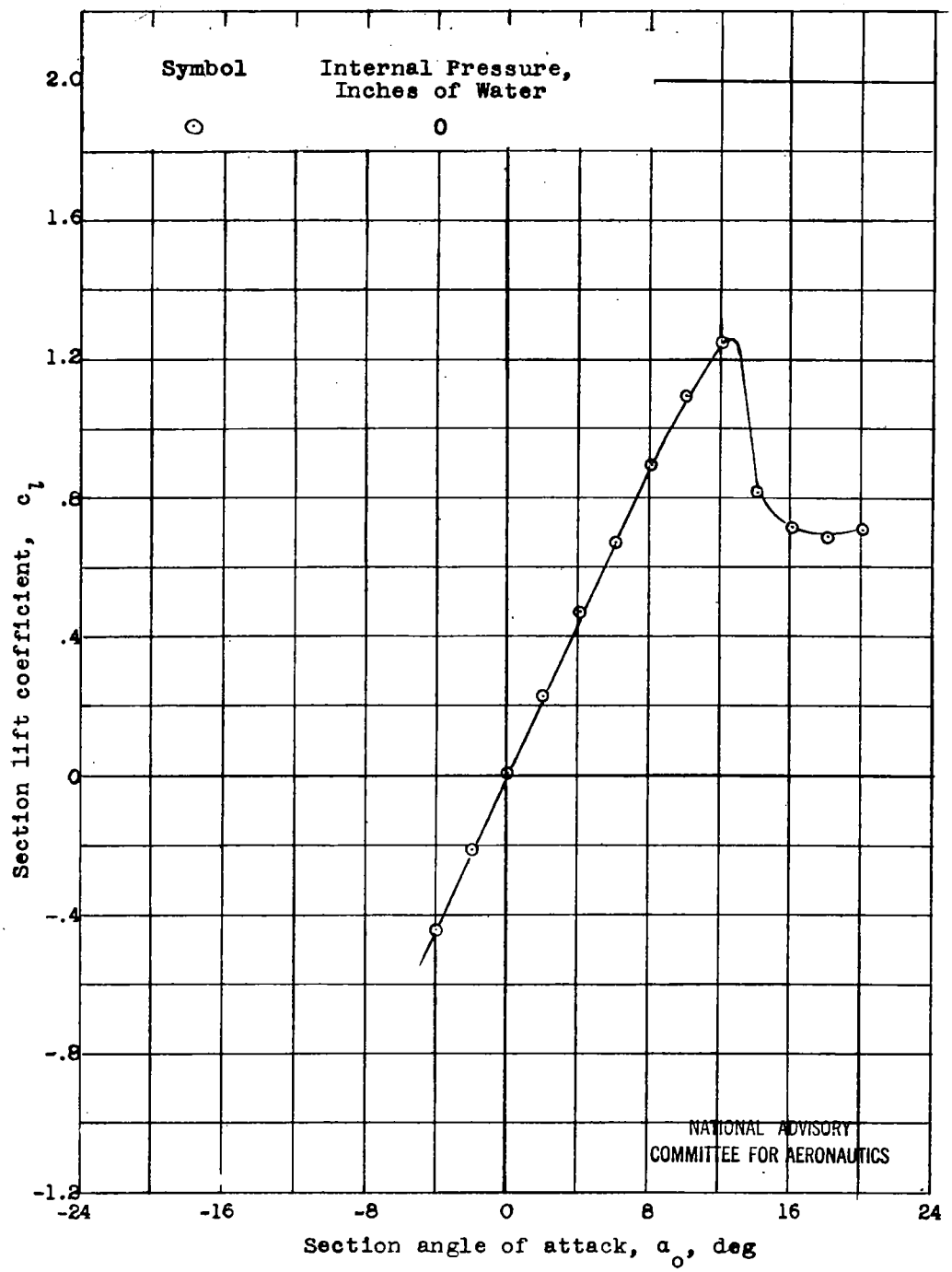

(b) Lift coefficient versus angle of attack.

Figure 25.- Continued.

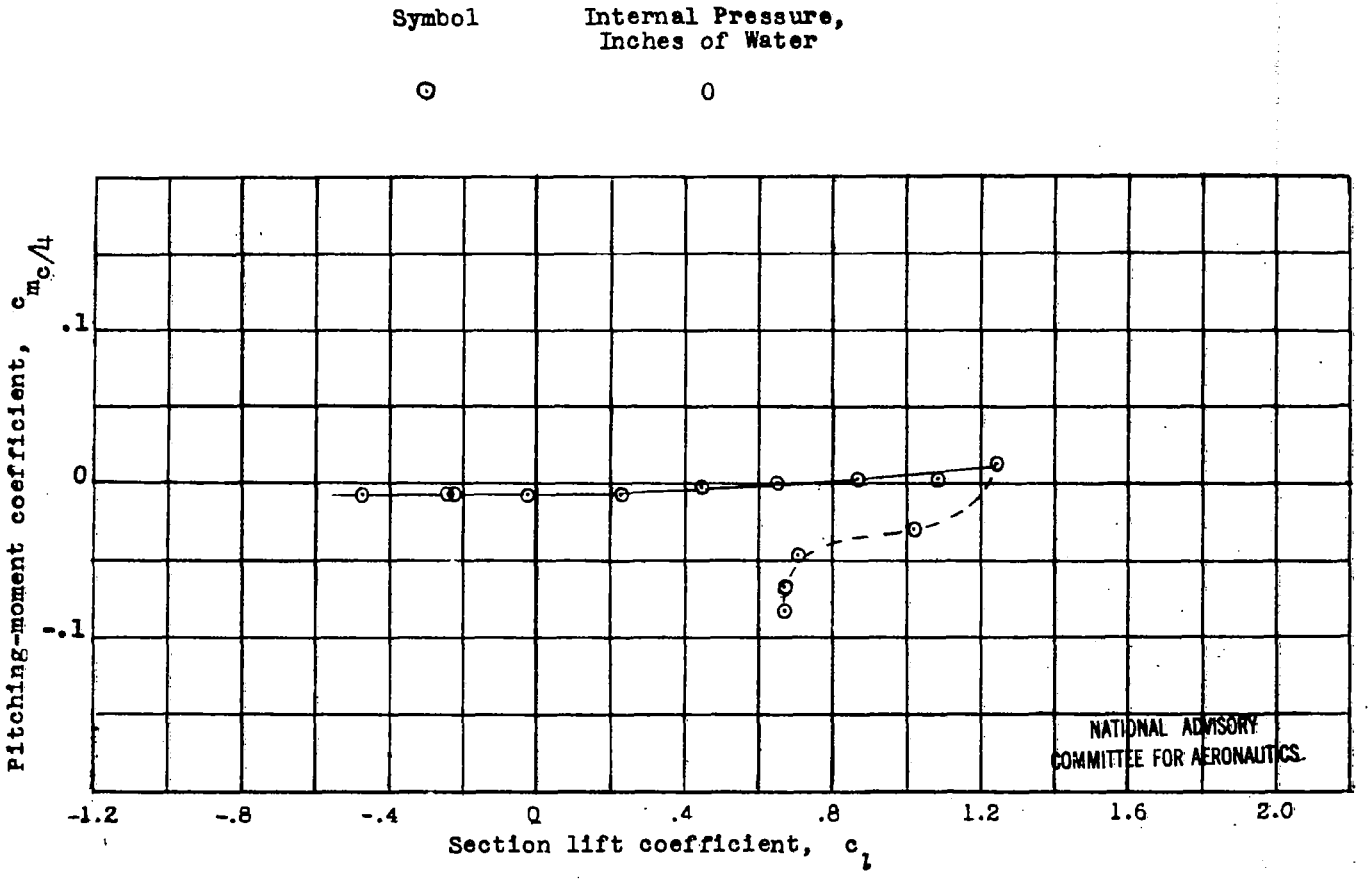

(c) Pitching-moment coefficient about quarter-chord point versus lift coefficient

Figure 25.- Continued.

Symbol	Internal Pressure Inches of Water	A.C. Position x/c
⊙	0	.247

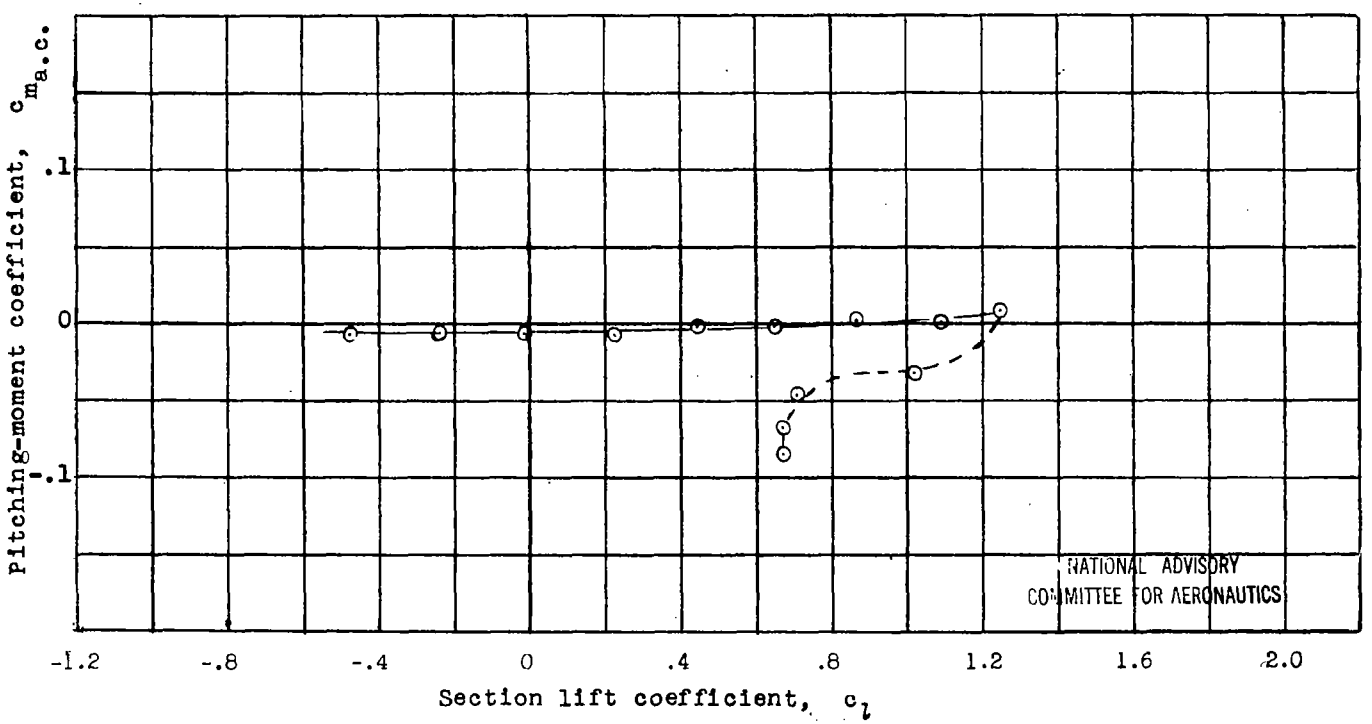

(d) Pitching-moment coefficient about aerodynamic center versus lift coefficient

Figure 25.- Concluded.

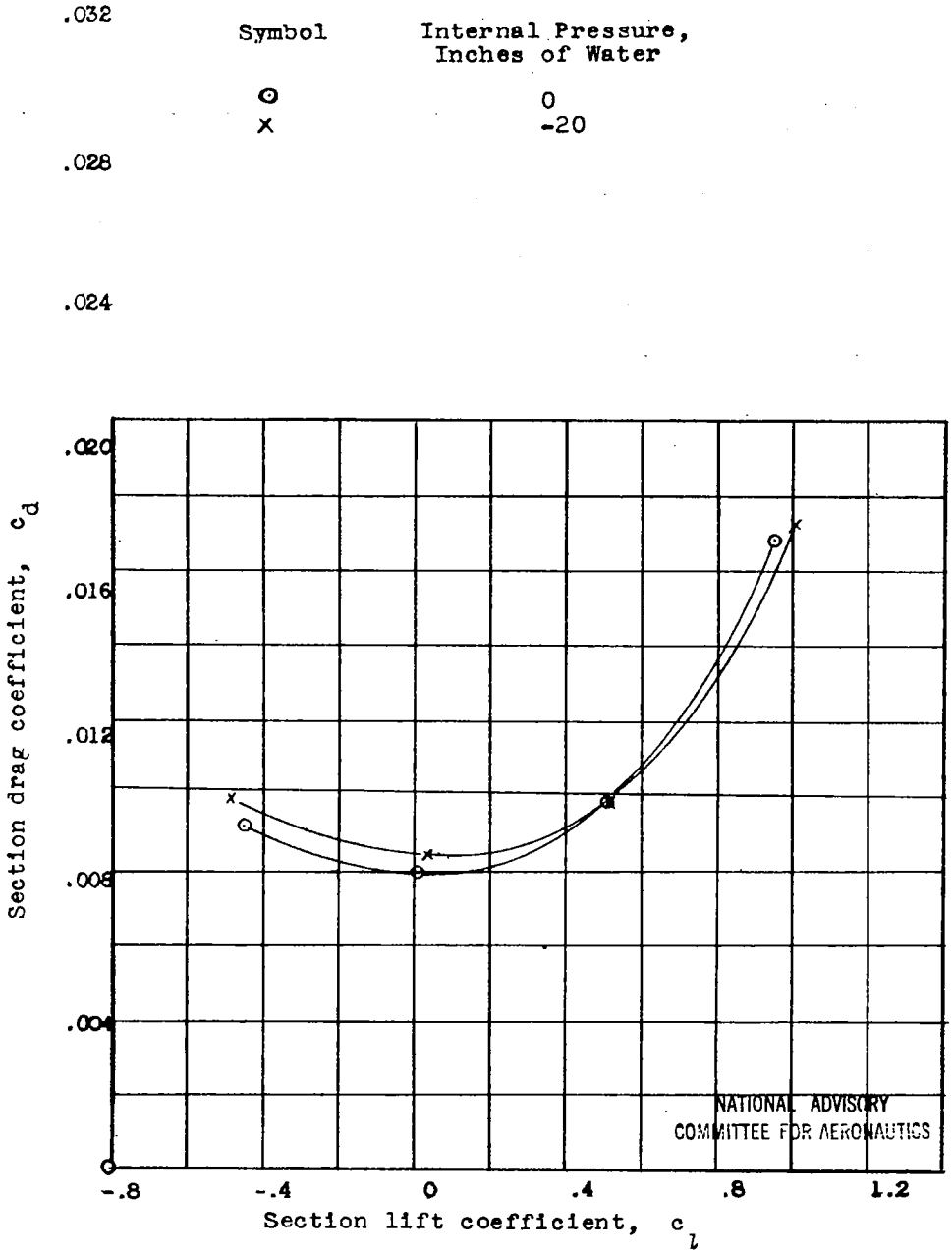

(a) Drag coefficient versus lift coefficient

Figure 26.- Aerodynamic data for the YR-4A No. 10 (Smooth Forward Portion) Helicopter test section. $R = 2.59 \times 10^6$, $M = 0.375$.

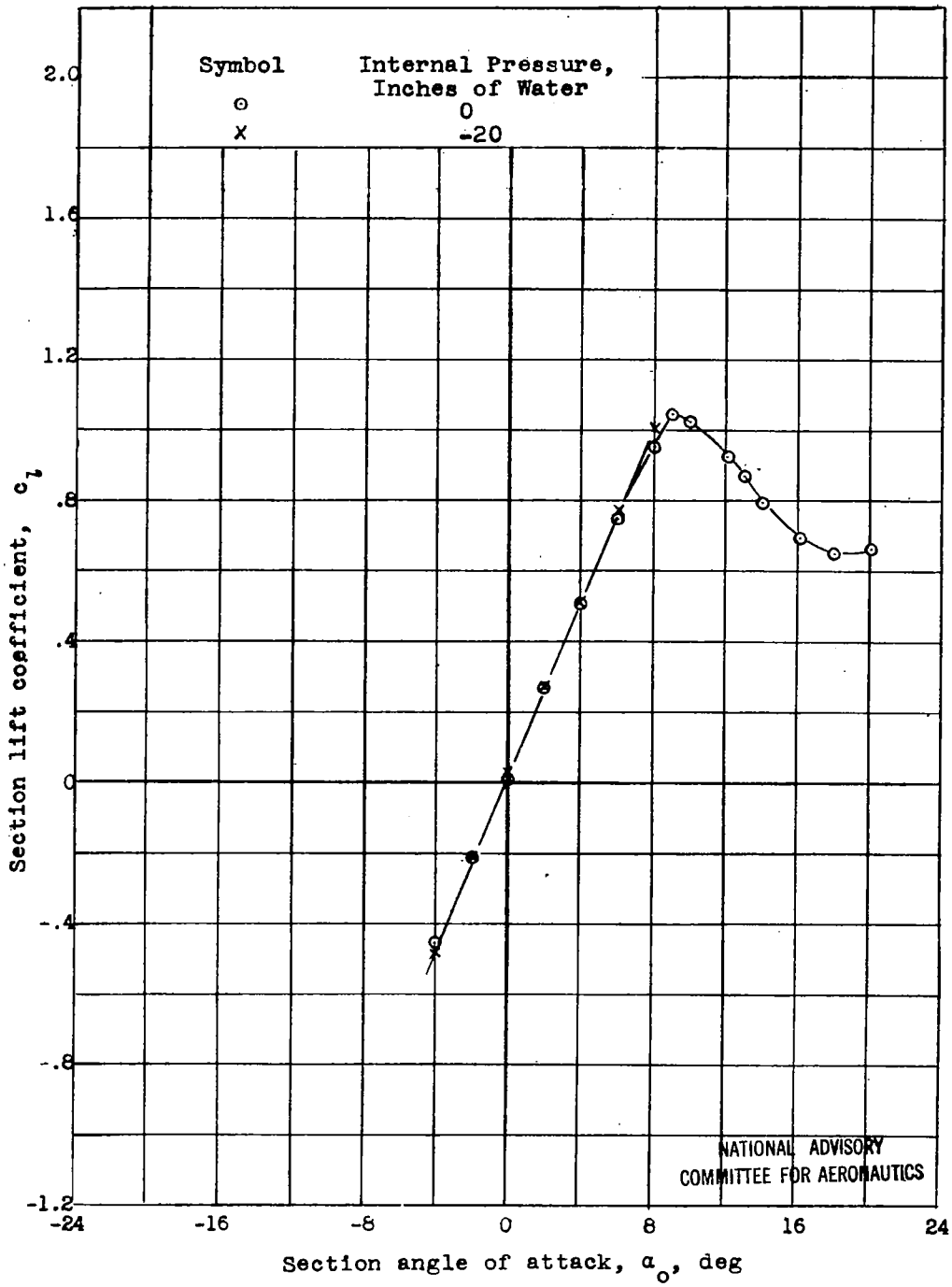

(b) Lift coefficient versus angle of attack.

Figure 26.- Continued.

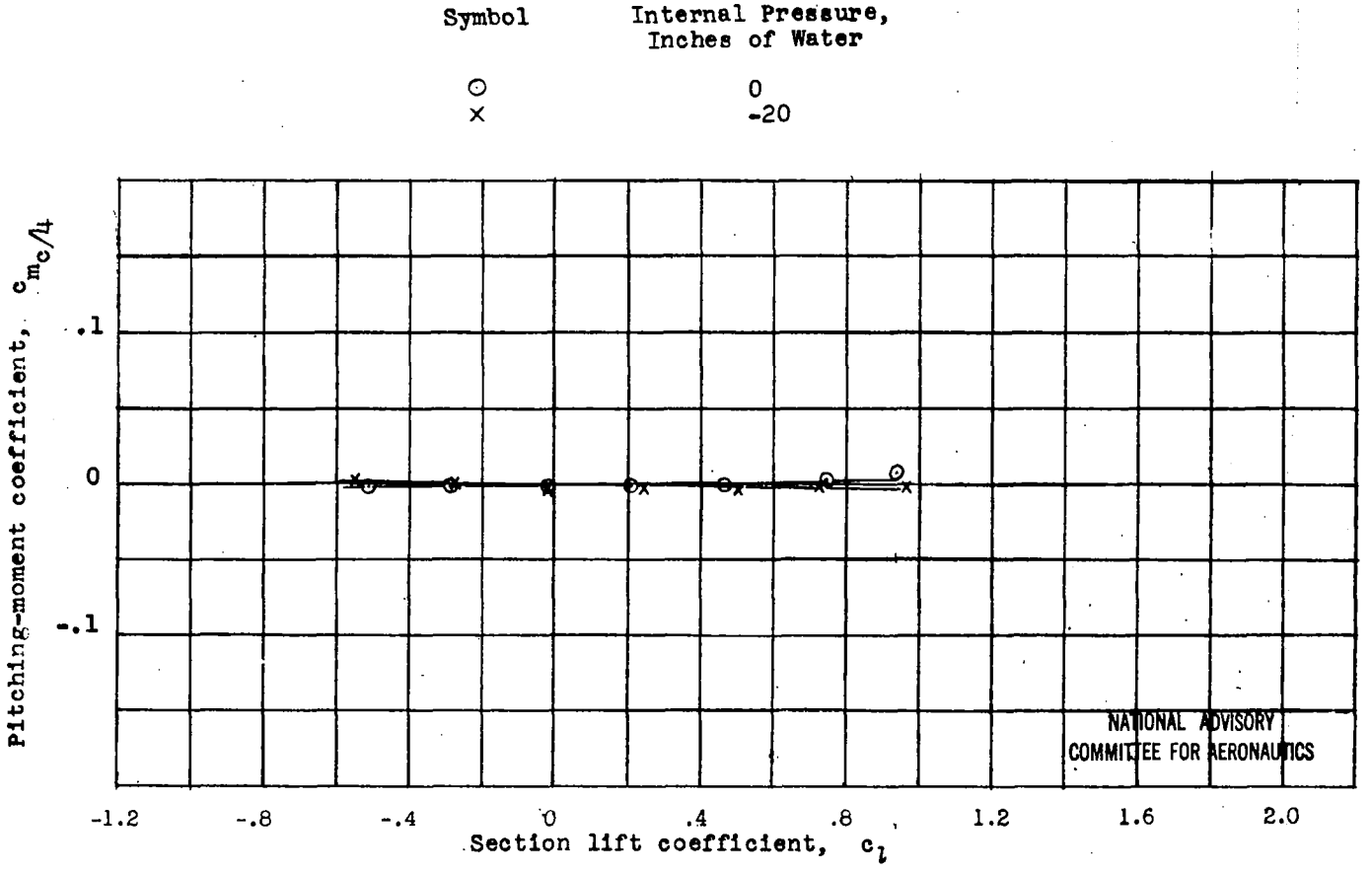

(c) Pitching-moment coefficient about quarter-chord point versus lift coefficient

Figure 26.- Continued.

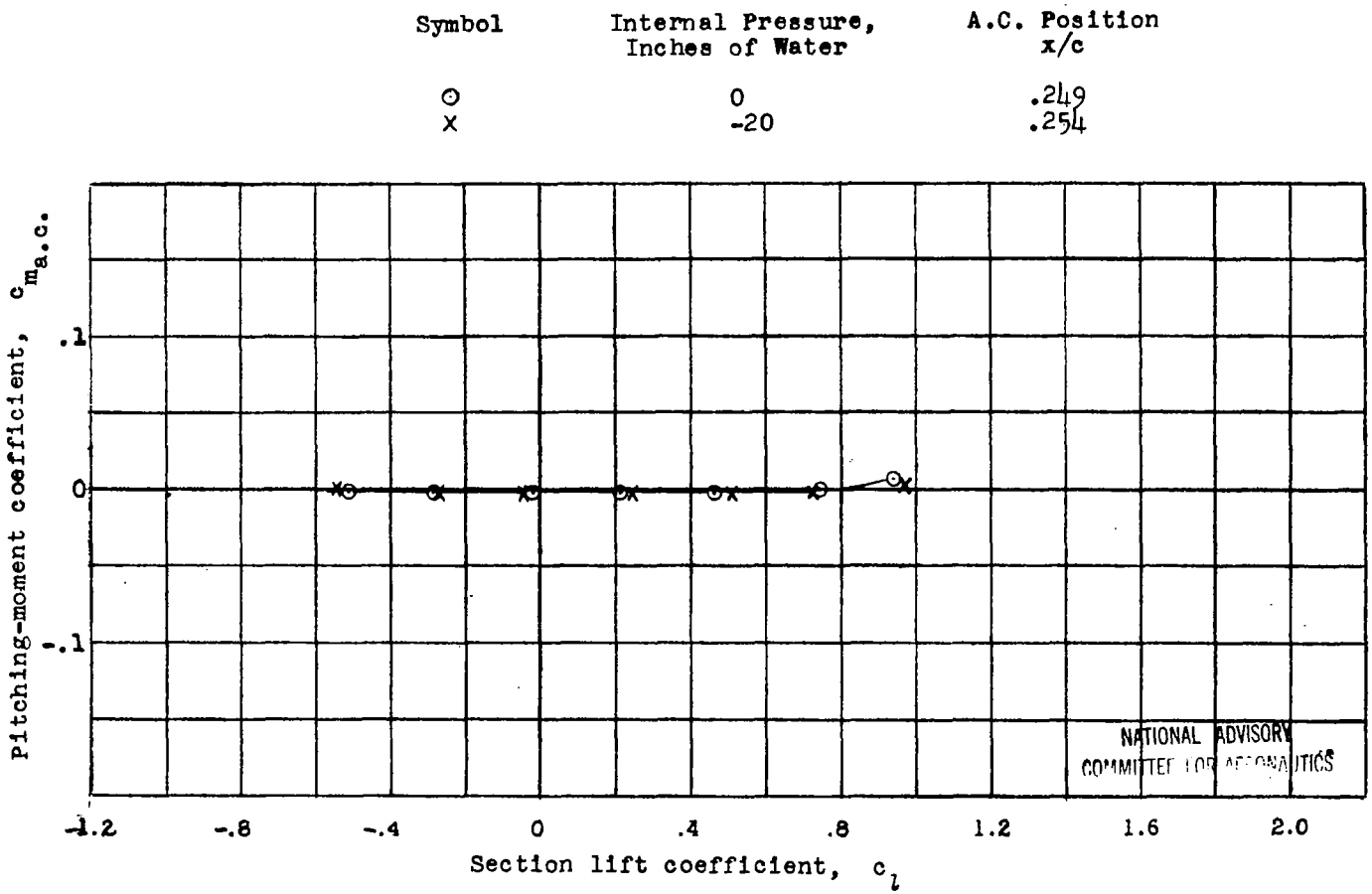

(d) Pitching-moment coefficient about aerodynamic centers versus lift coefficient

Figure 26.- Concluded.

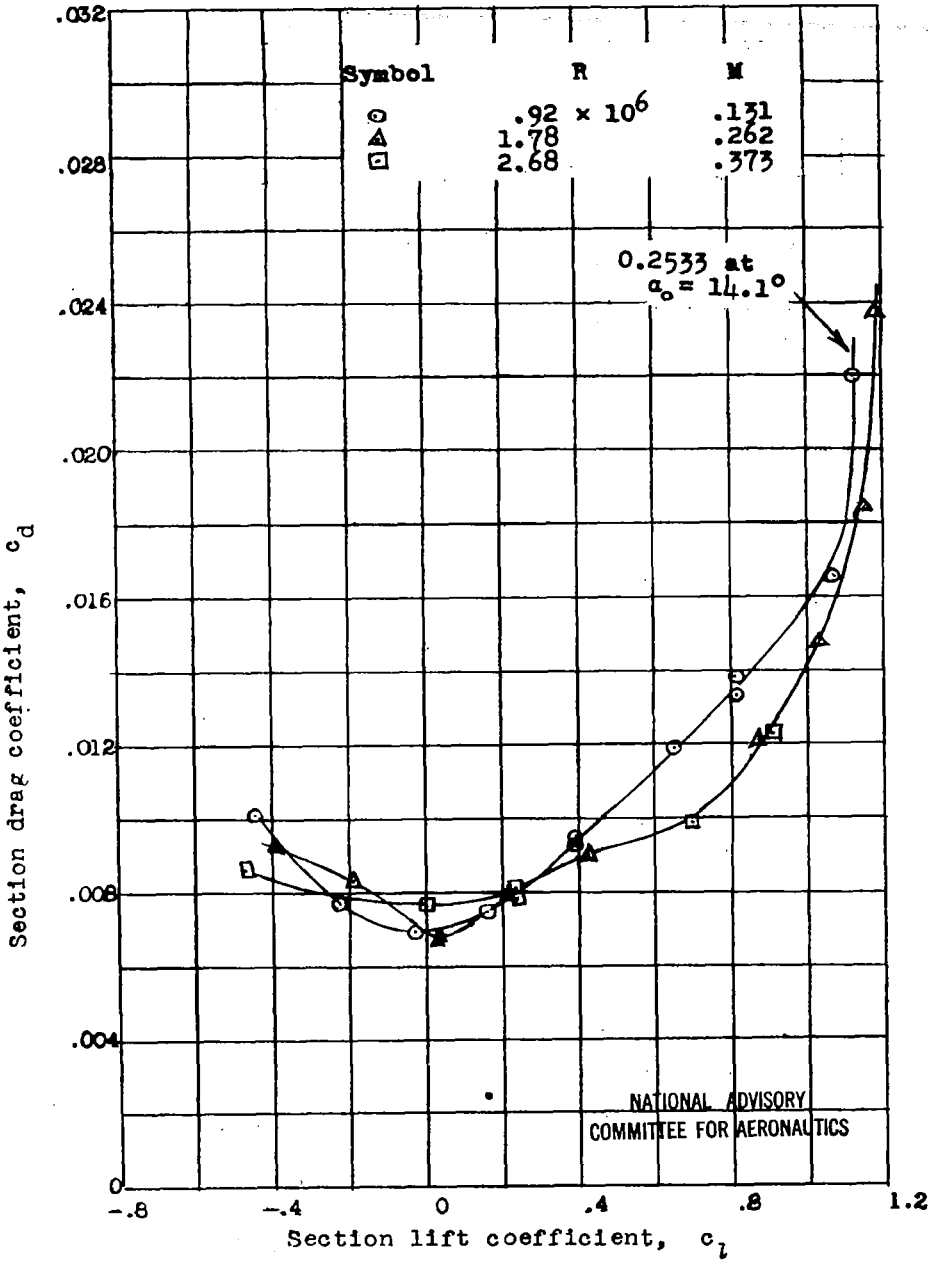

(a) Drag coefficient versus lift coefficient

Figure 27.- Aerodynamic data for the XR-6 No. 5 Helicopter test section.

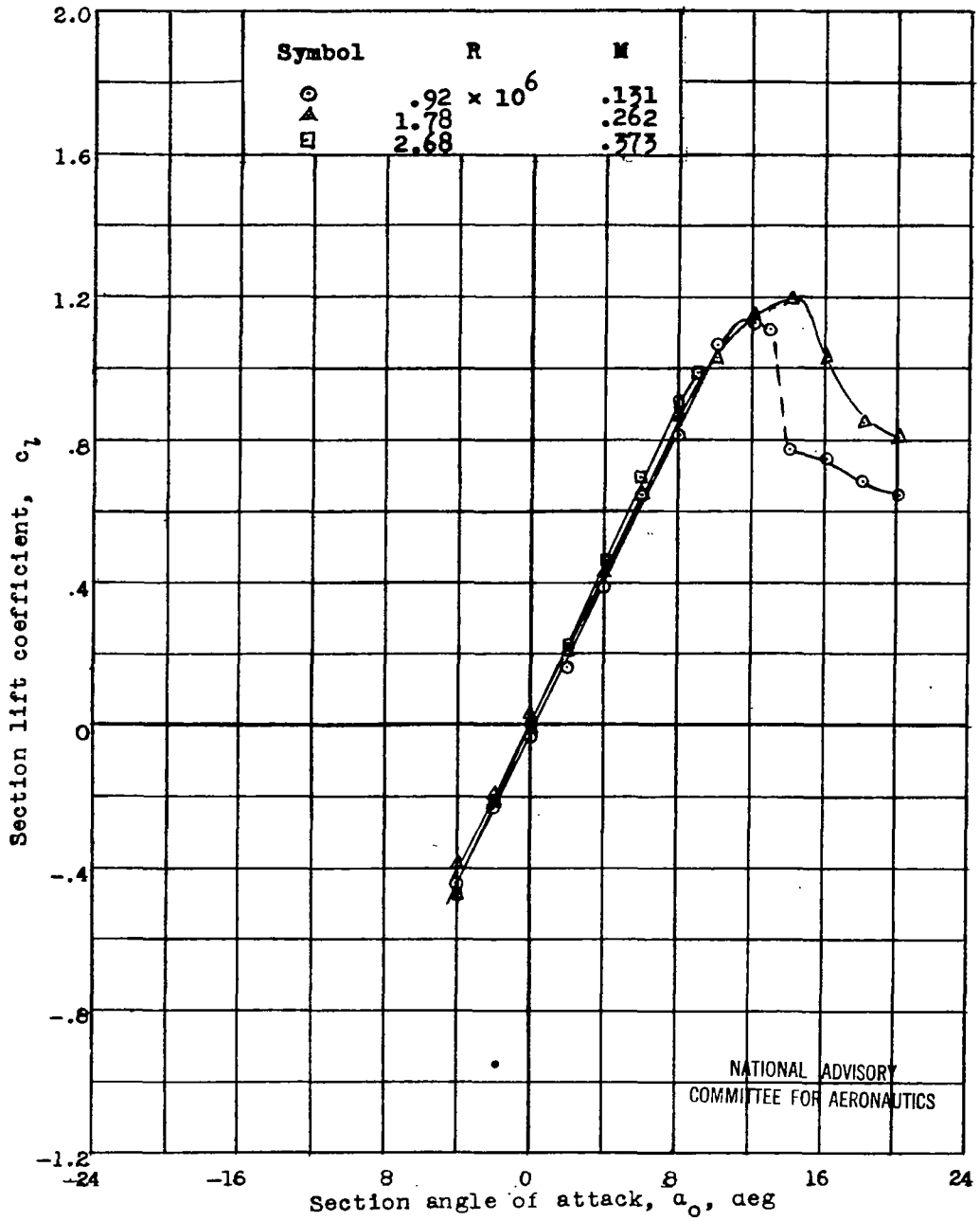

(b) Lift coefficient versus angle of attack

Figure 27.- Continued.

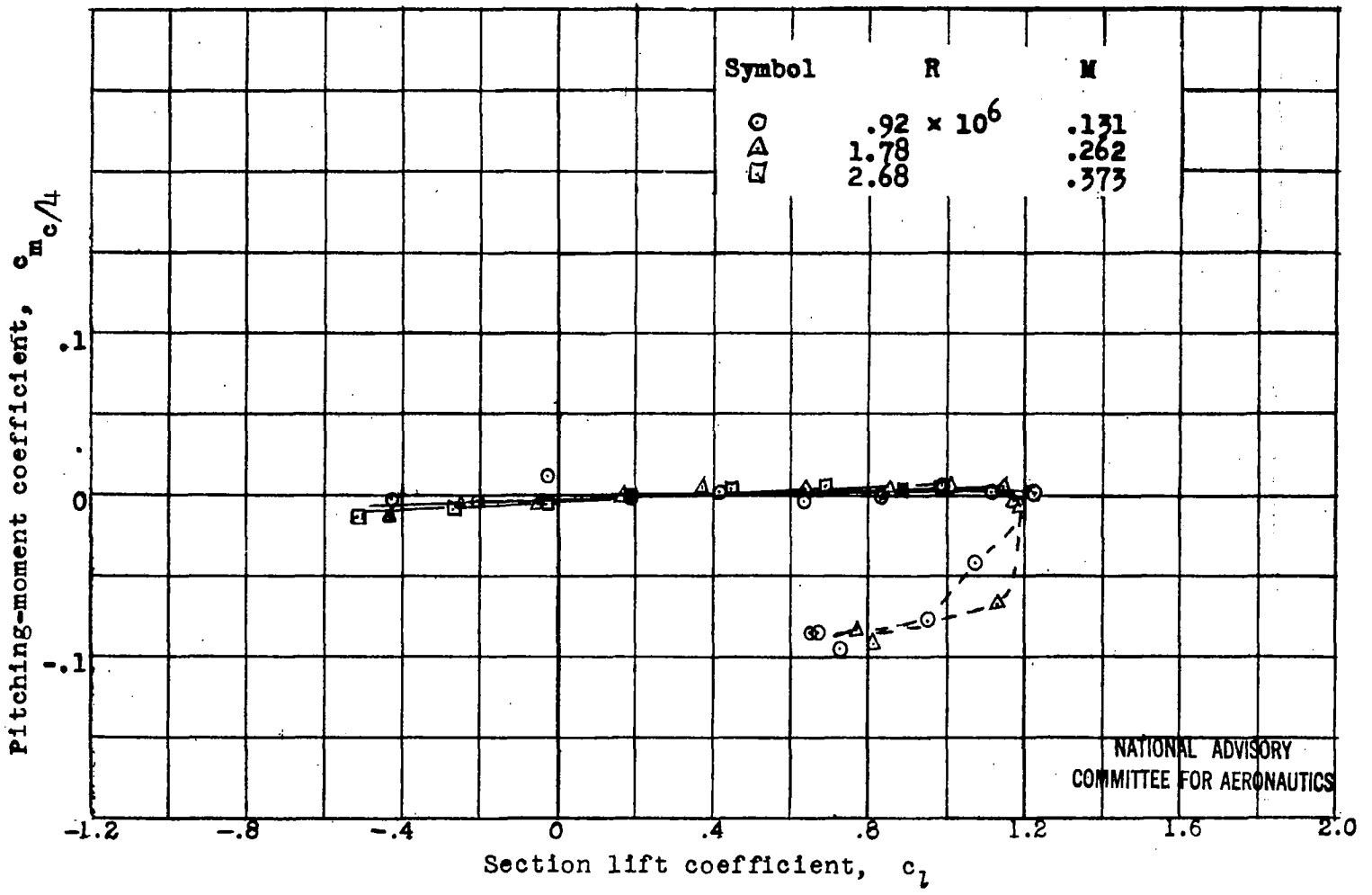

(c) Pitching-moment coefficient about quarter-chord point.

Figure 27.- Continued.

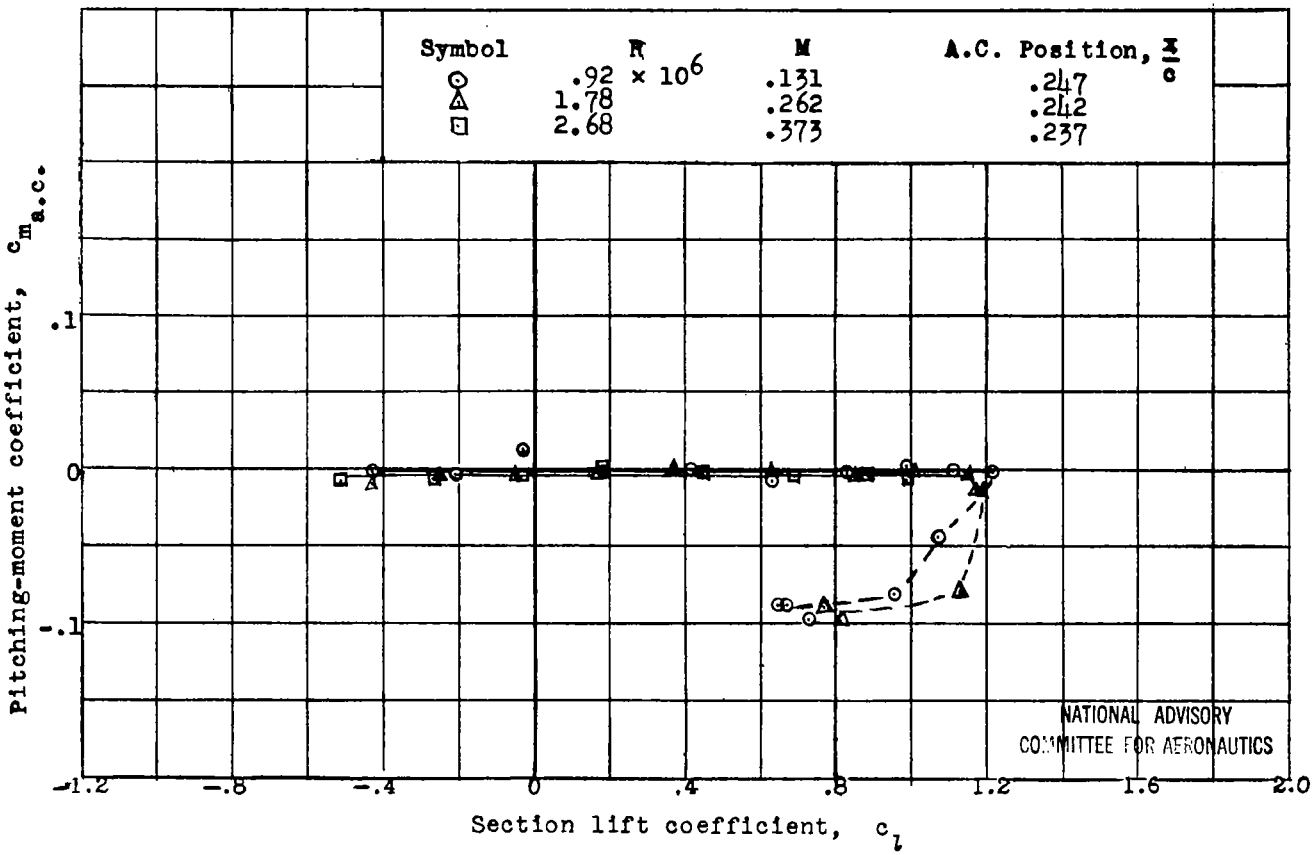

(d) Pitching-moment coefficient about aerodynamic center

Figure 27.- Concluded.

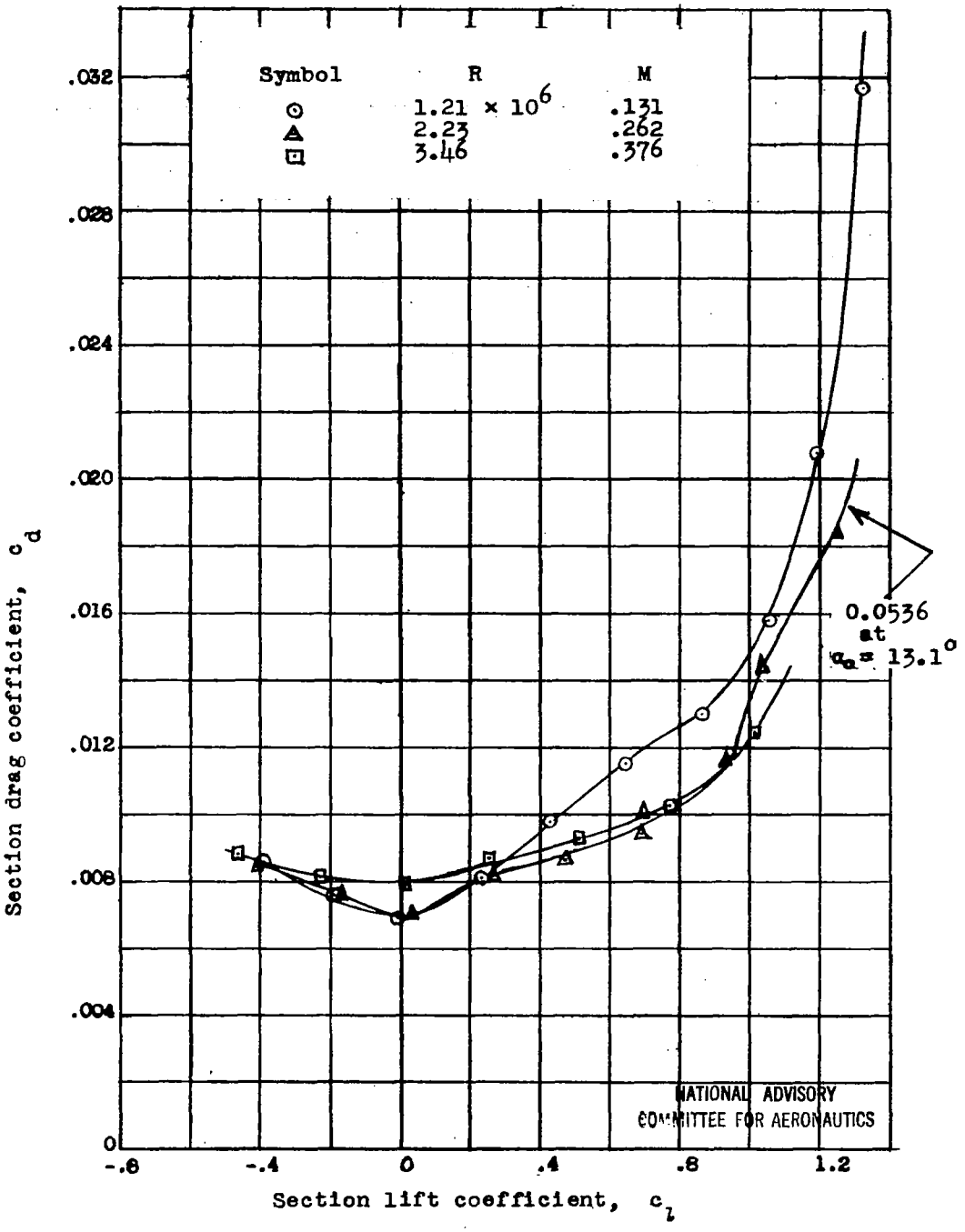

(a) Drag coefficient versus lift coefficient

Figure 28.- Aerodynamic data for the XR-6 No. 7 Helicopter test section.

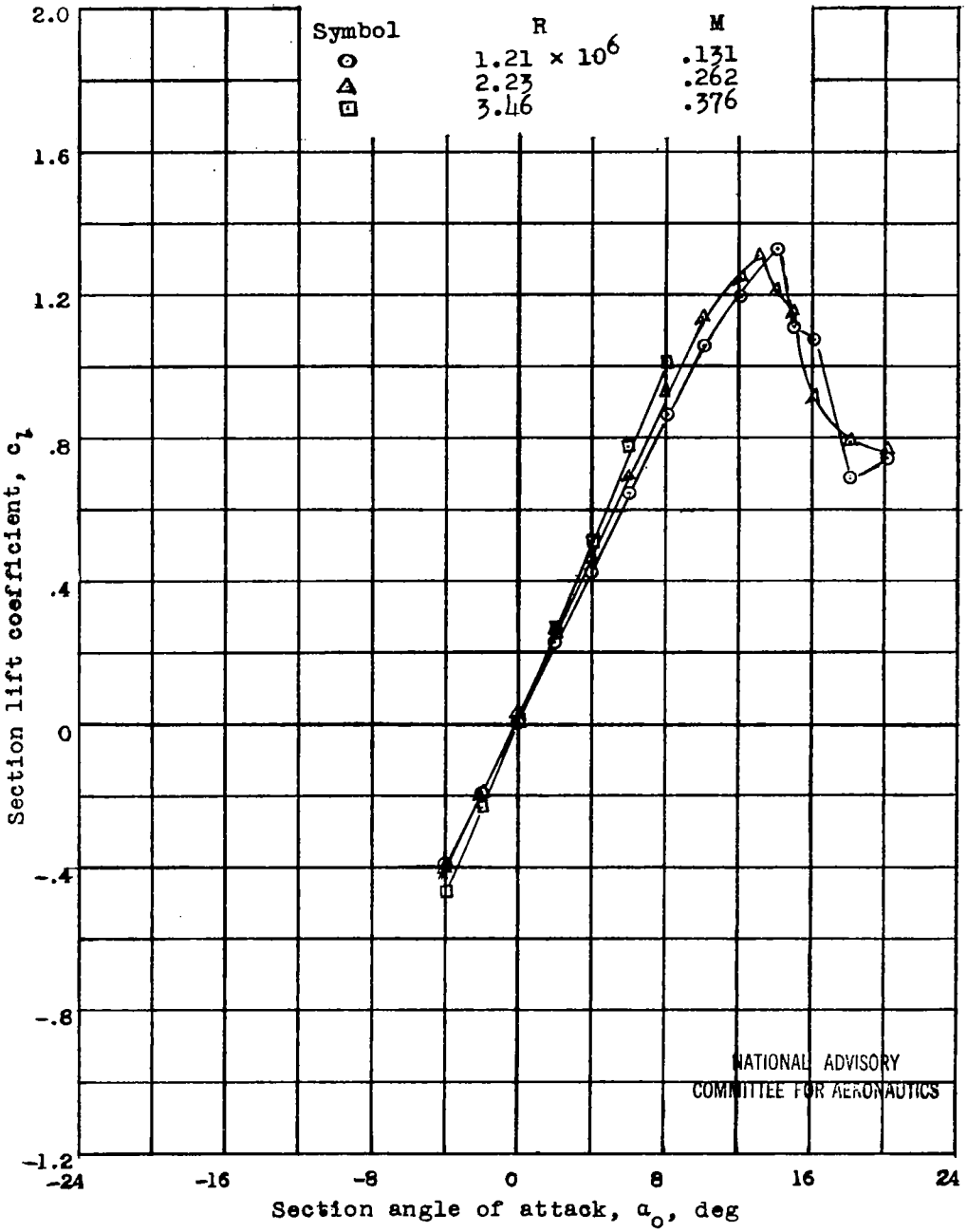

(b) Lift coefficient versus angle of attack

Figure 28.- Continued.

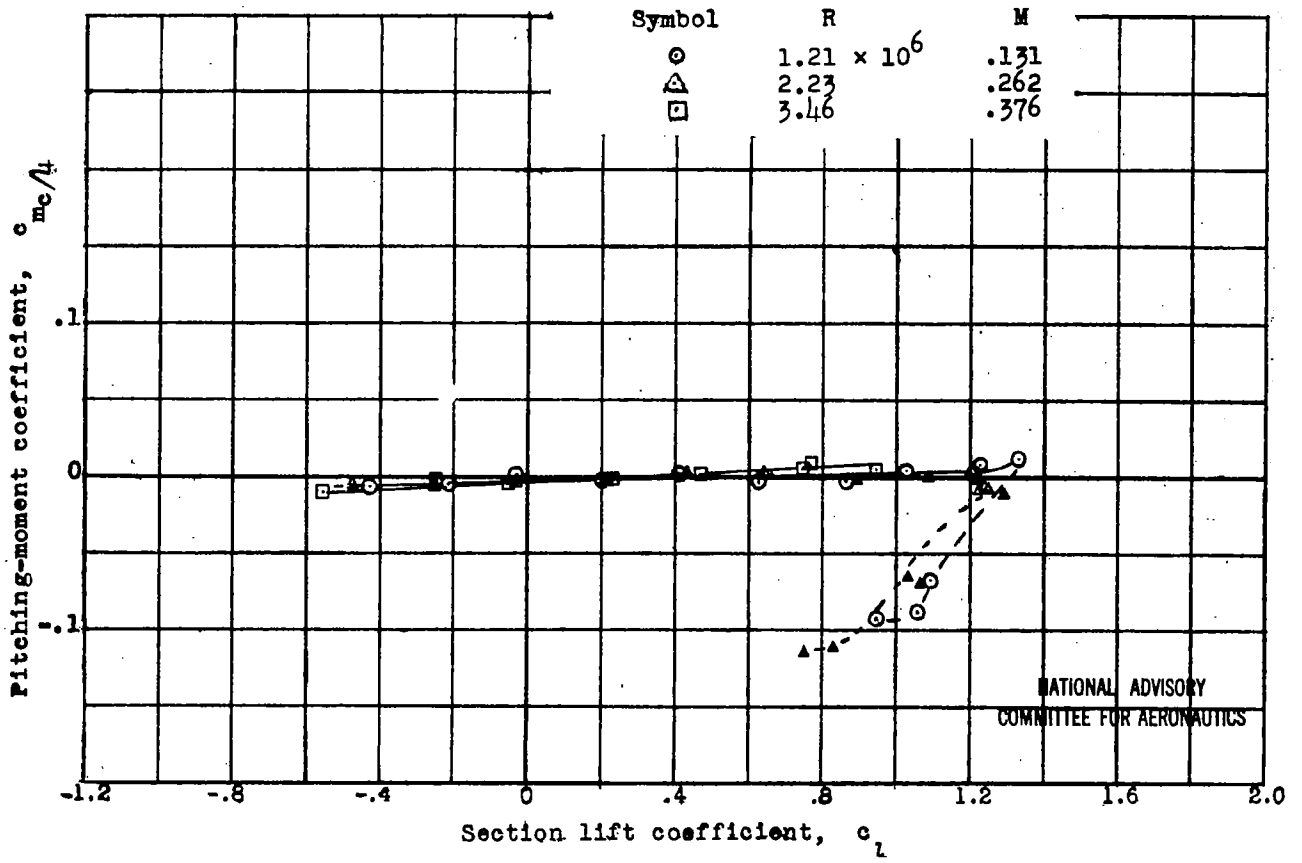

(c) Pitching-moment coefficient about quarter-chord point versus lift coefficient

Figure 28.- Continued.

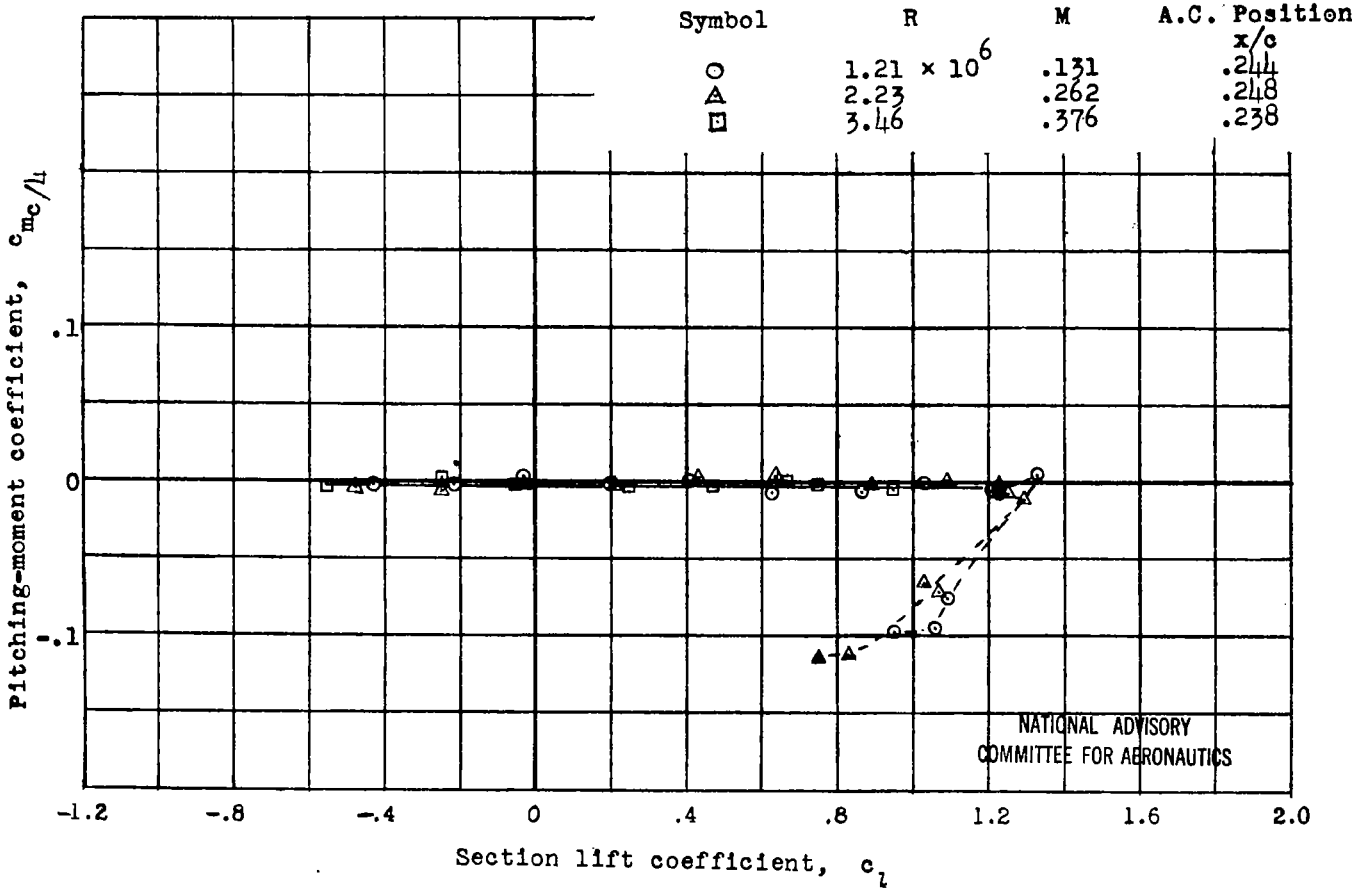

(d) Pitching-moment coefficients about aerodynamic centers versus lift coefficient

Figure 28.- Concluded.

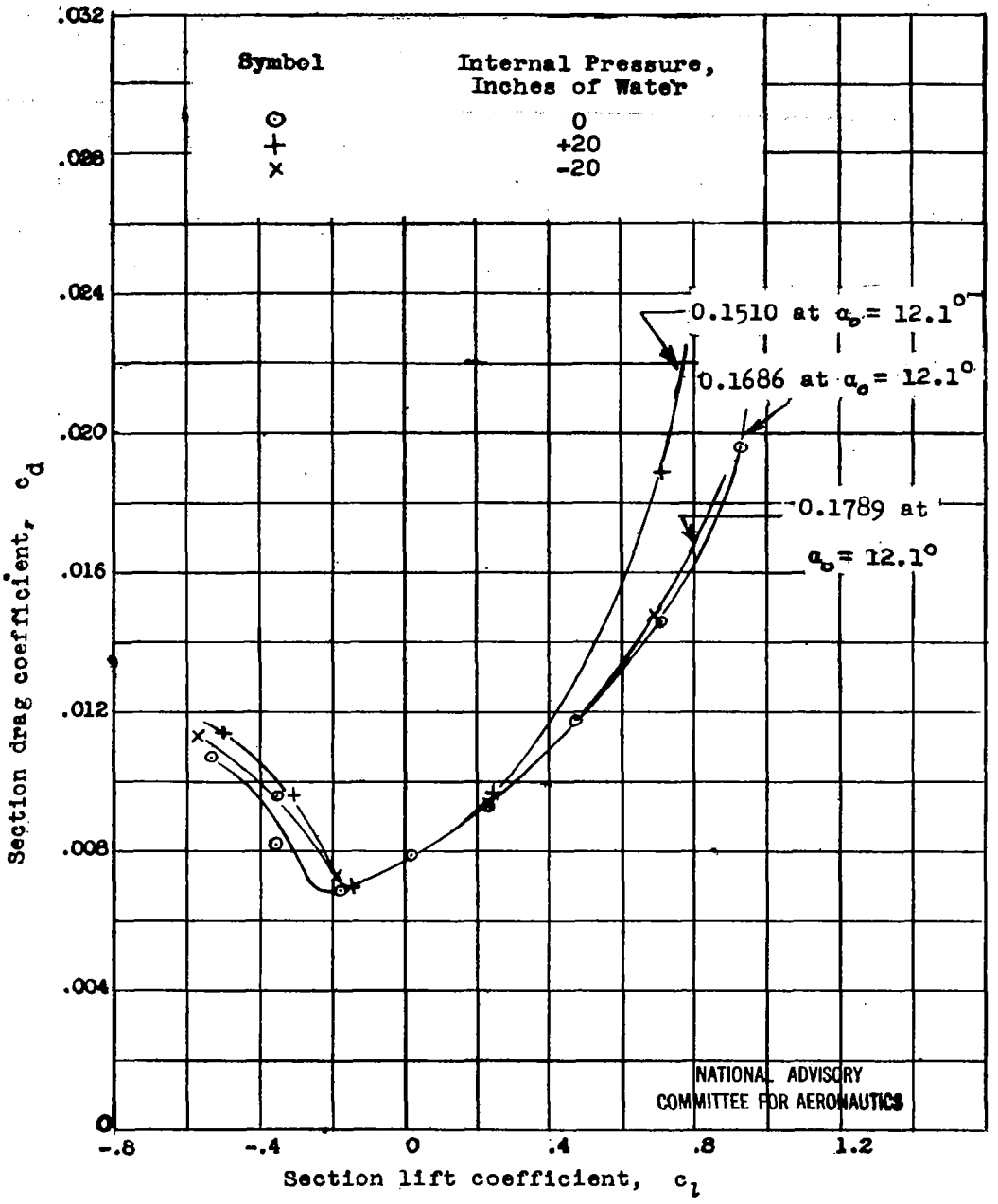

(a) Drag coefficient versus lift coefficient

Figure 29.- Aerodynamic data for the XR-5(a) Helicopter test section. R = 1.19 x 10^6, M = 0.131.

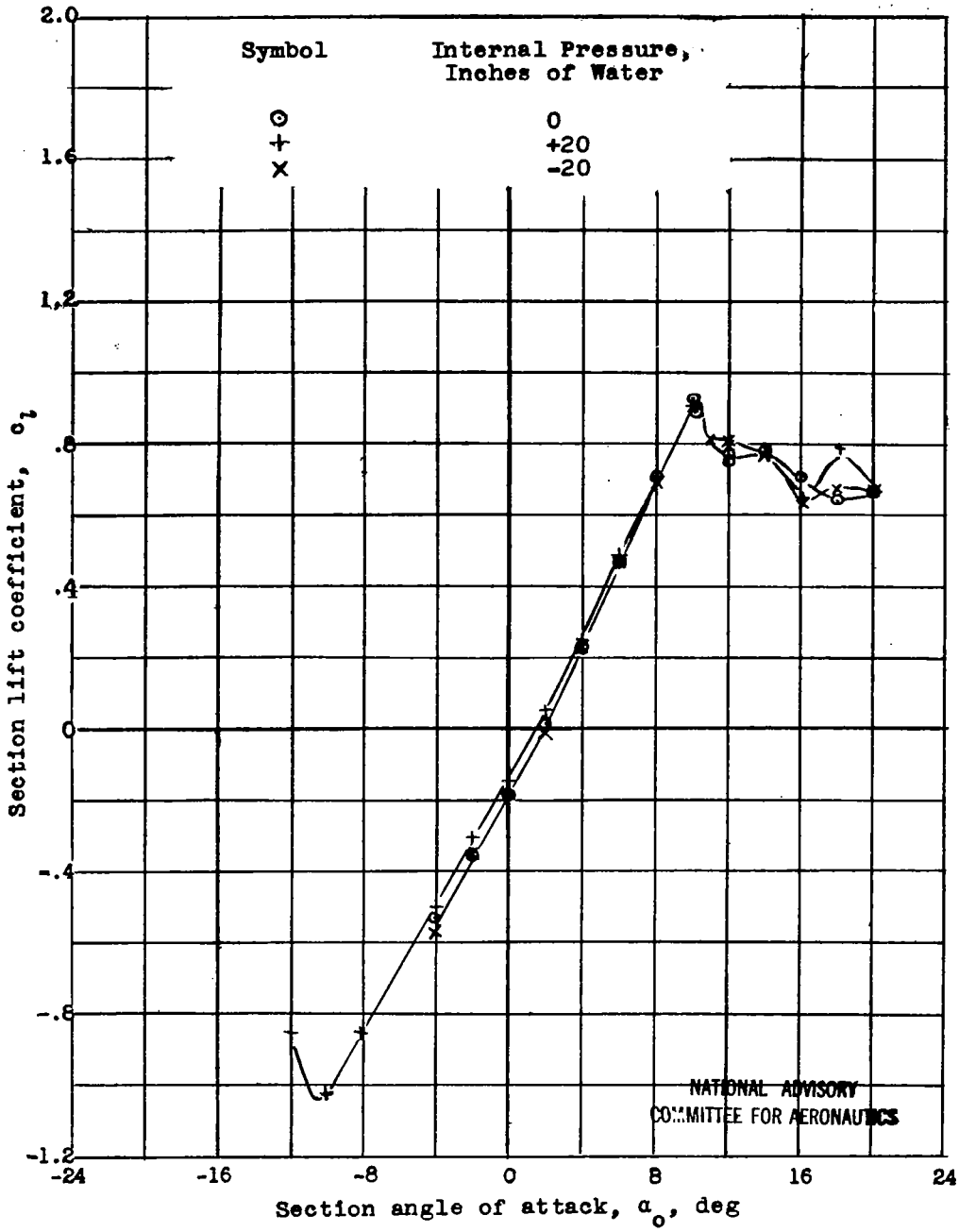

(b) Lift coefficient versus angle of attack

Figure 29.- Continued.

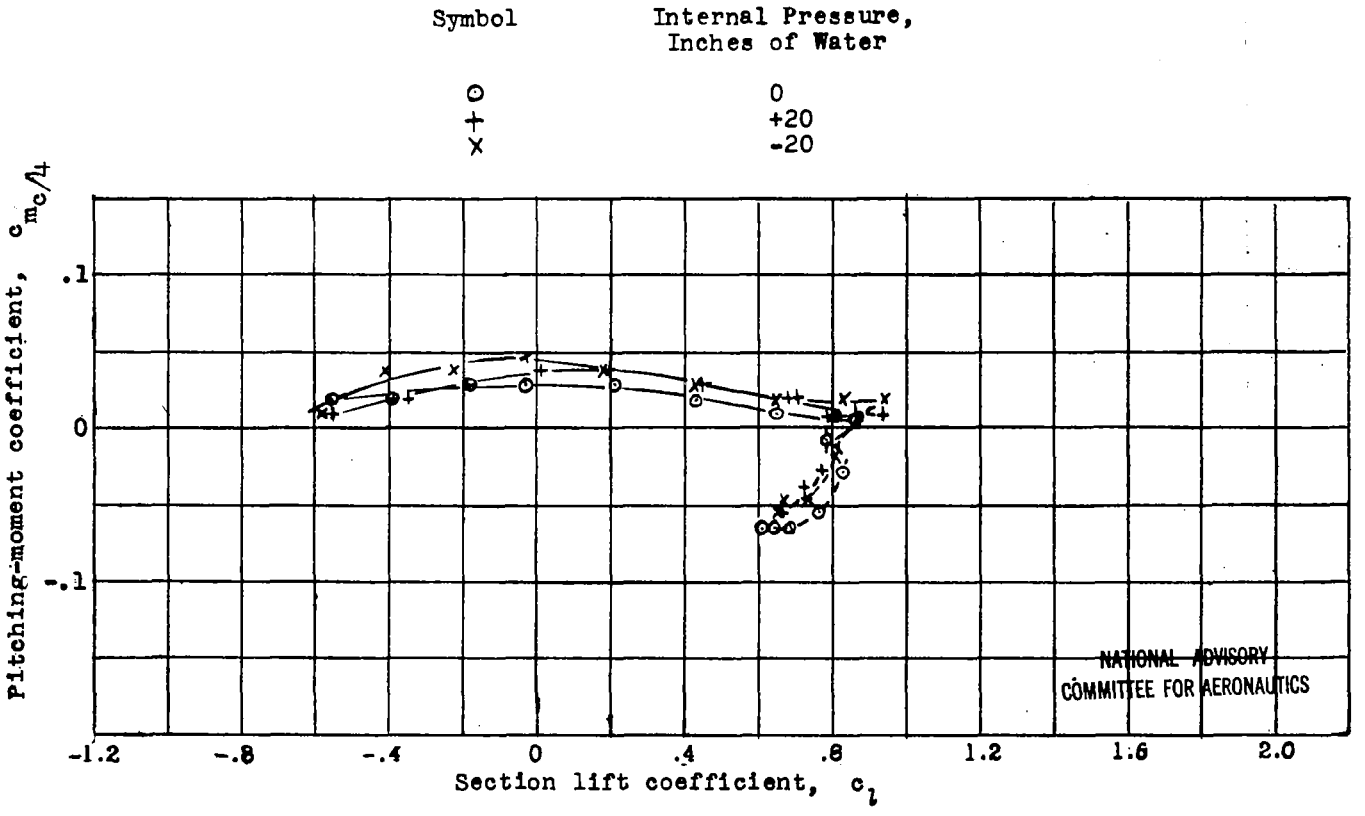

(c) Pitching-moment coefficient about quarter-chord point versus lift coefficient

Figure 29.- Concluded.

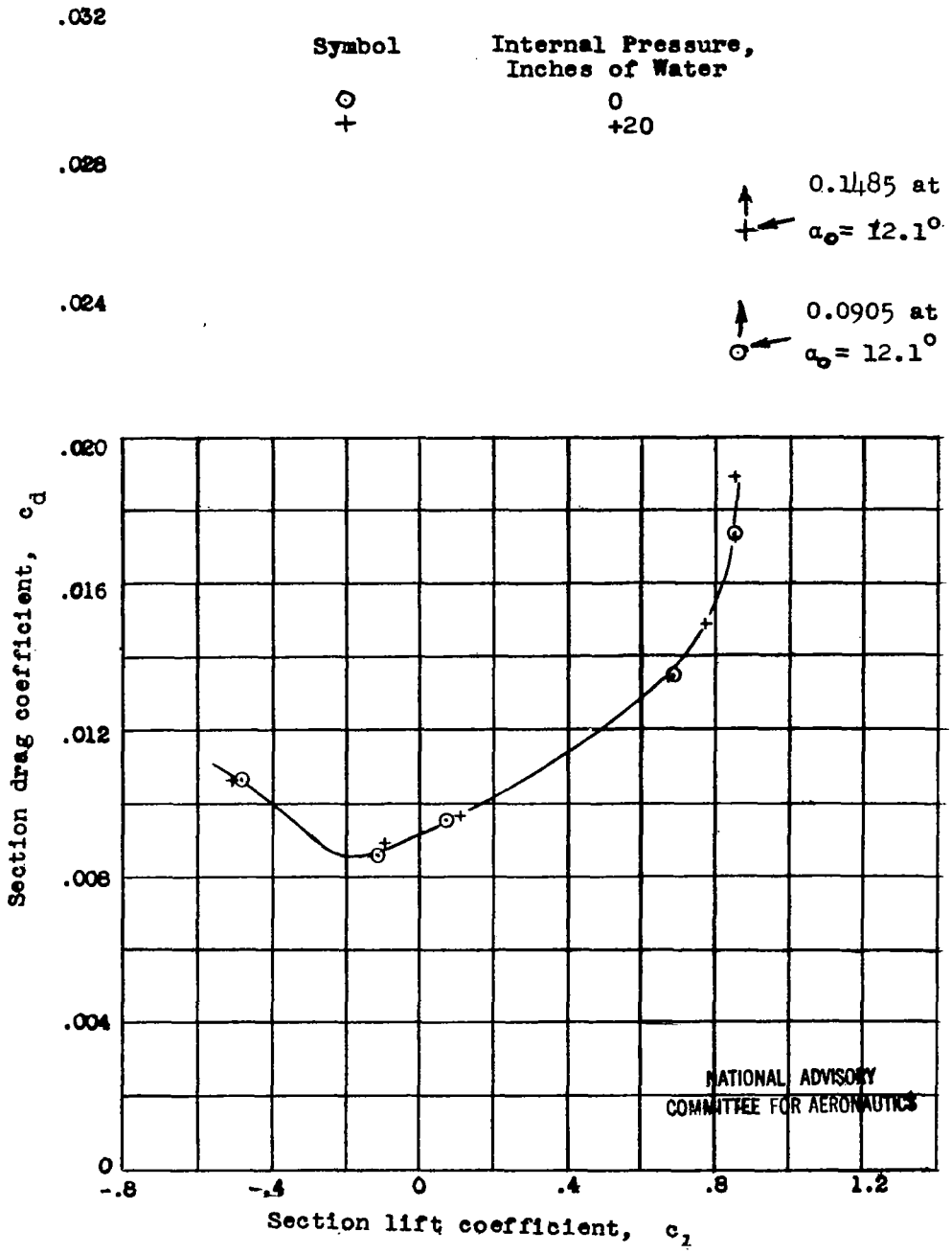

(a) Drag coefficient versus lift coefficient

Figure 30.- Aerodynamic data for the XR-5(a) Helicopter test section. $R = 2.40 \times 10^6$, $M = 0.261$.

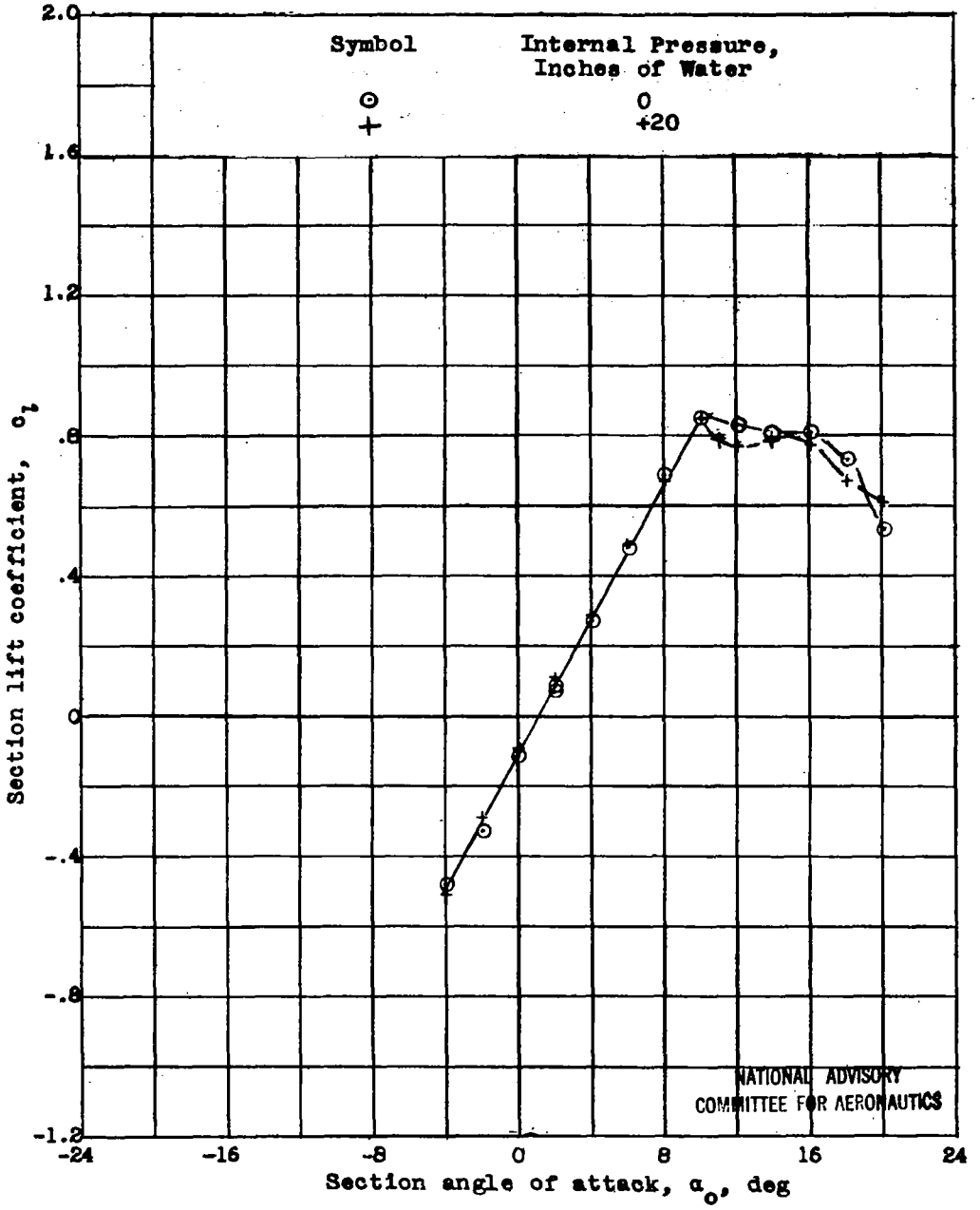

(b) Lift coefficient versus angle of attack.

Figure 30.- Continued.

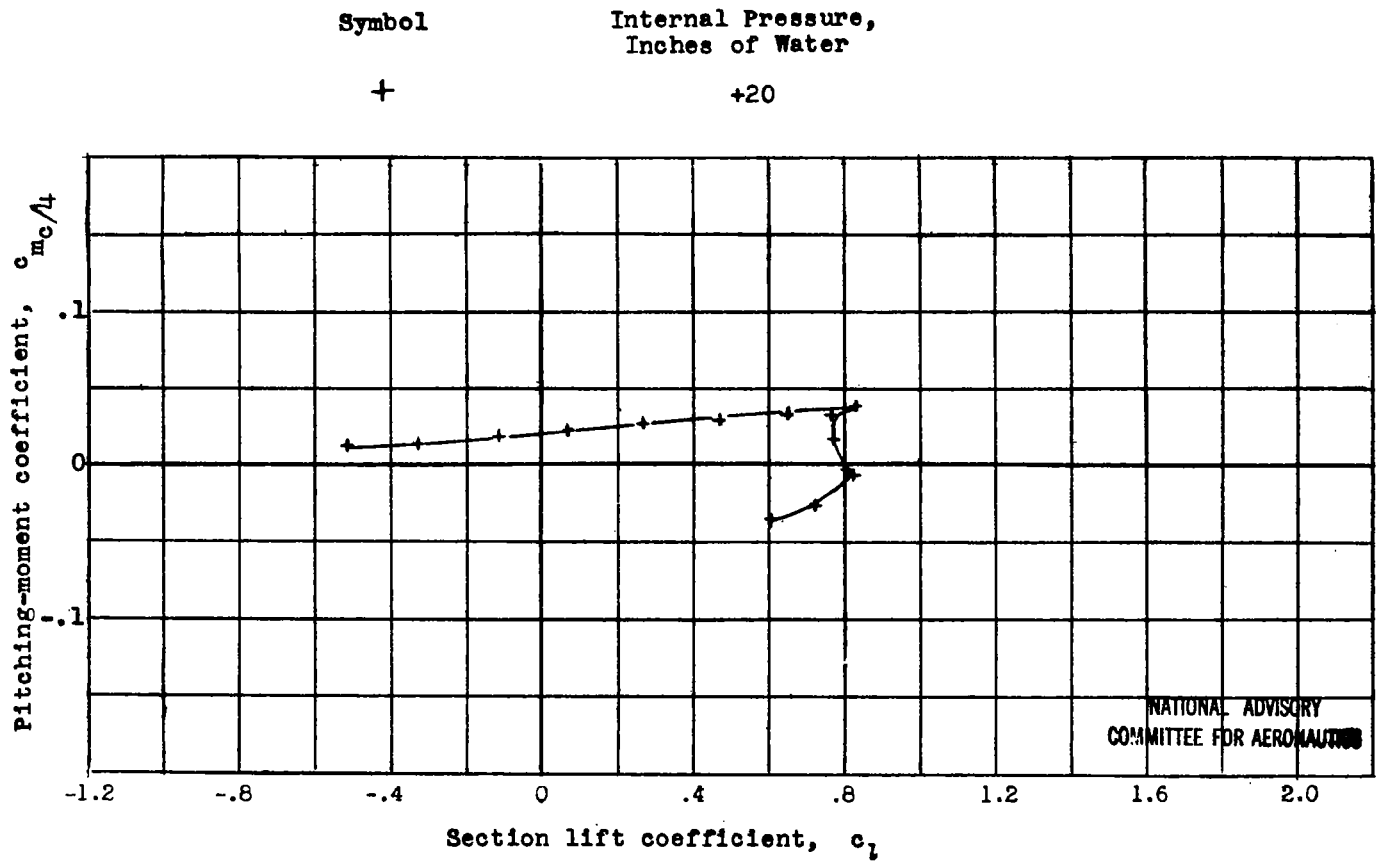

(c) Pitching-moment coefficient about quarter-chord point versus lift coefficient

Figure 30.- Concluded.

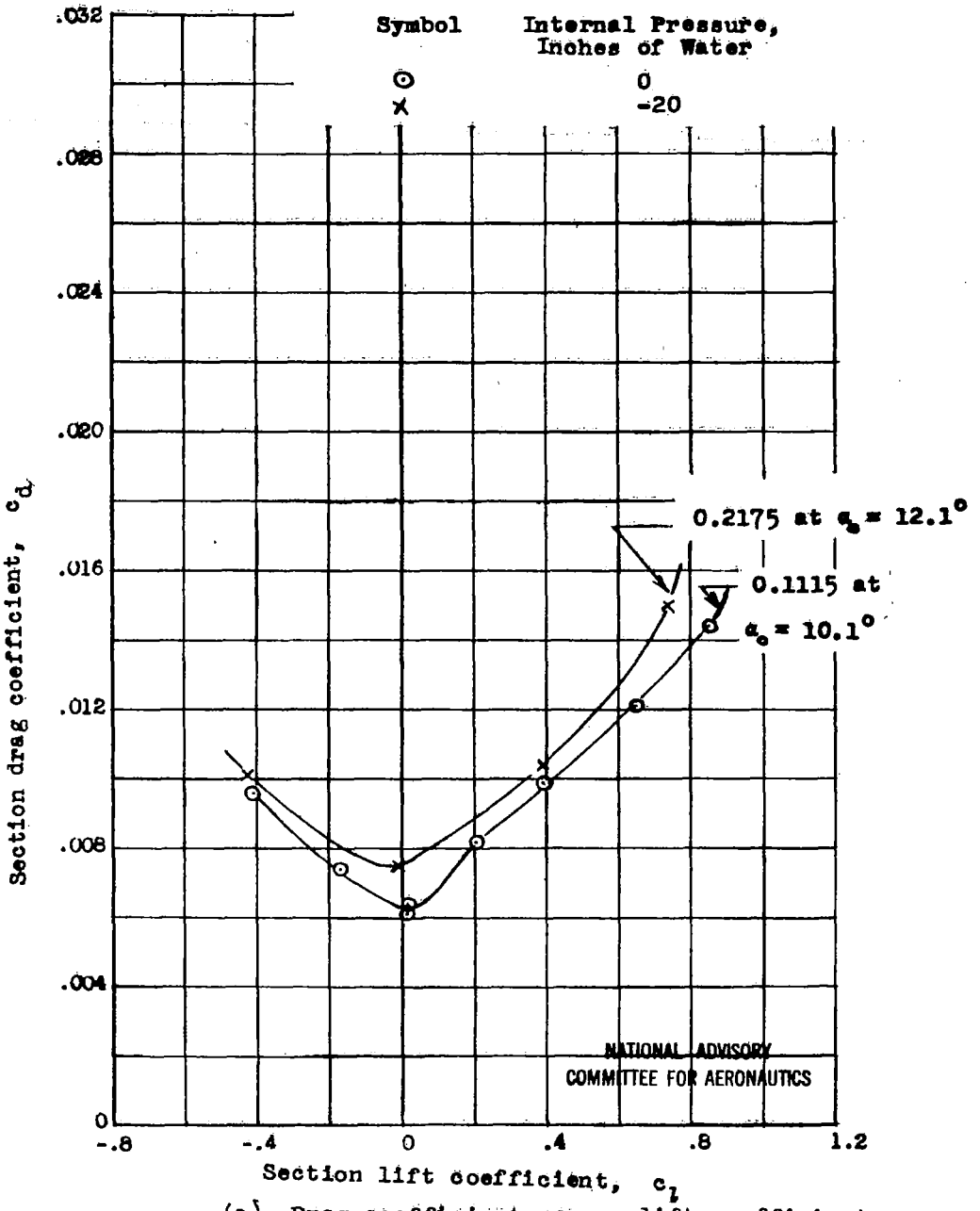

(a) Drag coefficient versus lift coefficient

Figure 31.- Aerodynamic data for the XR-5(b) Helicopter test section. $R = 1.20 \times 10^6$, $M = 0.136$.

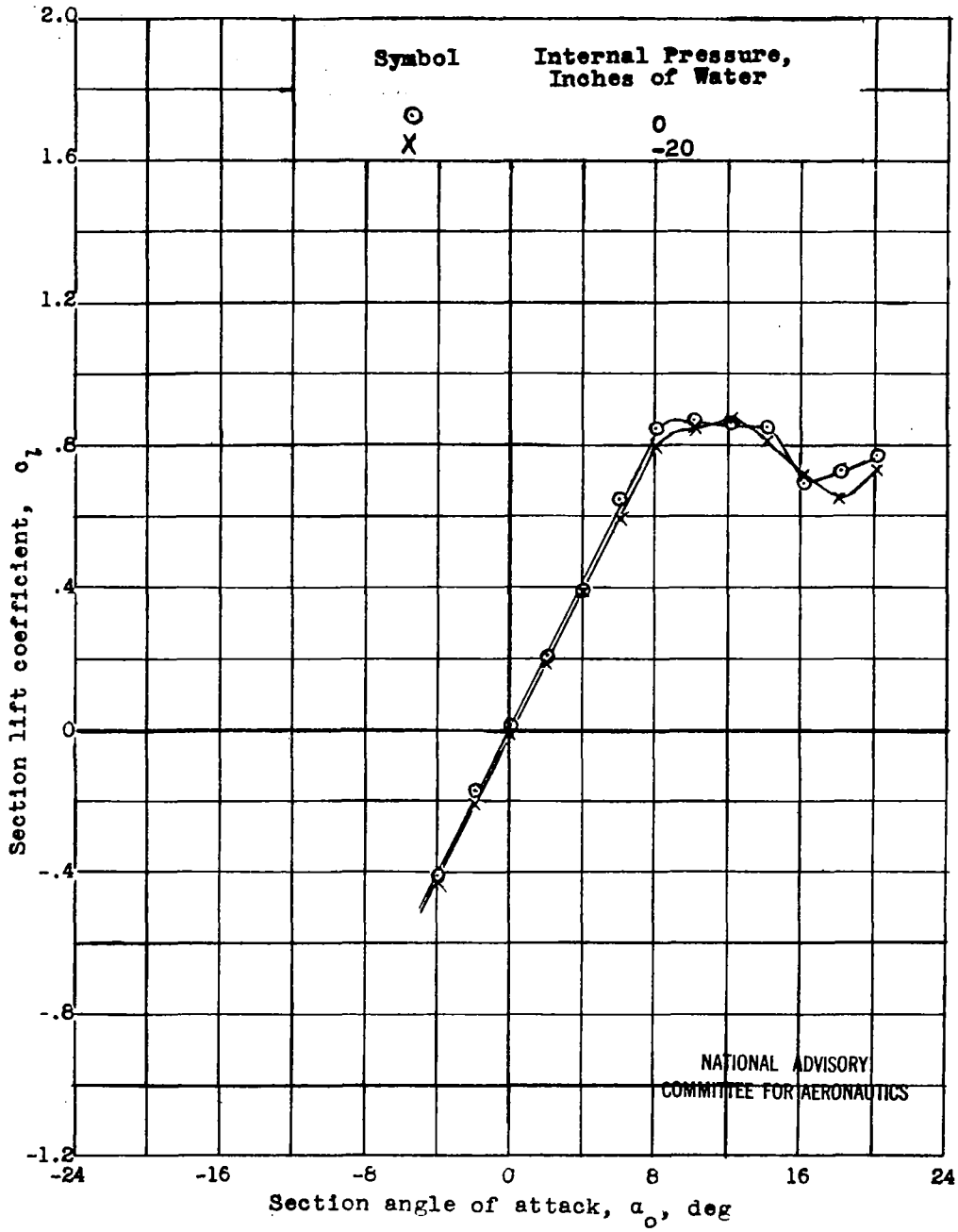

(b) Lift coefficient versus angle of attack.

Figure 31.- Continued.

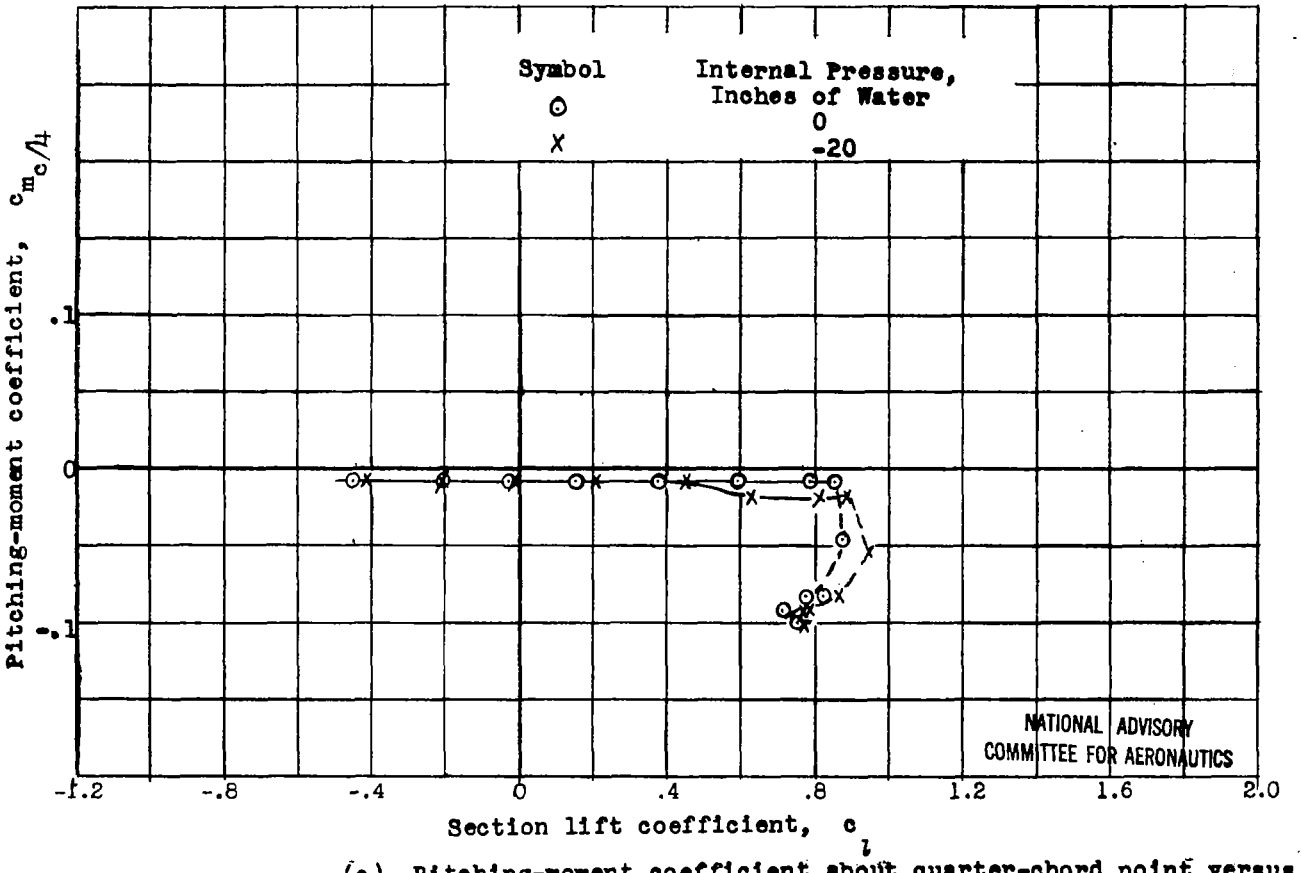

(c) Pitching-moment coefficient about quarter-chord point versus lift coefficient

Figure 3/.- Concluded.

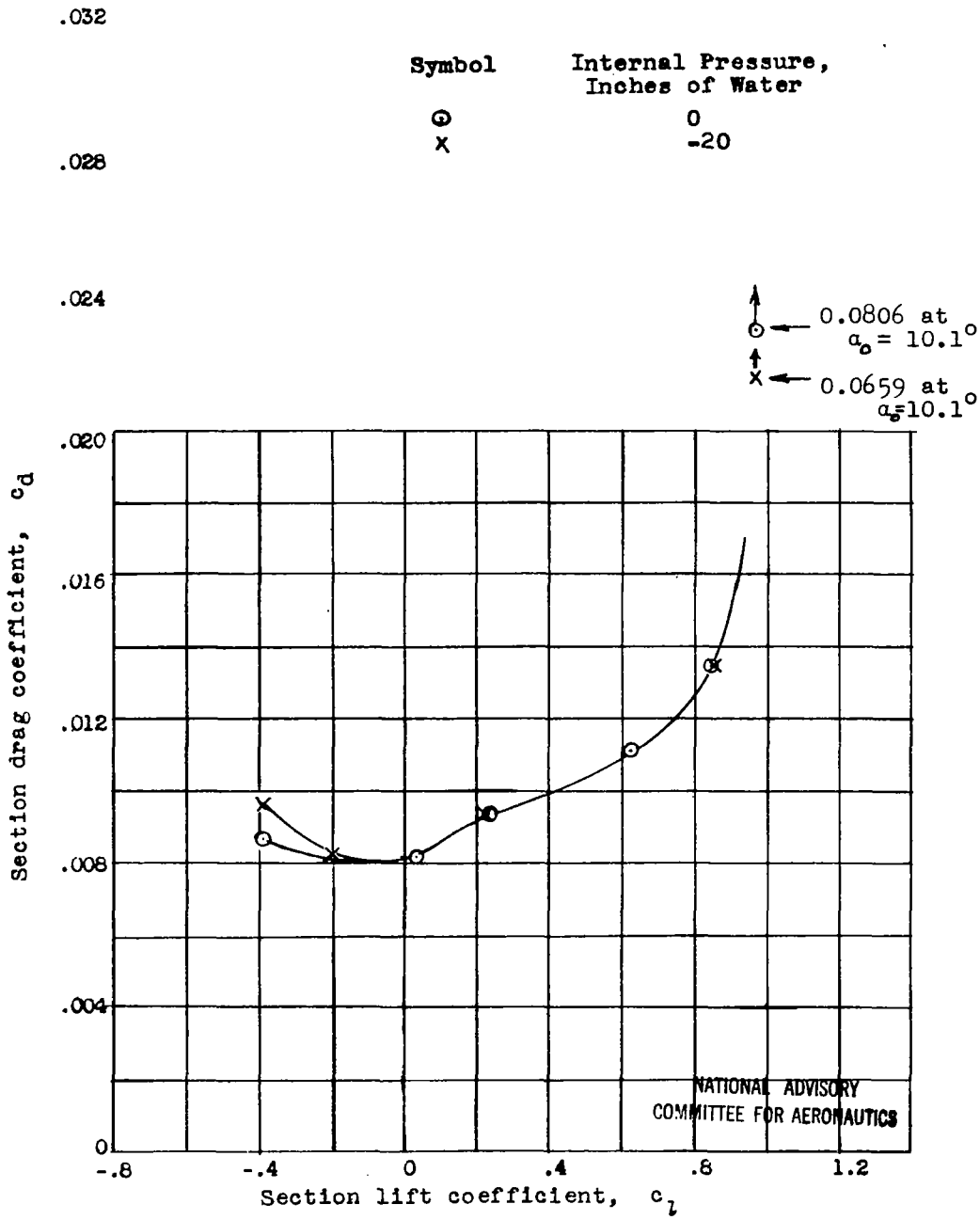

(a) Drag coefficient versus lift coefficient

Figure 32.- Aerodynamic data for the XR-5(b) Helicopter test section. R = 2.30 × 10^6, M = 0.262.

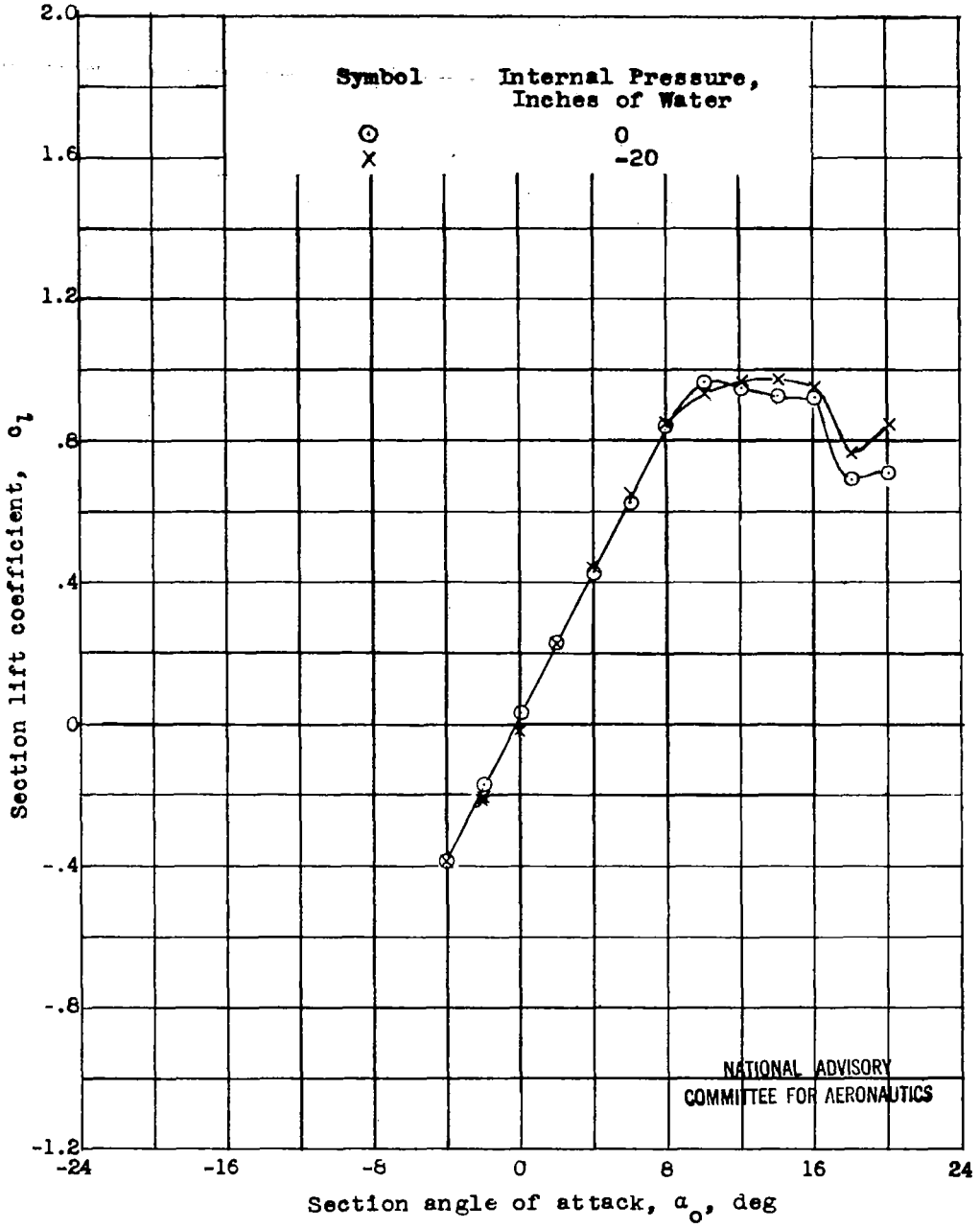

(b) Lift coefficient versus angle of attack

Figure 32.- Continued.

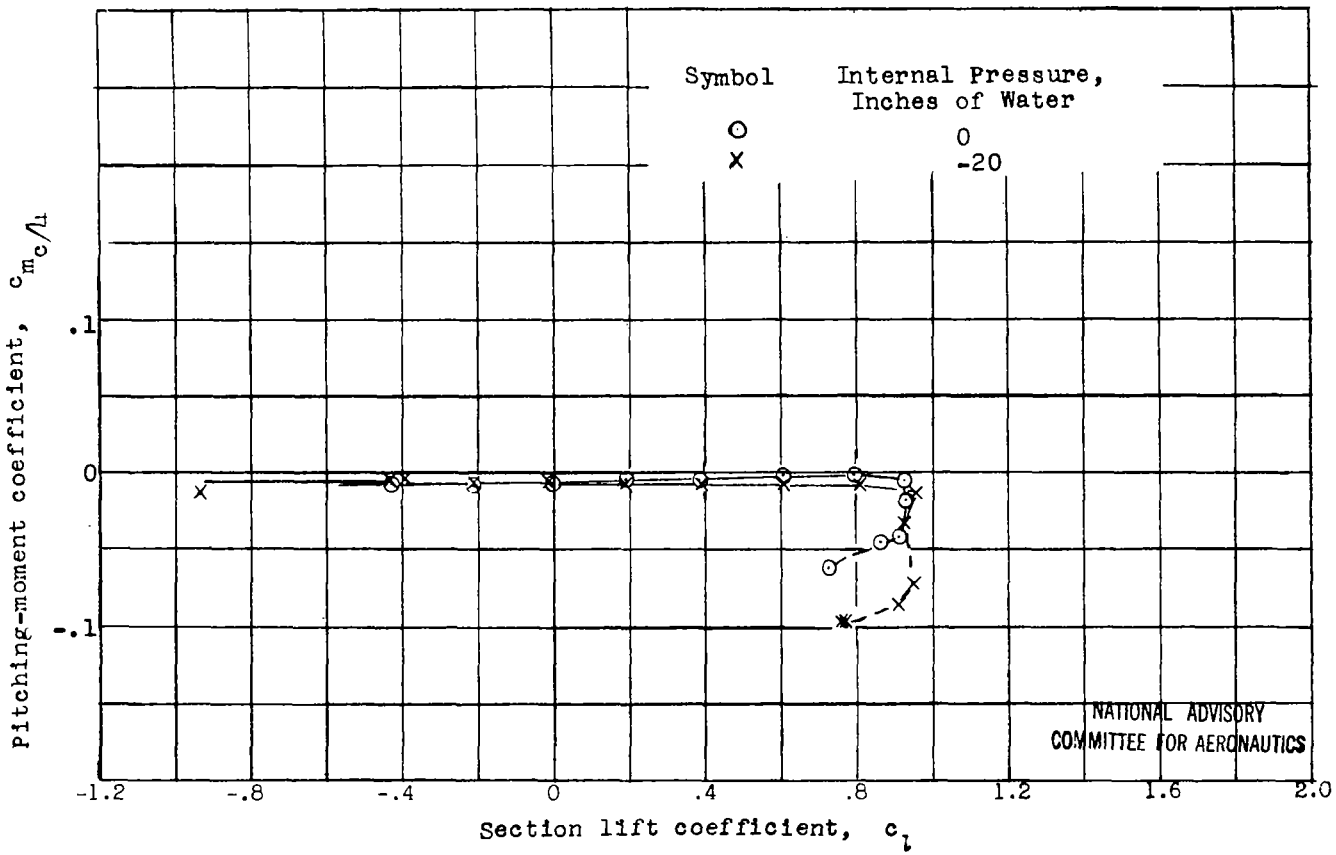

(c) Pitching-moment coefficient about quarter-chord point versus lift coefficient

Figure 32.- Concluded.

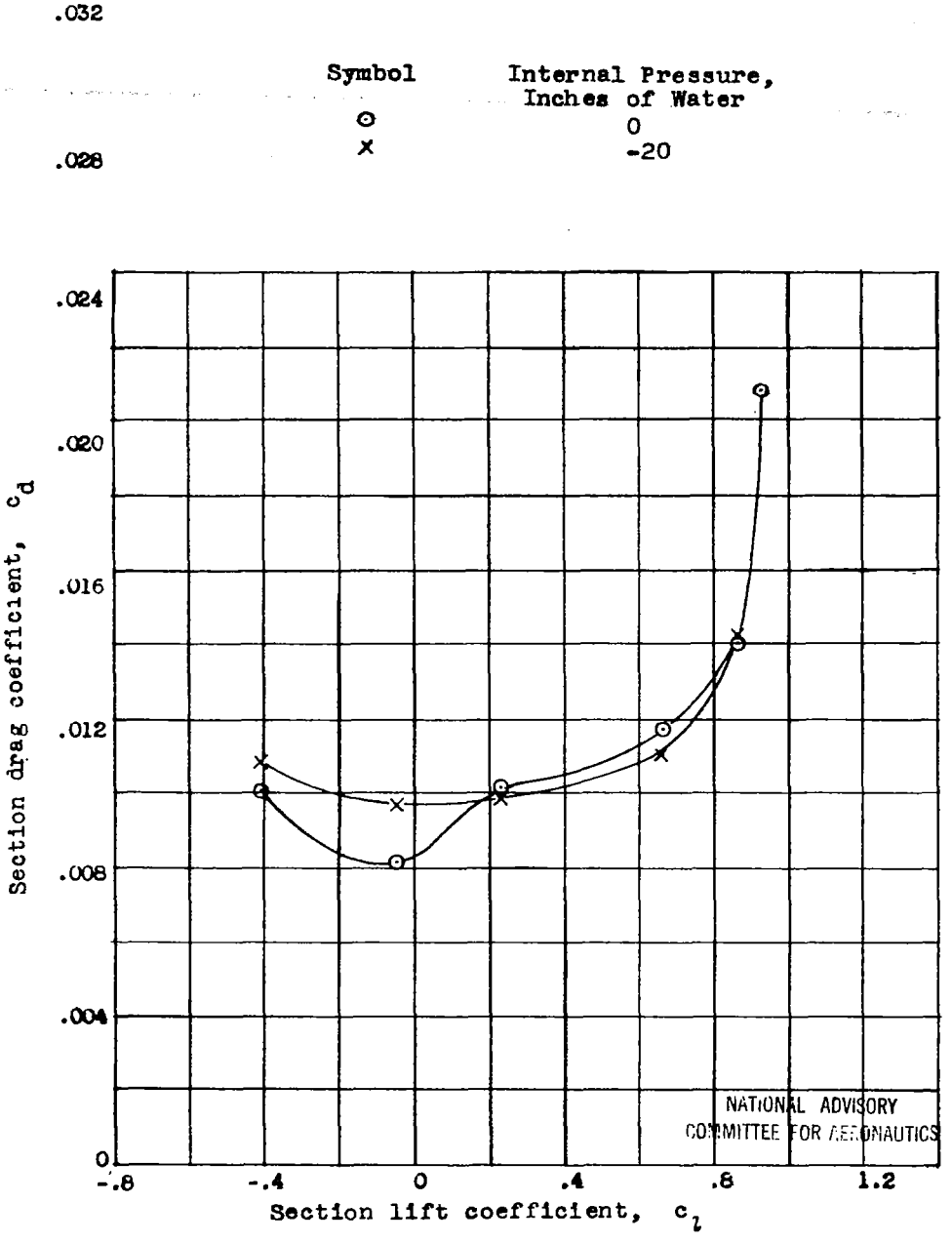

(a) Drag coefficient versus lift coefficient

Figure 33.- Aerodynamic data for the XR-5(b) Helicopter test section. $R = 3.16 \times 10^6$, $M = 0.373$.

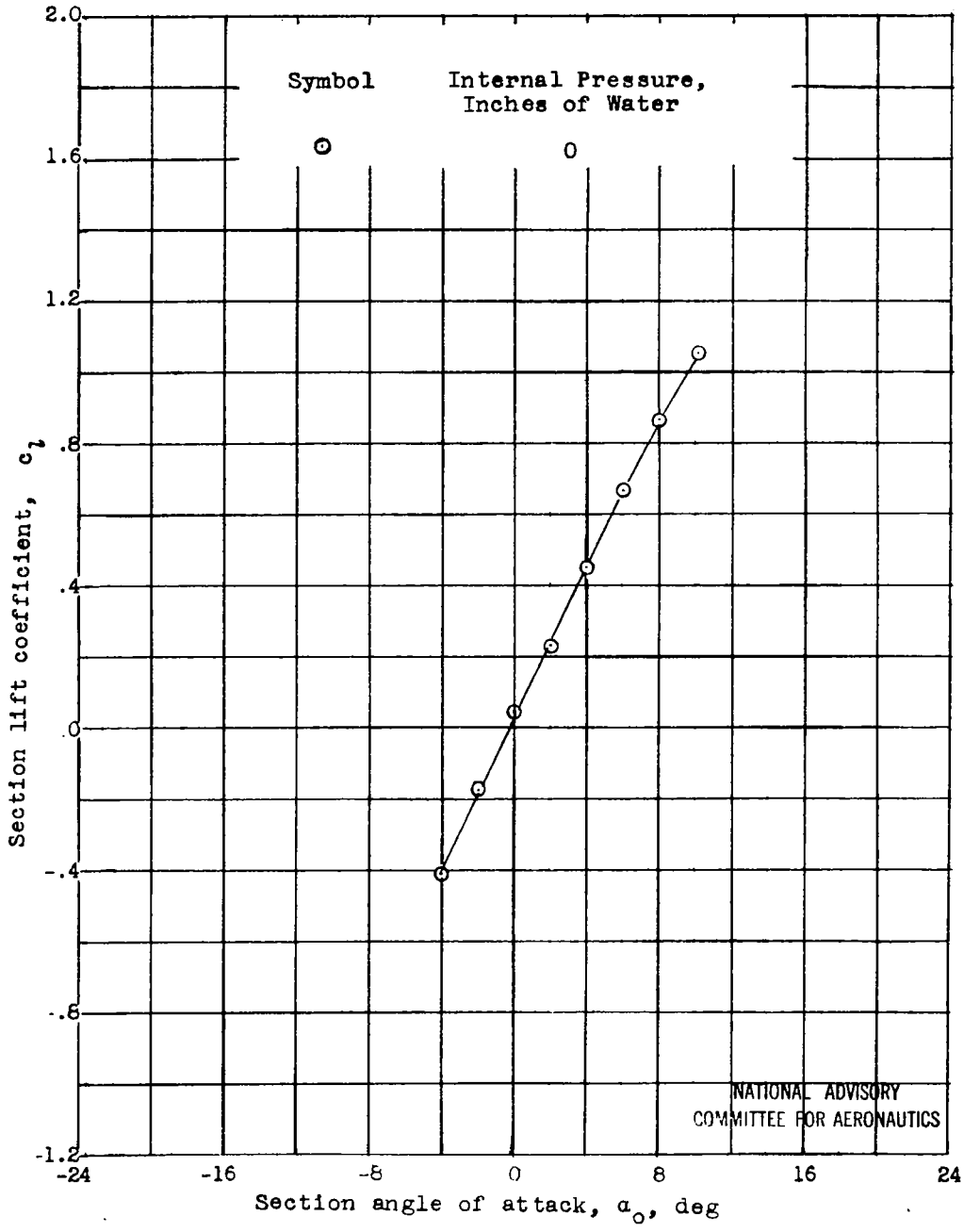

(b) Lift coefficient versus angle of attack

Figure 33.- Continued.

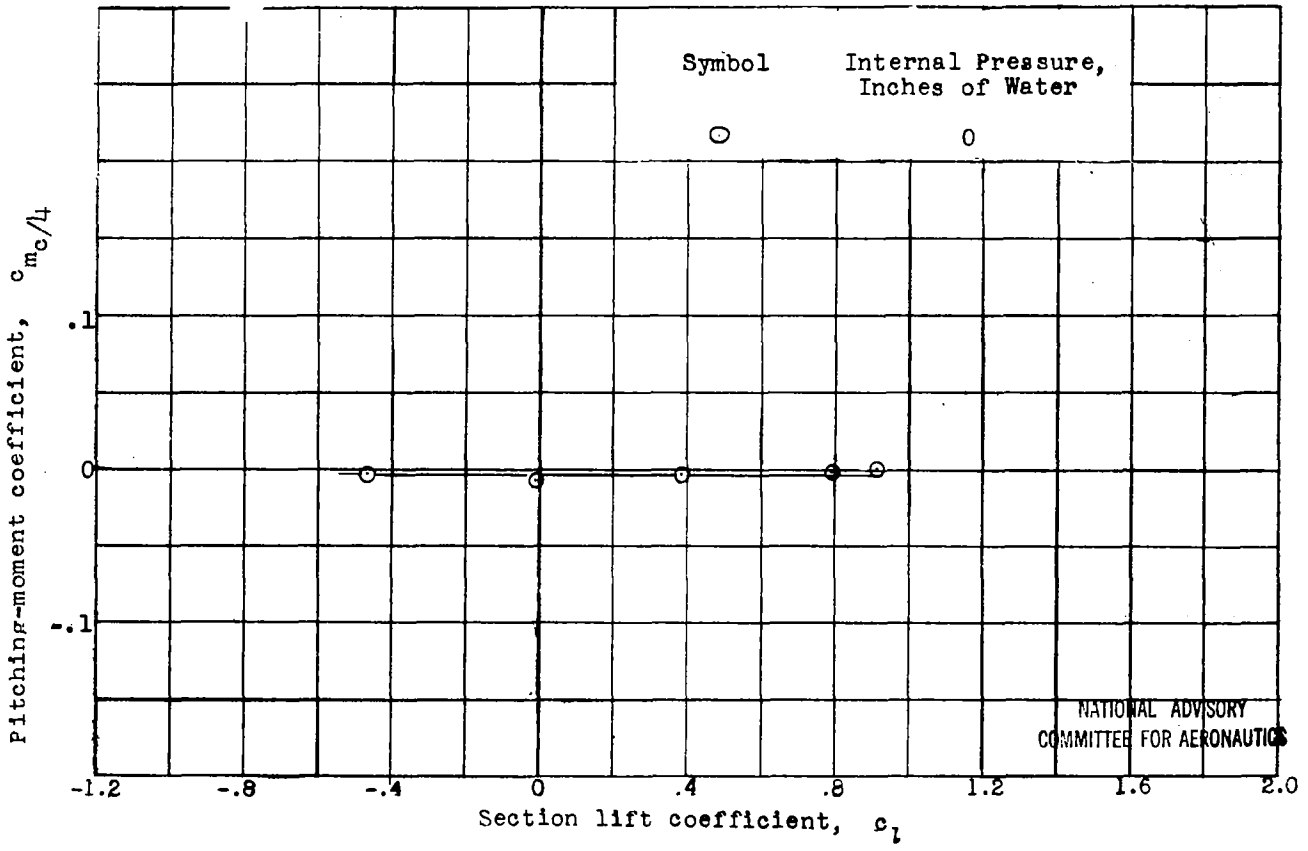

(c) Pitching-moment coefficient about quarter-chord point versus lift coefficient

Figure 33.- Continued.

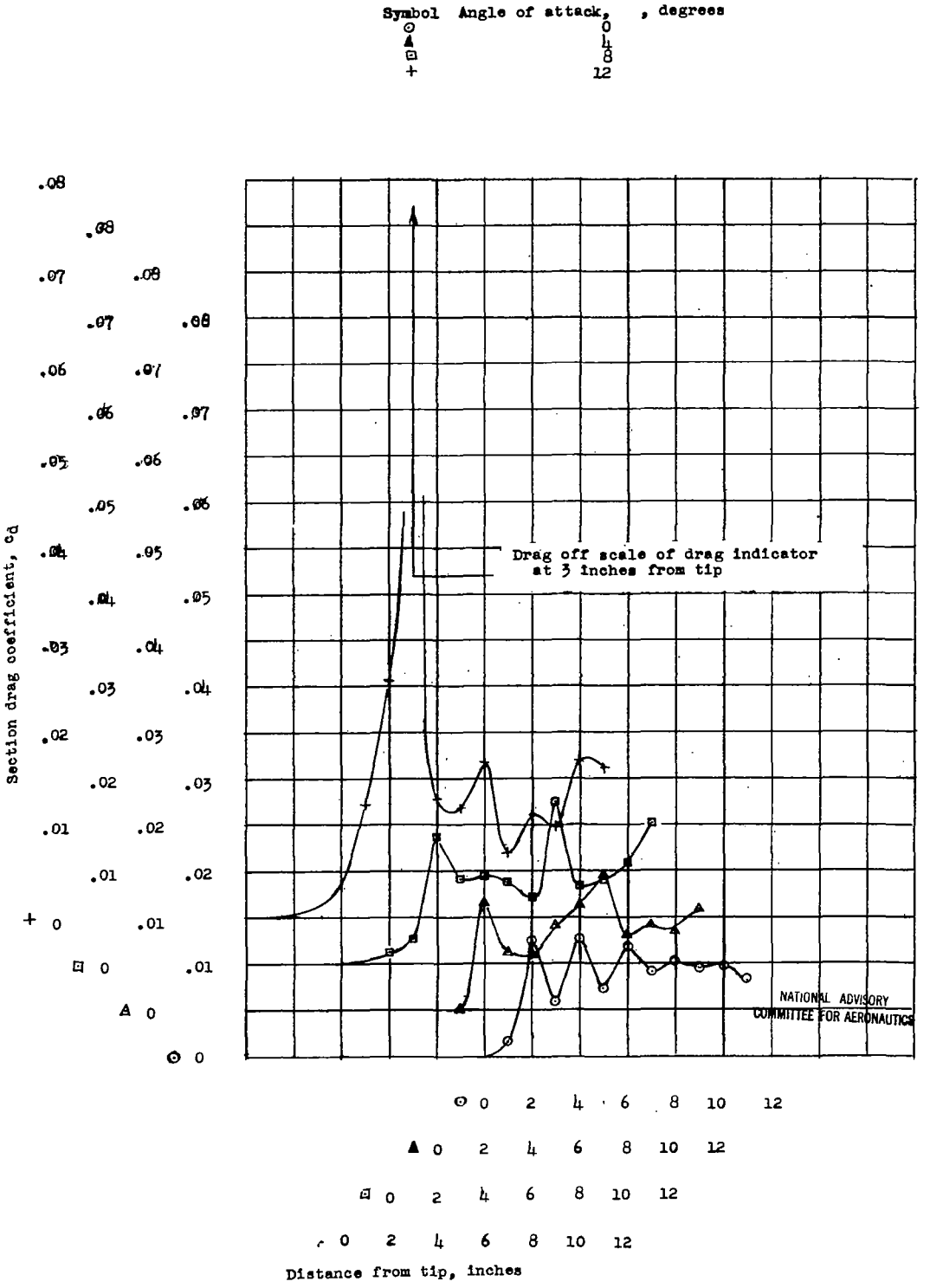

FIGURE 34.-Drag coefficient versus distance from model tip for the YR-4A No. 1 Helicopter blade tip section. R = 1.46, M = 0.280, internal pressure, 0 inches of water.

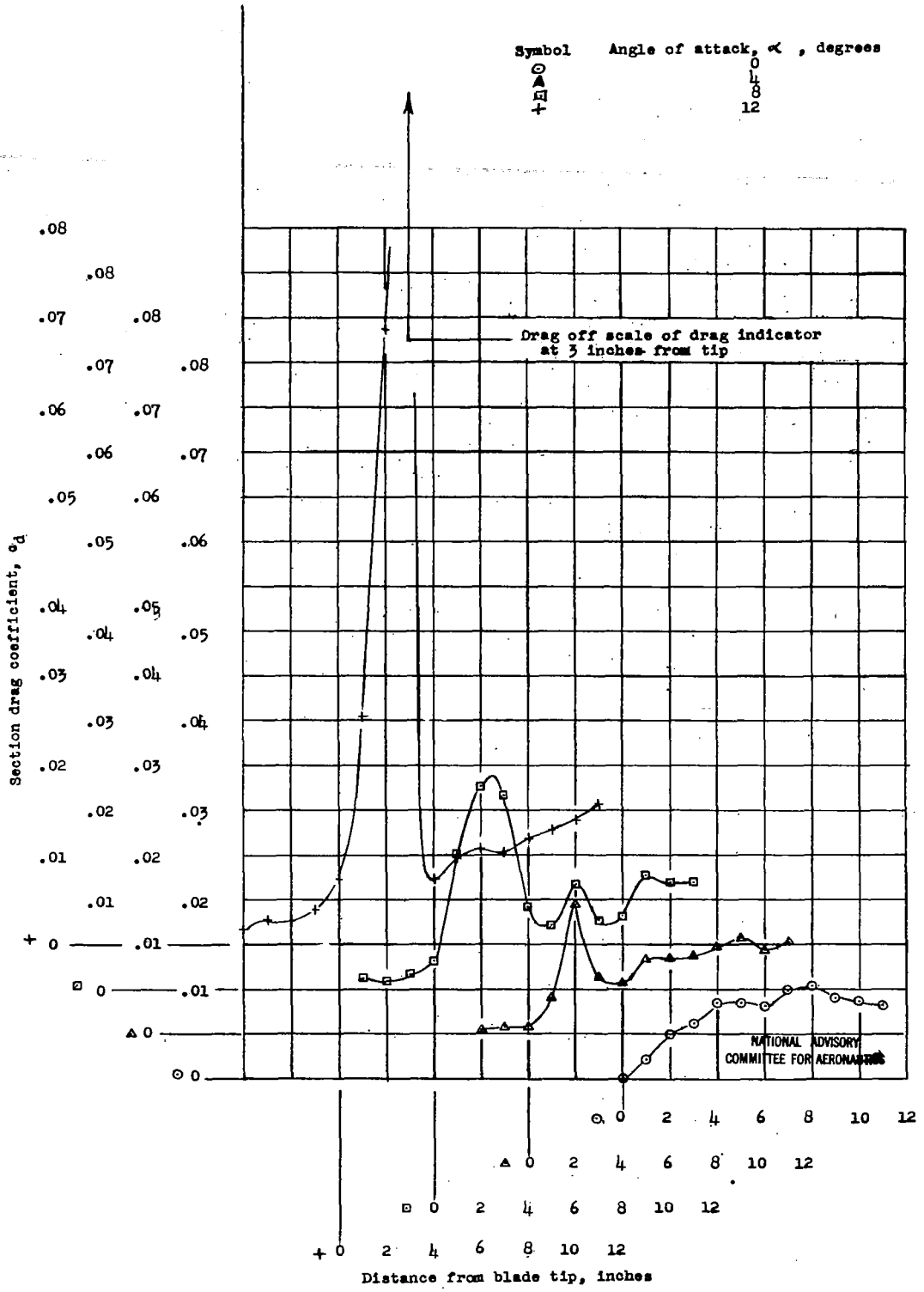

Fig. 35 Drag coefficient versus distance from model tip of XR-6 No. 2 Helicopter blade tip section.
$R = 1.46 \times 10^6$, $M = 0.280$

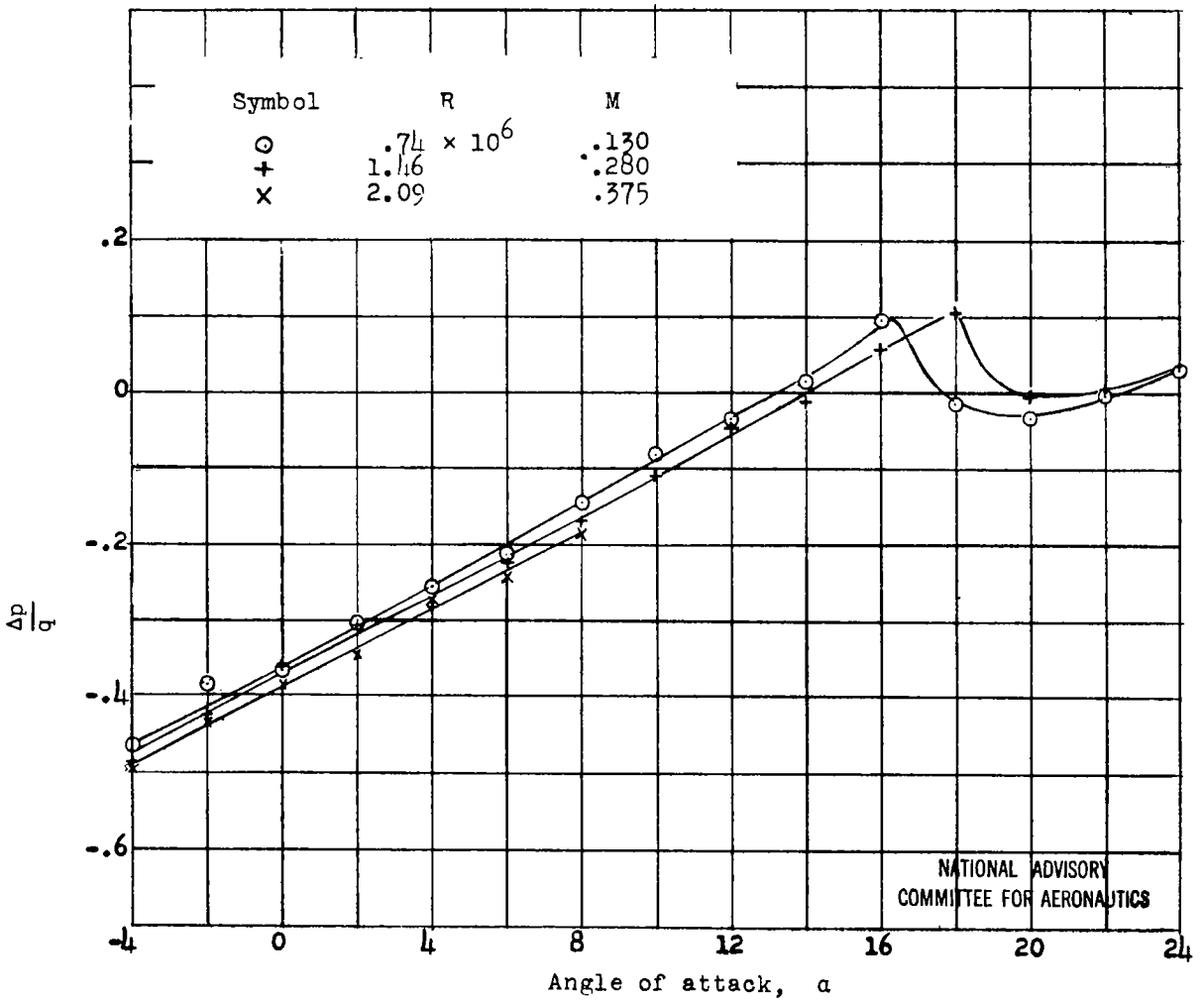

(a) Vent at x/c = 0.38

Figure 36.- Pressure coefficient versus angle of attack for various positions of the vent hole.

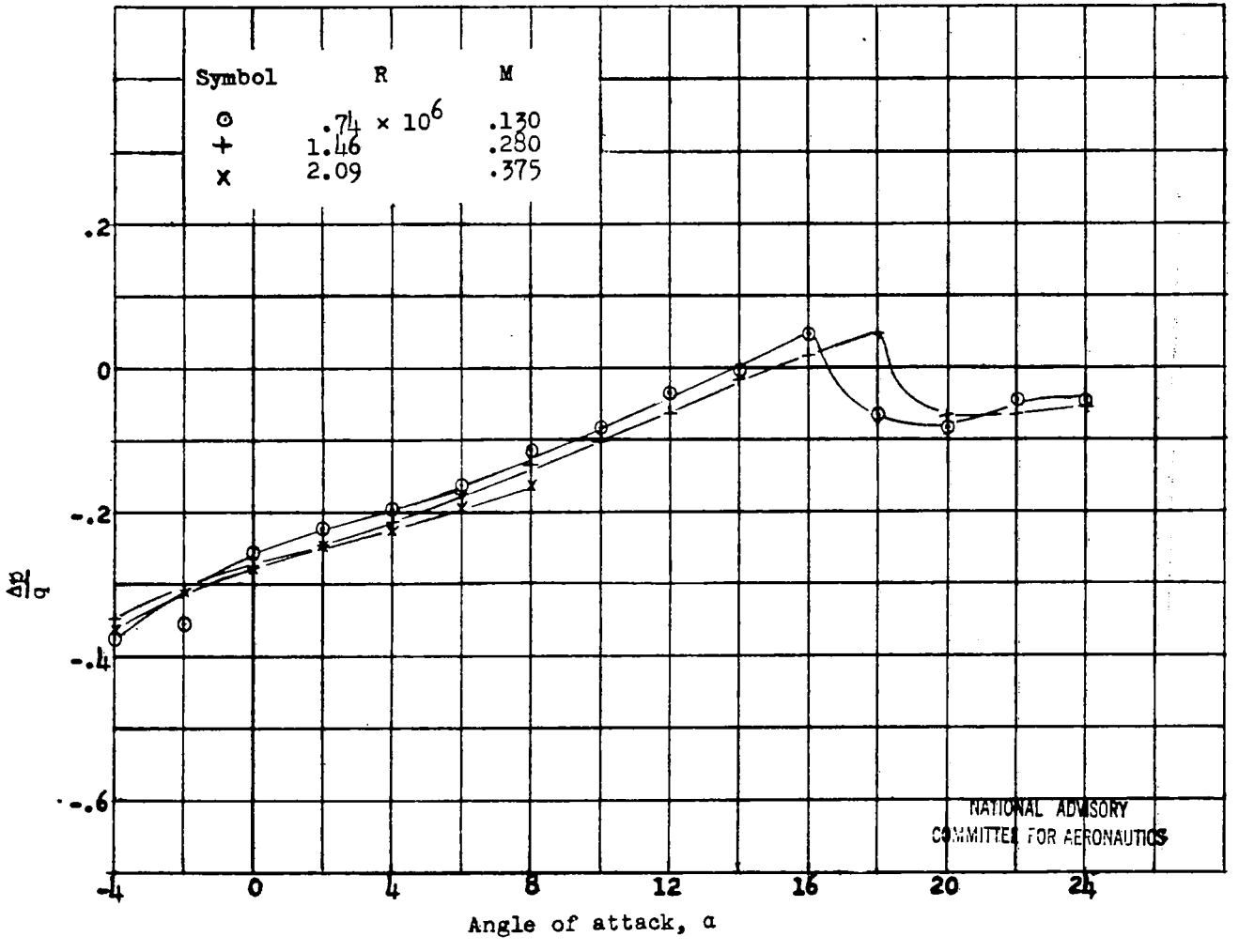

(b) Vent at x/c = 0.50

Figure 36.- Continued.

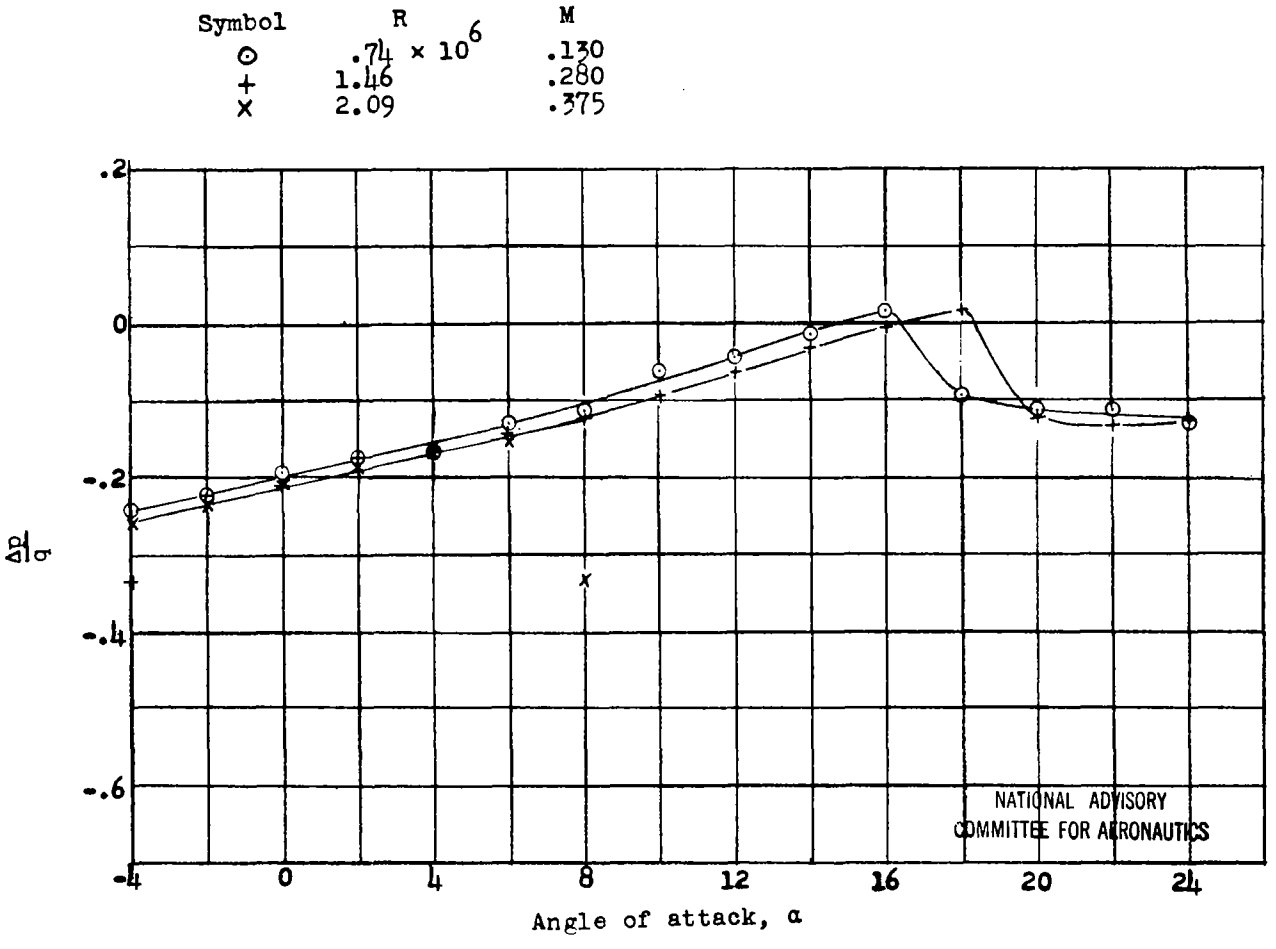

(c) Vent at x/c = .60

Figure 36.- Continued.

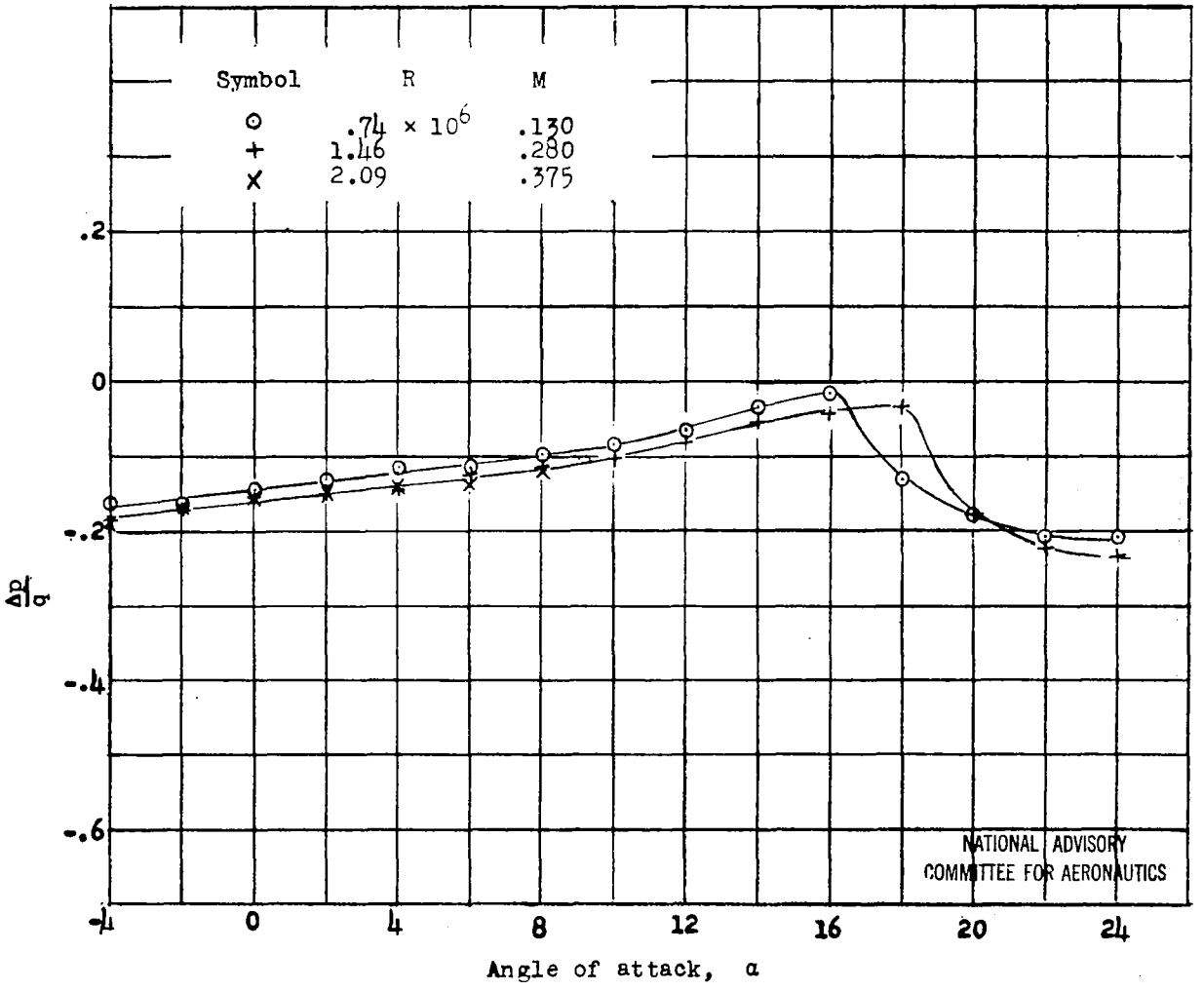

(d) Vent at x/c = 0.70

Figure 36.- Continued.

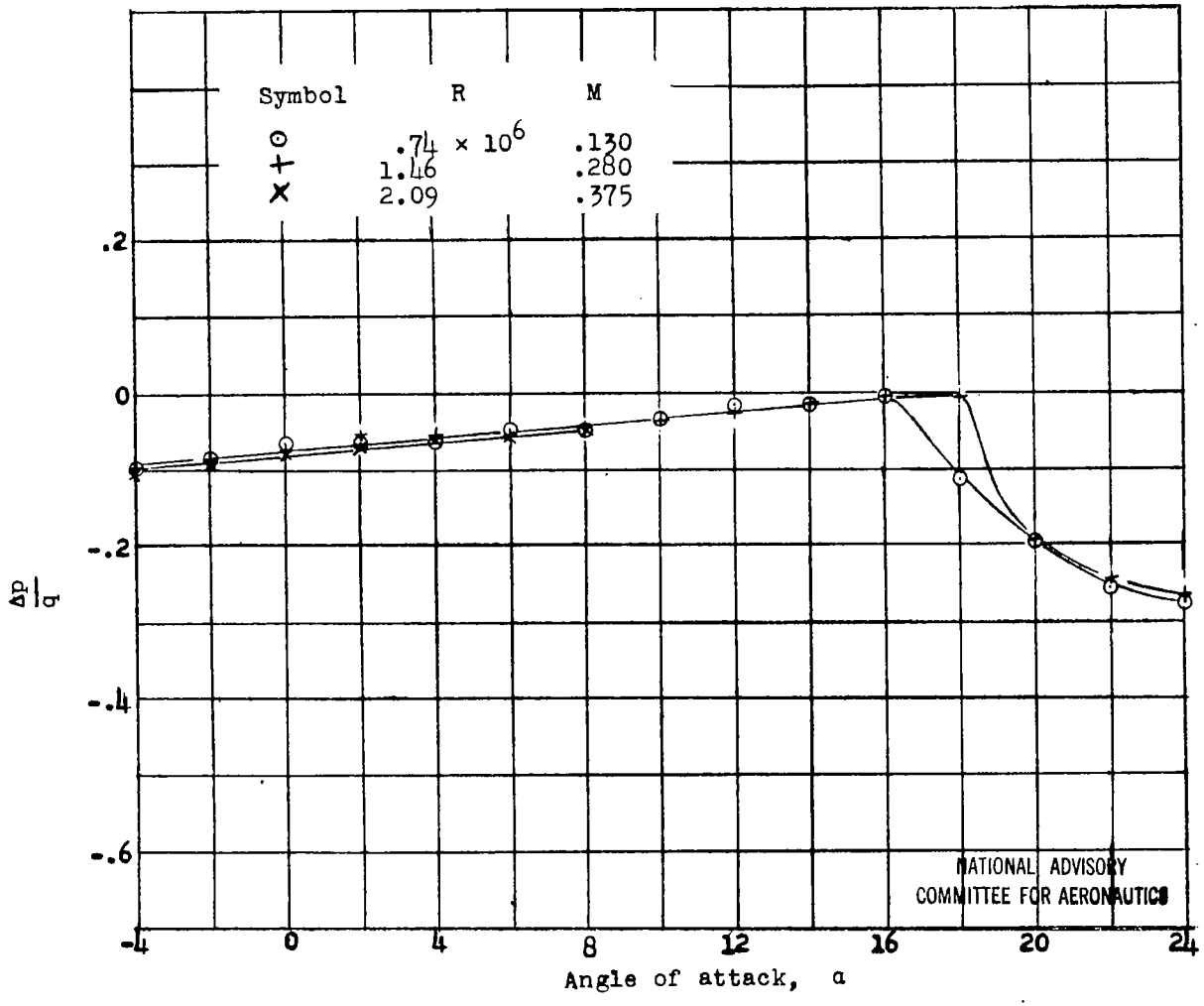

(e) Vent at x/c = 0.80

Figure 36.. Continued.

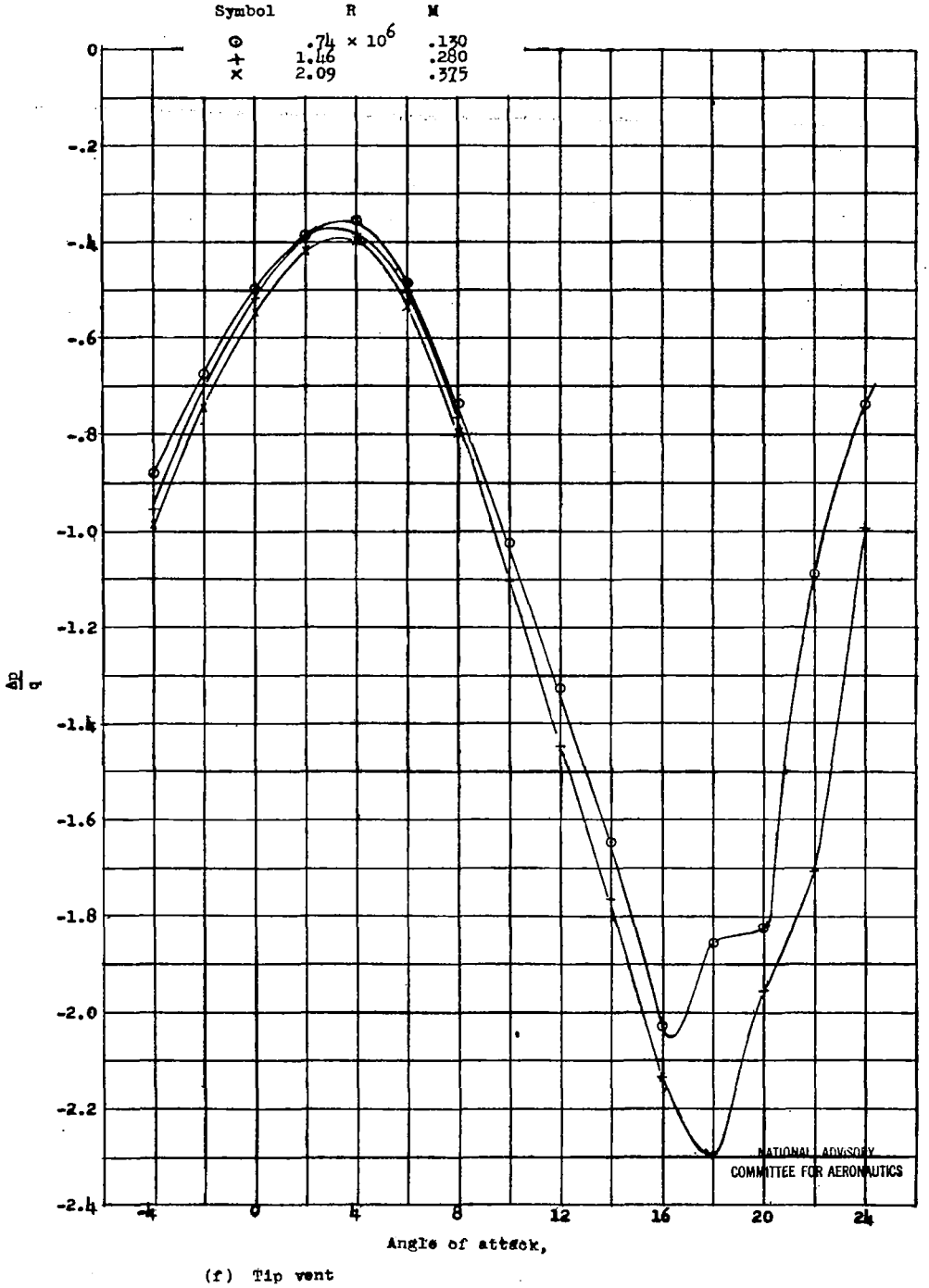

(f) Tip vent

Figure 36.- Concluded.

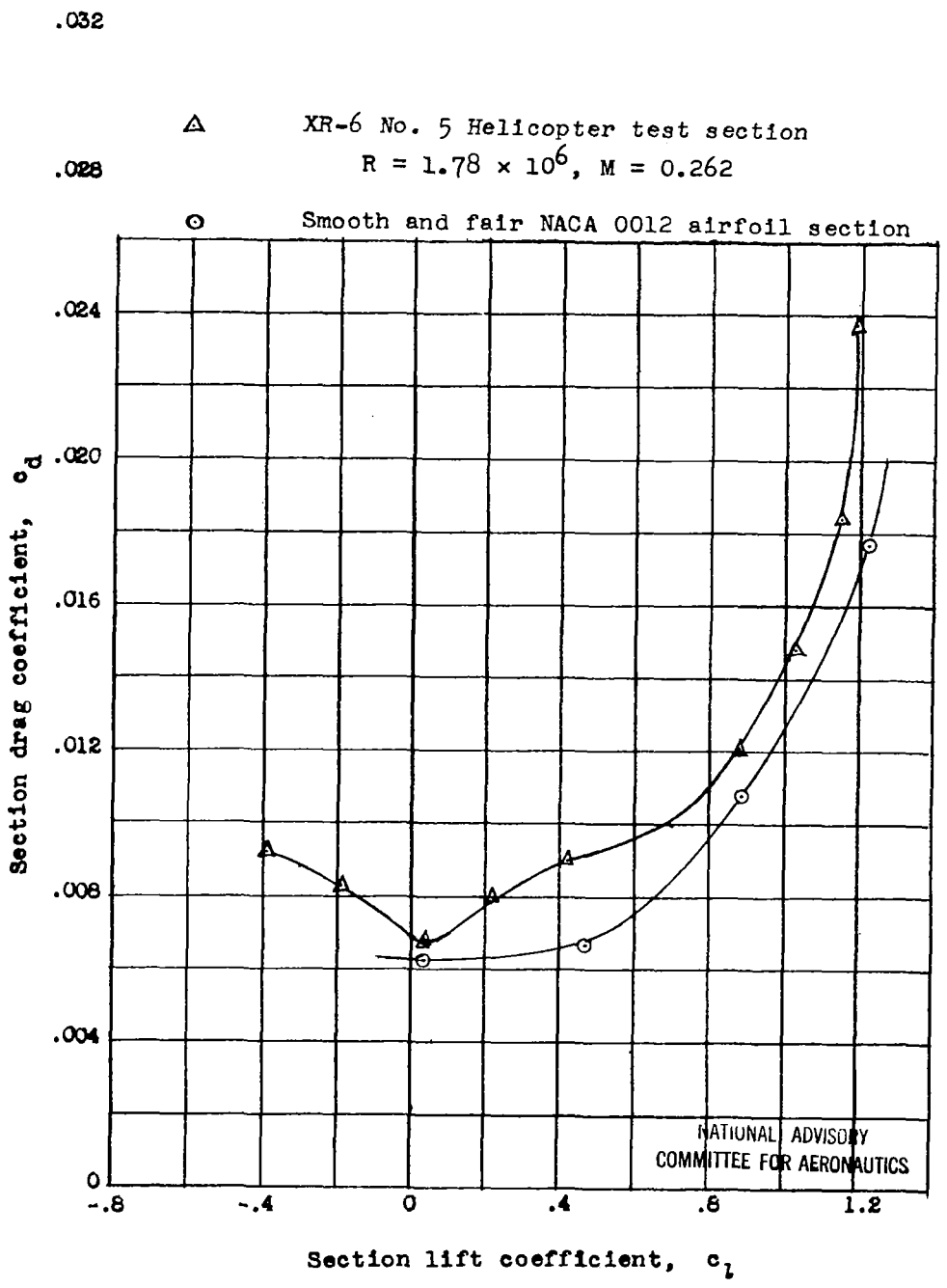

(a) Drag coefficient versus lift coefficient

Figure 37.- Aerodynamic data for a smooth and fair NACA 0012 airfoil section. R = 1.76 × 10^6, M = 0.130.

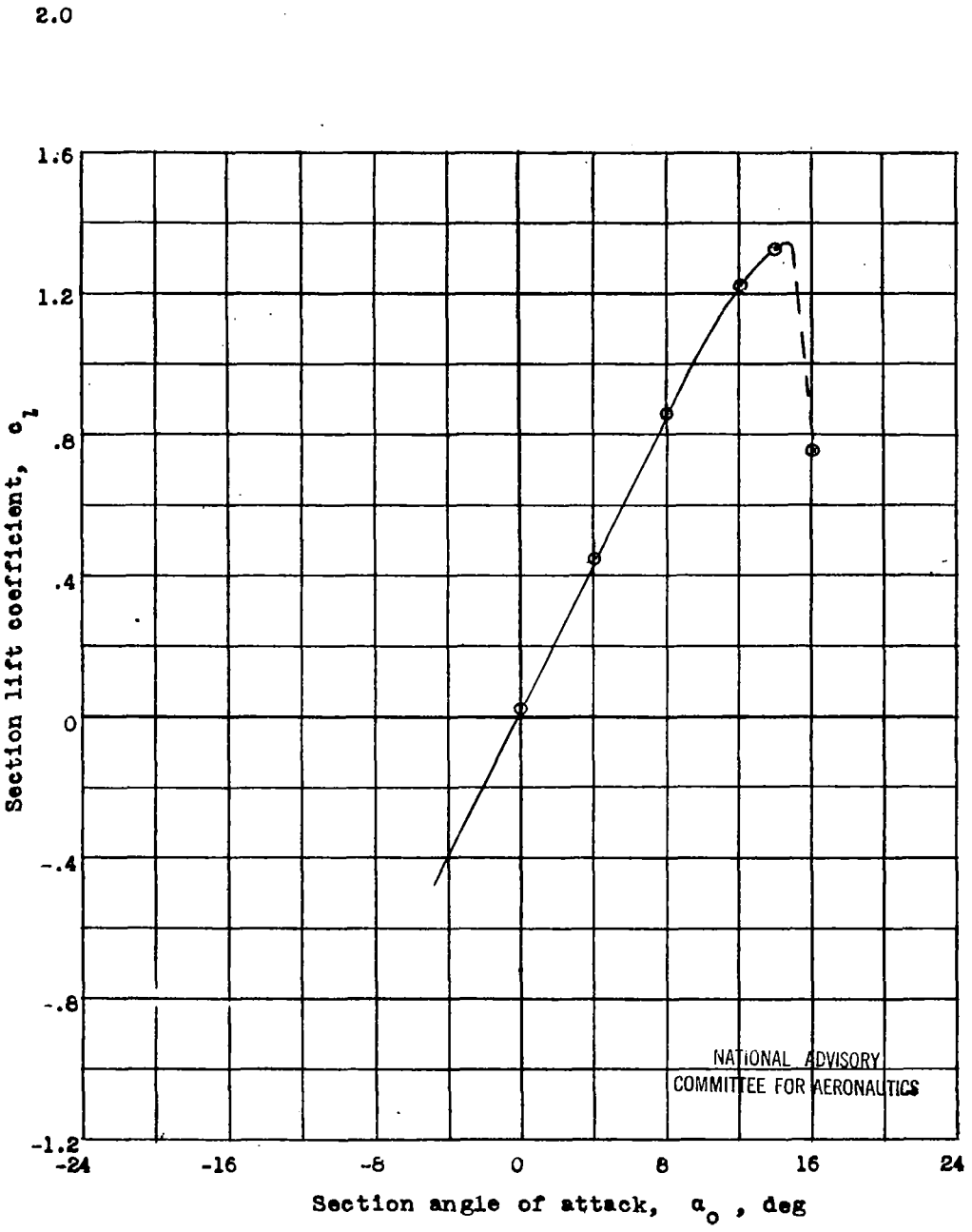

(b) Lift coefficient versus angle of attack

Figure 37.- Continued.